National Library of Canada
Canadian Theses Service
Ottawa, Canada
K1A 0N4

Bibliothèque nationale du Canada
Services des thèses canadiennes

CANADIAN THESES

THÈSES CANADIENNES

NOTICE

The quality of this microfiche is heavily dependent upon the quality of the original thesis submitted for microfilming. Every effort has been made to ensure the highest quality of reproduction possible.

If pages are missing, contact the university which granted the degree.

Some pages may have indistinct print especially if the original pages were typed with a poor typewriter ribbon or if the university sent us an inferior photocopy.

Previously copyrighted materials (journal articles, published tests, etc.) are not filmed.

Reproduction in full or in part of this film is governed by the Canadian Copyright Act, R.S.C. 1970, c. C-30. Please read the authorization forms which accompany this thesis.

AVIS

La qualité de cette microfiche dépend grandement de la qualité de la thèse soumise au microfilmage. Nous avons tout fait pour assurer une qualité supérieure de reproduction.

S'il manque des pages, veuillez communiquer avec l'université qui a conféré le grade.

La qualité d'impression de certaines pages peut laisser à désirer, surtout si les pages originales ont été dactylographiées à l'aide d'un ruban usé ou si l'université nous a fait parvenir une photocopie de qualité inférieure.

Les documents qui font déjà l'objet d'un droit d'auteur (articles de revue, examens publiés, etc.) ne sont pas microfilmés.

La reproduction, même partielle, de ce microfilm est soumise à la Loi canadienne sur le droit d'auteur, SRC 1970, c. C-30. Veuillez prendre connaissance des formules d'autorisation qui accompagnent cette thèse.

THIS DISSERTATION
HAS BEEN MICROFILMED
EXACTLY AS RECEIVED

LA THÈSE A ÉTÉ
MICROFILMÉE TELLE QUE
NOUS L'AVONS REÇUE

NL 339 (r 86/01)

Canada

THE STACK EFFECT IN HIGH-RISE BUILDINGS

by

KYU HYUN LEE

A thesis submitted to the School of Graduate Studies
in partial fulfillment of the requirement of
the degree of

MASTER OF APPLIED SCIENCE

in the

Department of Mechanical Engineering
University of Ottawa
Ottawa,Canada

1983

ABSTRACT.

In the present thesis, the characteristics of the pressure difference induced by the temperature difference across the building envelope (which is generally termed as "stack effect") was investigated both analytically and experimentally.

The emphasis was placed on the prediction of the correct value of the neutral pressure level (NPL) as it has been previously shown that the "stack effect equation" derived from the equation of the state of perfect gas can correctly calculate the pressure difference due to the stack effect, provided that the correct value of NPL is known.

The result of the present analysis based on the equation applied to a hypothetical high-rise building with no internal partition have shown to agree well with those obtained from the present experimental program. The model building which was used in the experiment was made of copper tube having 50.8 mm I.D and 18.3 m in length and consisted of 20 individually heated test sections to simulate the constant temperature difference across the wall in all elevations.

The study confirmed that the stack effect equation derived from the equation of state of perfect gas can correctly predict the pressure difference across the wall of a high-rise building induced by the temperature difference as long as the value of NPL is correct.

The study also showed that the recommendation of ASHRAE for the calculation of the value of NPL is extremely inadequate and that the value of NPL is strongly affected by the the characteristics of the wall openings (numbers and distribution) and of the flow passages. The effect of the temperature difference across the wall on the value of NPL, however, seems to be negligible. The effect of the physical sizes of buildings on the value of NPL has been shown to be insignificant when the dimensionless parameters D/Do and L/Lo are greater than 0.4 and 0.5, respectively.

ACKNOWLEDGEMENTS

The author wishes to express his deep sense of gratitude and appreciation to Dr. Yung Lee who initiated and supervised this work. His valuable suggestions, guidances and encouragements throughout this work have made it possible to obtain the desired results. The author is also very grateful to Dr. Lee for the generous financial support during the course of the present work.

Sincere thanks are also due to Dr.H.Tanaka of Civil Engineering, who provided his kind advice and encouragements, and other staff members of Department of Mechanical Engineering, who extended their help and coorperation in many ways.

Lastly, the author owes much to his wife.

TABLE OF CONTENTS

LIST OF TABLES

LIST OF FIGURES

NOMENCLATURE

A	Area
C	Friction factor pertaining to laminar flow
$\bar{C}_x$	Averaged coefficient defined by Eq.(3.12)
D	Diameter
g	Acceleration due to gravity
K_1	Coefficient defined by Eq.(1.1)
K	Minor loss coefficient
L	Length of flow path
N	Neutral pressure level
P	Pressure
Re_d	Reynolds number
T	Temperature
V	Velocity
Z	Height of building above ground

GREEK SYMBOLS

α_1, α_2	Function defined by Eq.(3.23)
β_1, β_2	Function defined by Eq.(3.23)
ρ	Density of air
μ	Viscosity

Δ	Difference

SUBSCRIPTS

1	Opening at bottom elevation
2	Opening at top elevation
a	Flow section a of openings
b	Flow section b of openings
exp	Experimental
i	inside or inner
o	outside or outer

Chapter I

INTRODUCTION

As a result of the rapidly rising energy cost and increasing concern over the depletion of energy resouces, the thermal performance of the building enclosure, both in residential and public buildings, has accordingly received greater attention recently.

In the design of a building, the calculation of the energy requirements for the air conditioning system plays an important role. It is also very important for the sizing and controlling of the air conditioning system, as well as the estimation of building operation costs.

The heat losses or gains of a building may be divided into three categories as follows;

(1) Conduction through the building envelope such as walls,ceilings, floors,etc.

(2) Fenestration such as heat transmission through the window and door systems.

(3) Air infiltration or exfiltration.

The theoretical understanding and prediction of the first two categories are relatively straightforward in

principle, though often quite complicated in practice. However, the last category may be of significant importance and yet it is the most uncertain to be accurately determined.

The factors that affect the characteristics of air infiltration or exfiltration are not only various, but they also depend upon quantities that are not easy to predict and measure. Hence, estimating the quantity of air infiltration requires knowledge of the pressure difference across the building exterior under various meteorological and occupancy conditions, as well as the air leakage characteristics of wall and window pane, etc.[1].

The pressure difference between the inside and the outside of a building may be due to (1) wind effects, (2) the density difference of the outside and inside air induced by temperature difference, which is called "chimney" or "stack" effect, and (3) mechanical ventilation.

The stack effect in a building occurs from the same causes as it does in a chimney or stack. When the inside temperature of a building is higher than that of the outside, in the absence of wind and mechanical ventilation, the stack effect due to the difference in air density generally produces a negative inside pressure and an inward air flow at low levels, and a positive inside pressure and an outward flow at high levels. The reverse occurs when the

inside temperature of a building is lower than that of the outside. With the stack effect acting alone in a building, a neutral pressure level(NPL) exists, where there is no pressure difference between the inside and the outside of a building.

The pressure difference induced by the stack or thermal effect alone can be approximated by the following equation:

$$(\Delta P)_s = K_1 \left(\frac{1}{T_o} - \frac{1}{T_i}\right)(N - Z) \qquad (1.1)$$

where

$(\Delta P)_s$=the pressure difference caused by the stack effect at the elevation(Z) above ground, Pa.

To=the outside temperature of the building,K.

Ti=the inside temperature of the building,K.

$K_1 = 3.44 \times 10^3$ Pa.K/m

N=the neutral pressure level(NPL) above ground from Z=0, m.

Z= the height of building above ground, m.

Eq.(1.1) is derived from the equation of the state of perfect gas and has been shown to be very correct for the

actual situation, provided that the neutral pressure level is accurately known [2].

As seen in Eq.(1.1), the amount of draft, or the pressure difference, produced in a building depends on the difference between the temperatures of the inside and the outside air, as well as on the building height. During cold weather, these action is not negligible in a high rise building. Even for one or two story houses, the effect in winter is sufficient to affect certain aspects of the air infiltration significantly [3].

As taller buildings are built recently, the stack effect increases proportionately. In -18°C weather, a 240 m. building can develop a stack effect with pressure difference totaling 500 Pa along the air flow paths. Such pressure differences should not be ignored from a number of points of view, especially in the aspect of energy conservation and occupancy conditions in multistory buildings.

For the accurate prediction of the stack effect in a building, it is very important to know the correct value of the neutral pressure level. A recommended method for the calculation of the neutral pressure level(NPL) of a building with openings at the top and bottom levels only was proposed by the American Society of Heating, Refrigerating and Air Conditioning Engineers(ASHRAE)[4] as follows:

$$N = \frac{H}{1 + \left(\frac{A_1}{A_2}\right)^2 \left(\frac{T_i}{T_o}\right)} \qquad (1.2)$$

where

H=total vertical height of a building between the exterior wall openings at the top and bottom elevations(m).

A_1=size of opening area at bottom elevation(m^2)

A_2=size of opening area at top elevation(m^2)

To=outside temperature, K°.

Ti=inside temperature, K°.

N=the neutral pressure level measured from the bottom opening elevation(m).

The recommended equation, Eq.(1.2), is derived from the Bernoulli's principle, thus neglecting the flow resistance along the flow paths of the building enclosures.

From the previous field studies, it was confirmed that the vertical pattern of pressure differences across the exterior walls of building depends on the vertical distribution of openings in the exterior wall and on the air flow resistance across the wall[4,5,6,7].

Hence, it is very doubtful if the recommended equation, Eq.(1.2), can accurately predict the correct value of the neutral pressure level. Little information, however, is available at this time as to the factors affecting the neutral pressure level and the profile of pressure differences induced by the stack effect in a high rise building.

Therefore, this study was initiated to investigate the characteristics of the stack effect and to propose a reliable method for the calculation of the neutral pressure level.

In the present study, the vertical distribution of pressure differences in a tall building due to stack effect alone was investigated by using a simple idealized model of a highrise building having no internal partition for various thermal conditions and for different wall opening distibutiohs.

The main objectives of the present study by both experiment and analysis are set as follws:

1) to verify the stack equation,Eq.(1.1),

2) to investigate the effect of the flow resistance along the flow path of the wall openings

and also of the vertical distribution of the openings in the exterior wall of building on the neutral pressure level,

3) to investigate the effect of temperature difference across the wall on the neutral pressure level for a given vertical distribution of the exterior wall openings, and

4) to study the effect of the size of the exterior wall opening on the value of the neutral pressure level.

The results also are compared against those recommended by ASHRAE.

Chapter II

LITERATURE SURVEY

The stack effect in a building is a phenomenon due to the temperature difference across the building envelope, when a tall building acts like a chimney, with air entering openings in a part of building, flowing through the building, and leaving out of openings in the other part of the building. Since it often causes undesirable pressure differentials and air flows, the stack effect can create functional problems for the building occupants .

This stack effect increases with temperature difference and the height of building, and is therefore one of the major causes of air leakage, or air infiltration, in a high rise building especially during the winter season in Canada.

The studies of the stack effect in the building can be divided into two major categories. The first category deals with the physical measurements of the air infiltration rate induced by the stack effect only, or combined effect of wind and mechanical ventilation through the field study in the buildings. The other group involves the numerical

estimation and prediction of the stack effect alone or combined with wind and mechanical ventilation using the mathematical model or numerical simulations.

2.1 PHYSICAL MEASUREMENT OF STACK EFFECT IN THE BUILDING

The earlier investigations were concerned mostly with the field studies of the stack effect in a high rise building to obtain overall air leakage characteristics and patterns of pressure differences caused by the stack effect alone or by the stack effect in combination with pressure differences induced by wind and the operation of mechanical ventilation systems.

Tamura and Wilson [7] have conducted the pressure measurements on a nine story office building under the influence of stack action alone as well as under the combined actions of mechanical ventilation and the stack effect. The height of the building above ground was 34 m(112 ft 10 in) to the main roof level and the internal dimensions of a typical floor was 23x81 m . The tests to investigate the stack effect were coducted in the evening when the building was unoccupied, during periods of low wind speed, and over various ranges of outside temperatures.

The results of the measurements reported that the neutral pressure level was 0.72 of the building height over various ranges of the outside temperature conditions with the mechanical ventilation system turned off and the dampers to the return air shaft opened. It also reported that the neutral pressure level moved to 62% of the building height when vertical air shaft was sealed and that the vertical profile of the pressure differentials across the exterior walls depends on the vertical distribution of openings in the exterior wall. The results of their field measurements are presented in Fig.2.1.

Tamura and Wilson [8] also have conducted another subsequent measurements on three buildings of A, B, and C, which is 17, 34, and 44 stories repectively. The results showed that the natural pressure levels were approximately 40, 35, and 52 % of the building height for building A, B and C, respectively, with ventilation system off and with wind speed under 16 Km/h. The measurements made under several temperature differences across the exterior walls indicated that the temperature differences had very little effect on the neutral pressure levels. They also showed the result that the pressure differentials across the exterior walls were approximately proportional to the corresponding pressure difference due to the stack effect of Eq.(1.1).

Shaw and Jones [3] conducted the analysis of air leakage characteristics of 11 school buildings through field tests using the pressurization method. The analysis showed that the contribution of stack effect to air infiltration was shown to be quite significant, even for a single level building, and a major contributing factor to annual heat consumption.

Lee, Tanaka and Shaw [2] have conducted the measurement of pressure differences on a twenty storey compartmentalized building. They found that the pressure induced by the wind and the stack effect were predominant for the particular building during the winter season. Their study found that the stack effect was linearly proportional to the difference of the reciprocal of the outside and inside absolute temperatures, and varied almost linearly with height. They also showed that the neutral pressure level occured at 70% of the total building height and that the vertical distribution of pressure differentials was affected by the occupancy conditions of the building.

2.2 NUMERICAL ESTIMATION AND PREDICTION OF STACK EFFECT

As the pressure distributions and flow patterns in buildings can be influenced by the building design characteristics, the building construction, and the

occupancy conditions, the direct measurements used in the field study are usually neither easy nor feasible. However, the net effect of stack action, affecting air infiltration into the building, can be analysed and estimated using computer and an appropriate mathematical model. It would be helpful in interpreting the results of such pressure measurements to understand how these pressure differentials and the resulting air flow are affected by the various parameters such as the vertical distributions of the wall openings, the flow resistance of the internal separations of a building, and the temperature differences across the exterior walls.

Such informations would be useful in establishing the requirements for the control of air infiltration caused by the stack effect alone or combined with wind and mechanical ventilation action, and therefore for the improvement of the occupancy environment of the buildings.

An analytical study of the distribution of pressure differences caused by the stack effect for a ten story building has been carried out by Tamura and Wilson[9], using a mathematical model based on the mass balance and energy equations.

The analysis has shown that under the uniform distribution of vertical openings the neutral pressure level

was located at mid-height of the building. With no internal flow resistance of interior separations, there was no pressure drop across the floors. This analysis showed that the pressurization, providing an excess of supply or exhaust air, offered possibilities for the control of pressure differences from the stack effect by altering the distribution of pressure differences in order to lower the neutral pressure level to ground level.

Barret and Locklin [10] have carried out a computer analysis of stack effect with a hypothetical 75 story office building having curtain-wall construction. The analysis showed that the validity of the predictions of the pressure differentials resulted from the effect depended on an advance knowledge of the flow resistances of building components along the air flow paths. It also reported that the safety aspect of building performance resulting from the stack effect may be evaluated with the computer simulation and is not a negligible one in a high rise building. The result showed that the computer analysis is useful in identifying the nature and location of problems resulting from the stack effect in a particular building, in predicting the magnitude of these problems, and in assessing the effectiveness of corrective means prior to building consruction.

Shaw, Sander and Tamura[11] have developed a method to estimate the air leakage induced by the stack effect in a building by using the known flow coefficient and flow exponent obtained from the field test of 4 multi-story buildings as well as from the computer analysis of models. They also have conducted other measurements of 4 additional multi-story buildings, using the previous test method. They reported that the infiltration rates calculated using this method were in good agreement with the measured values. They proposed an equation for the air infiltration resulting from the stack effect as follows.

$$Q_s = C_w S(0.0342\gamma P[\frac{\Delta T}{T_i T_o}])\frac{(\beta H)^{n_w+1}}{n_w+1} \qquad (2.1)$$

where

Q_s = total infiltration rate caused by the stack effect, m/s.

C_w = exterior wall flow coefficient, m /s.m .Pa

S = perimeter of the building, m

γ = ratio of actual to theoretical pressure difference.

P = atmospheric pressure, Pa.

To = absolute temperature outside, K.

Ti = absolute temperature inside , K.

ΔT = inside-outside temperature difference, Ti-To, K.

n_w = flow exponent

β = ratio of the height of the neutral pressure

level above the ground to the height of building.

It is apparent from the above review of studies on the stack effect in buildings that the detailed information of the characteristics of the stack effect has , generally speaking, not been completely investigated. A reliable method to predict the value of the neutral pressure level, which is essential for the accurate estimation of the stack effect, has not been developed.

Thus in this study, efforts will be made to obtain solutions to the problems discussed above.

Chapter III

ANALYTICAL STUDIES

3.1 THE STACK EFFECT

The Stack effect in buildings is similar to the thermal effect in a chimney. The amount of draft or the pressure difference in a chimney depends on the difference between the temperatures of the flue gas and the outside air as well as on the chimney height. During cold weather a similar action occurs in buildings, although the inside to outside air temperature difference is much less and the opening conditions of the buildings are quite different from that of the chimney.

Even for one or two storey houses the stack effect in winter is strong enough to induce the air infiltration significantly. In a high rise building it can lead to a considerable pressure differences across the exterior walls of the building[3].

The stack effect can be illustrated with the aid of Fig.3.1(a), which represents a building with no internal

separations, a single opening at the bottom level, and an inside air temperature greater than that of the outside. The figure shows the variations of the absolute air pressure with the height of building. The figure also shows that under the steady temperature conditions, with no wind and mechanical ventilation actions, the pressure difference between the inside and the outside is equal at the level of the opening. The absolute pressures decrease with the height of the building because of the reduction of the density with elevations above ground. This phenomenon of decreasing air pressures with height is straightforward[12] and is noticeable in the ear discomfort which results from rapid changes in elevation, as one experiences travelling in a non-pressurized aircraft.

Fig.3.1(a) also indicates that since the outside air is denser than that of the inside air, the reduction in pressure with height is more rapid on the outside of the building. It also shows that the absolute pressure in the inside is greater than that of the outside at all levels above the opening. This pressure difference is called the stack or the thermal effect. It acts across the walls of the building and is equal to the horizontal distance between the lines representing the inside and outside pressures. The maximum value of the pressure difference induced by the stack effect occurs at the top level in this particular case

and equals the total pressure difference caused by the thermal effect of the building.

If the single opening shown in Fig.3.1(b), on the other hand, is at the top level of the building, the absolute pressure inside and outside should be equal at the top of the building. Therefore, the inside pressure is less than that of the outside at all lower levels and the maximum pressure difference across the walls of the enclosure at bottom should be equal in magnitude but opposite in direction to that of Fig.3.1(a).

The openings through which air can infiltrate or exfiltrate occur in the walls of buildings at various levels. Fig.3.1(c) represents a heated building with no internal separations and openings of equal size in the exterior wall of the top and bottom levels. In this case, the air in the building is warmer than that of the outside, and therefore lighter than that of the outside in density, so that it tends to rise and escape through the upper opening while the colder outside air infiltrates through the lower opening at the bottom level to replace it. As the air flow takes place from the high pressure side to the low pressure side, the pressure outside must be higher than that of the inside at the bottom level and lower than that of the inside at the top level.

An example of the distribution of the inside and outside pressures required to satisfy these conditions is illustrated in Fig.3.1(c). The lines representing the absolute pressures of the inside and the outside of the building should have a cross point indicating that there is no pressure difference across the exterior wall of the building. This is the level that is called the neutral pressure level (NPL), neutral pressure plane, or neutral pressure zone, where the the inside and outside pressure of the building are equal.

In Fig.3.1(a) the neutral pressure level is at the level of the bottom opening. But in Fig.3.1.(b) the neutral pressure level occurs at the level of the top opening. The pressure difference across the exterior wall increases in proportion to the distance from the neutral pressure level. As shown in Eq.(1.1), it is evident that the pressure difference across the wall also increases in proportion to the temperature difference between the inside and the outside of the building. Hence the total theoretical pressure difference across the building enclosure caused by the stack effect, which can be calculated from Eq.(1.1), equals the sum of the pressure differences across the exterior walls at the top and bottom levels of the building.

The leakage openings in the exterior walls of a building are not always distributed uniformly from the bottom to the top of the building. But from the mass balance principle the inflow in the inward flow section of the building always should be equalled to the outflow.

If the openings at the bottom level are larger than those at the top level, and therefore may impose a smaller resistance to flow, the pressure difference across the bottom level may be less than that of the pressure difference across the top level. This may takes place with a shift of the inside pressure line shown in Fig.3.1.(c) to the right and a lowering of the neutral pressure level.

3.2 GOVERNING EQUATIONS

As a first step in the analysis of the characteristics of the stack effect in a highrise building, a model building having openings only at the top and bottom elevations as shown in Fig.3.2 is used in the present analysis.

The model shown in Fig.3.2 represents a high rise building with no internal partitions between floors and with the openings at the top and bottom levels only.

For the present analysis the following assumptions are made:

(1) The temperatures in the inside and outside of the building are uniform and steady.

(2) The air flows in the in-flow and out-flow paths are steady.

(3) The inside temperature of the building is higher than that of the outside.

(4) There are no wind or mechanical actions on the building.

The stack effect induced by the present temperature difference across the wall yields a negative inside pressure and inward air flow at the lower opening of the bottom level. On the other hand, it produces a positive pressure and outward air flow at the upper opening of the top level.

From the given conditions and assumptions, the pressure differences at the corresponding openings of each level can be represented by the following equations:

$$\Delta P_1 = \Delta P_{(K.E)_1} + \Delta P_{(f)_1} + \Delta P_{(ml)_1} \qquad (3.1)$$

$$\Delta P_2 = \Delta P_{(K.E)_2} + \Delta P_{(f)_2} + \Delta P_{(ml)_2} \qquad (3.2)$$

where

ΔP_1 =pressure difference across the exterior wall at the elevation of bottom opening.

ΔP_2 =pressure difference across the exterior wall at the elevation of top opening.

$\Delta P_{(K.E)}$=kinetic energy loss term at the corresponding flow path at the opening.

$\Delta P_{(f)}$ =friction loss term at the corresponding flow path at the opening.

$\Delta P_{(ml)}$=minor loss term caused by the abrupt change of flow directions and area at the corresponding openings.

Here the subscripts 1 and 2 denote the bottom and top levels, respectively.

Substituting the corresponding terms into Eqs(3.1) and (3.2), the energy equations at each level may be given as:

$$\Delta P_1 = P_{o_1} - P_{i_1} = \frac{1}{2}\rho_{a_1} v_{a_1}^2 \left\{1 + f_{a_1}\frac{La_1}{Da_1} + (K_c + K_e)_{a_1}\right\} + \frac{1}{2}\rho_{b_1} v_{b_1}^2 \left\{1 + f_{b_1}\frac{L_{b1}}{D_{b1}} + (K_{re})_{b_1}\right\} \quad (3.3)$$

$$\Delta P_2 = P_{i_2} - P_{o_2} = \frac{1}{2}\rho_{a_2} v_{a_2}^2 \left\{1 + f_{b_1}\frac{La_2}{Db_2} + (K_c + K_e)_{a_2}\right\} + \frac{1}{2}\rho_{b_2} v_{b_2}^2 \left\{1 + f_{b_2}\frac{L_{b2}}{D_{b2}} + (K_e)_{b_2}\right\} \quad (3.4)$$

The subscripts a and b refer respectively to flow sections a and b at the openings of the corresponding elevation of the system shown in Fig.3.2.

Applying the mass conservation relations at each opening of both levels, the continuity equations of the system may be given by:

$$\rho_{a_1} v_{a_1} A_{a_1} = \rho_{b_1} v_{b_1} A_{b_1} \tag{3.5}$$

$$\rho_{b_1} v_{b_1} A_{b_1} = \rho_i v_i A_i \tag{3.6}$$

$$\rho_i v_i A_i = \rho_{a_2} v_{a_2} A_{a_2} \tag{3.7}$$

$$\rho_{a_2} v_{a_2} A_{a_2} = \rho_{b_2} v_{b_2} A_{b_2} \tag{3.8}$$

Since Po=Pa=Pb, the velocity terms at the corresponding sections of the flow paths of the system may be represented as follows using the equation of state of a perfect gas for air.

$$V_{a_1} = \left\{\frac{T_{a_1}}{T_{b_1}}\right\}\left\{\frac{A_{b_1}}{A_{a_1}}\right\} V_{b_1} \tag{3.9}$$

$$V_{a_2} = \left\{\frac{T_{a_2}}{T_{b_2}}\right\}\left\{\frac{A_{b_2}}{A_{a_2}}\right\} V_{b_2} \tag{3.10}$$

Assuming that the flows at each flow section of the opening of each level are laminar and are in the developing regions, the friction factors for the corresponding flow sections may be expressed as follows:

$$f_x = \frac{\overline{C}_x}{Re_d} \tag{3.11}$$

where

f_x = friction factor at the corresponding flow sections.

$\overline{C}_x$ = averaged coefficient pertaining to the developing laminar flow at the corresponding flow sections, which is defined as

$$\overline{C}x = \frac{\int_o^L C_x dx}{\int_o^L dx} \tag{3.12}$$

and

$$C_\infty = 64$$

Red=Reynold's number at the corresponding flow sections.

Substituting the continuity equations of Eqs.(3.5) to (3.8) into Eq.(3.11) and simplifying:

$$f_{a_1}\frac{L_{a_1}}{D_{a_1}} = \overline{C}_{a_1}\left\{\frac{RT_{b_1}}{P_o}\right\}\left\{\frac{\mu_{a_1} L_{a_1}}{D_{b_1}}\right\}\frac{1}{V_{b_1}} \qquad (3.13)$$

$$f_{b_1}\frac{L_{b_1}}{D_{b_1}} = \overline{C}_{b_1}\left\{\frac{RT_{b_1}}{P_o}\right\}\left\{\frac{\mu_{b_1} L_{b_1}}{D_{b_1}}\right\}\frac{1}{V_{b_1}} \qquad (3.14)$$

$$f_{a_2}\frac{L_{a_2}}{D_{a_2}} = \overline{C}_{a_2}\left\{\frac{RT_{b_2}}{P_o}\right\}\left\{\frac{\mu_{a_2} L_{a_2}}{D_{b_2}}\right\}\frac{1}{V_{b_2}} \qquad (3.15)$$

$$f_{b_2}\frac{L_{b_2}}{D_{a_2}} = \overline{C}_{b_2}\left\{\frac{RT_{b_2}}{P_o}\right\}\left\{\frac{\mu_{b_2} L_{b_2}}{D_{b_2}}\right\}\frac{1}{V_{b_2}} \qquad (3.16)$$

Assuming that the coefficients at the corresponding opening are all the same ($C1 \cong Ca1 \cong Cb1$, $C2 \cong Ca2 \cong Cb2$) and substituting Eqs.(3.12) to (3.15) into Eqs.(3.3) and (3.4), the energy equations at each level become:

$$\Delta P_1=\frac{1}{2}\left(\frac{P_o}{R}\right)V_{b_1}^2\left\{\frac{T_{a_1}}{T_{b_1}^2}\left[\frac{A_{b_1}}{A_{a_i}}\right]^2\left(1+(K_c+K_{e_{ai}})\right)+\frac{1}{T_{b_1}}\left[1+(K_{re})_{b_1}\right]\right\}$$

$$+\frac{1}{2}C_1V_{b_1}\left\{\frac{T_{a_1}}{T_{b_1}}\left(\frac{A_{b_1}}{A_{a_1}}\right)^2\frac{\mu_{a_1}L_{a_1}}{D_{b_1}^2}+\frac{\mu_{b_1}L_{b_1}}{D_{b_1}^2}\right\} \qquad (3.17)$$

$$\Delta P_2=\frac{1}{2}\left(\frac{P_o}{R}\right)V_{b_2}^2\left\{\frac{T_{a_2}}{T_{b_2}^2}\left(\frac{A_{b_2}}{A_{a_2}}\right)^2\left[1+(K_c+K_e)_{a_2}\right]+\frac{1}{T_{b_2}}\left[1+(K_e)_{b_2}\right]\right\}$$

$$+\frac{1}{2}C_2V_{b_2}\left\{\frac{T_{a_2}}{T_{b_2}}\left[\frac{A_{b_2}}{A_{a_2}}\right]^2\frac{\mu_{a_2}L_{a_2}}{D_{b_2}^2}+\frac{\mu_{b_2}L_{b_2}}{D_{b2}^2}\right\} \qquad (3.18)$$

Let

$$a_1=\frac{1}{2}\left(\frac{P_o}{R}\right)\left\{\frac{T_{a_1}}{T_{b_1}^2}\left[\frac{A_{b_1}}{A_{a_1}}\right]^2\left(1+(K_c+K_e)_{a_1}\right)+\frac{1}{T_{b1}}\left[1+(K_{re})_{b_1}\right]\right\}$$

$$b_1=\frac{1}{2}C_1\left\{\frac{T_{a_1}}{T_{b_1}}\left[\frac{A_{b_1}}{A_{a_1}}\right]^2\frac{\mu_{a_1}L_{a_1}}{D_{b_1}^2}+\frac{\mu_{b_1}L_{b_1}}{D_{b_1}^2}\right\}$$

$$a_2=\frac{1}{2}\left(\frac{P_o}{R}\right)\left\{\left(\frac{T_{a_2}}{T_{b_2}^2}\right)\left[\frac{A_{b_2}}{A_{a_2}}\right]^2\left(1+(K_c+K_e)_{a_2}\right)+\frac{1}{T_{b_2}}\left[1+(K_e)_{b_2}\right]\right\}$$

$$b_2=\frac{1}{2}\ C_2\left\{\frac{T_{a_2}}{T_{b_2}}\left[\frac{A_{b_2}}{A_{a_2}}\right]^2\frac{\mu_{a_2}L_{a_2}}{D_{b_2}^2}+\frac{\mu_{b_2}L_{b_2}}{D_{b_2}^2}\right\}$$

Then the energy equations, Eqs.(3.17) and (3.18), representing the pressure differentials at the top and bottom elevations, become:

$$(\Delta P)_{s_1} = a_1 V_{b_1}^2 + b_1 V_{b_1} \tag{3.19}$$

$$(\Delta P)_{s_2} = a_2 V_{b_2}^2 + b_2 V_{b_2} \tag{3.20}$$

From the equation of the stack effect, Eq.(1.1), the pressure differences caused by the stack effect at both elevations may be given as follows:

$$(\Delta P)_{s_1} = K_1 \left(\frac{1}{T_o} - \frac{1}{T_i} \right) N \tag{3.21}$$

$$(\Delta P)_{s_2} = K_1 \left(\frac{1}{T_o} - \frac{1}{T_i} \right) (N - H) \tag{3.22}$$

The pressure differentials induced by stack effect at both elevations obtained from Eqs.(3.20) and (3.21) should be balanced with the energy equations, Eqs.(3.18) and (3.19), which represent the pressure differences across the wall at both elevations. Therefore, the solution for the value of the neutral pressure level for the present case may be obtained from Eqs.(3.18) to (3.21). Finally, the solution for the neutral pressure level may be expressed as follows:

$$N = \left(\frac{1}{1 + \frac{X_2}{X_1}}\right) H \qquad (3.23)$$

where

N=the neutral pressure level above ground, m.

$X_1 = \alpha_1 V_{b_1} + \beta_1$

$X_2 = \alpha_2 V_{b_1} + \beta_2$

H=vertical height of building above the opening at bottom level, m.

$$\alpha_1 = \frac{1}{2} \frac{P_o}{R} \left\{ \frac{T_{a_1}}{T_{b_1}} \left[\frac{A_{b_1}}{A_{a_1}}\right]^2 + \frac{1}{T_{b_1}} + (K_c + K_e)_a \left[\frac{T_{a_1}}{T_{b_1}}\right] \left(\frac{A_{b_1}}{A_{a_1}}\right)^2 + (K_{re})_{b_1} \frac{1}{T_{b_1}} \right\}$$

$$\beta_1 = \frac{1}{2} C_l \left\{ \frac{\mu_{a_1} L_{a_1}}{D_{a_1}} \left(\frac{T_{a_1}}{T_{b_1}}\right) \left(\frac{A_{b_1}}{A_{a_1}}\right) + \frac{\mu_{b_1} L_{b_1}}{D_{b_1}} \right\}$$

$$\alpha_2=\frac{1}{2}\ \frac{P_o}{R}\left\{\frac{T_{a_2}}{T_{b_1}}\left(\frac{A_{b_1}}{A_{a_2}}\right)^2+\frac{T_{b_2}}{T_{b_1}}\left(\frac{A_{b_1}}{A_{b_2}}\right)+\quad(K_c+K_e)_{a_2}\left(\frac{T_{a_2}}{T_{b_1}}\right)\left(\frac{A_{b_1}}{A_{a_2}}\right)^2\right.$$

$$\left.+(K_e)_{b_2}\frac{T_{b_2}}{T_{b_1}}\left(\frac{A_{b_1}}{A_{b_2}}\right)^2\right\}$$

$$\beta_2=\frac{1}{2}\,C_2\left\{\frac{\mu_{a_2}L_{a_2}}{D_{a_2}}\left(\frac{T_{a_2}}{T_{b_1}}\right)\frac{A_{b_1}}{A_{a_2}}\quad+\frac{\mu_{b_2}L_{b_2}}{D_{b_2}}\left(\frac{T_{b_2}}{T_{b_1}}\right)\frac{A_{b_1}}{A_{b_2}}\right\}$$

The velocity terms can also be obtained from substituting the continuity equations, Eqs.(3.5) to (3.8), into the energy equations, Eqs.(3.3) and (3.4). Hence, the velocity at the flow section b of the bottom level may be given as:

$$V_{b_1}=\frac{1}{2\,a}\left\{-b+\sqrt{b^2-4ac}\right\}\qquad(3.24)$$

where

$$a=\frac{1}{2}\left(\frac{P_o}{R}\right)\left(\frac{A_{b_1}}{A_{a_2}}\right)^2\left\{\frac{T_{a_2}}{T_{b_1}^2}+\frac{1}{T_{b_2}}\left(\frac{T_{a_2}}{T_{b_1}}\right)^2+(K_c+K_e)_{a_2}\left(\frac{T_{a_2}}{T_{b_1}^2}\right)\right\}$$

$$+\frac{1}{2}\left(\frac{P_o}{R}\right)\left\{(K_e)_{b_2}\left(\frac{T_{b_2}}{T_{b_1}}\right)\left(\frac{A_{b_1}}{A_{b_2}}\right)^2+\left(\frac{T_i}{T_{b_1}}\right)\left(\frac{A_{b_1}}{A_i}\right)^2+\frac{T_{a_1}}{T_{b_1}^2}\left(\frac{A_{b_1}}{A_{a_1}}\right)^2\right.$$

$$+\frac{1}{T_{b_1}}+(K_c+K_e)_{a_1}\left(\frac{T_{a_1}}{T_{b_1}^2}\right)\left(\frac{A_{b_1}}{A_{a_1}}\right)^2+(K_{re})_{b_1}\left(\frac{1}{T_{b_1}}\right)\Bigg\}$$

$$b=\frac{1}{2}\Bigg\{C_2\left[\frac{\mu_{a_2}L_{a_2}}{D_{a_2}}\left(\frac{T_{a_2}}{T_{a_1}}\right)\left(\frac{A_{b_1}}{A_{a_2}}\right)+\frac{\mu_{b_2}L_{b_2}}{D_{b_2}^2}\left(\frac{T_{b_2}}{T_{b_1}}\right)\left(\frac{A_{b_1}}{A_{b_2}}\right)\right]$$

$$+\left(\frac{64\mu_i L_i}{D_i^2}\right)\frac{T_i}{T_{b_1}}\left(\frac{A_{b_1}}{A_i}\right)+C_1\left[\frac{\mu_{a_1}L_{a_1}}{D_{a_1}^2}\left(\frac{T_{a_1}}{T_{b_1}}\right)\left(\frac{A_{b_1}}{A_{a_1}}\right)\right.$$

$$\left.+\frac{\mu_{b_1}L_{b_1}}{D_{b_1}^2}\right]\Bigg\}$$

and

$$c=\left(\frac{P_o g}{R}\right)\left(\frac{1}{T_o}-\frac{1}{T_i}\right)H$$

3.3 METHOD OF SOLUTION.

As shown in Eq.(3.22), it is required to obtain the values of the parameter X_1 and X_2 for the prediction of the neutral pressure level(NPL).

From Eq.(3.22) the neutral pressure level also can be represented in the following functional form:

$$N=N(\ T,\ A,\ L,\ C,\ Kt\ ) \qquad (3.25)$$

where

T=temperature of air at the corresponding

flow sections.

A=size of the opening area at the flow sections(Aa1, Aa2, Ab1, Ab2, Ai).

L=flow length at the corresponding flow sections(La1, La2, Lb1, Lb2, Li).

C=coefficient of the friction factor(C1, C2).

Kt=minor loss factors at the flow paths (Kc, Ke, Kre).

All the calculations to obtain the numerical values and to evaluate the parameters in Eq.(3.27) were performed by using HP 9835A computer.

The flow diagram of the computer program for the computation can be found in Fig.3.3. Samples of the values of Cx calculated by Eq.(3.12) are given in Tab.3.1.

The value of Cx with smooth transition at the entrance was estimated from Ref[13].

It was noticed that the calculated value of the neutral pressure level for a given condition is very sensitive to the values Cx and the temperatures at the flow sections of the wall openings, which is to be used to evaluate the physical properties in Eqs.(3.19) to (3.24).

The analytical results of the neutral pressure level for the cases studied are presented in Figs.5.5 to 5.11 and 5.20 to 5.21, compared with the results of the experiment.

The effect of temperatures at the inlet and outlet of the flowpaths of each opening(Ta_1, Tb_1, Ta_2, Tb_2), and the coefficient, C, on the neutral pressure level are also presented in Figs.3.4 and 3.5.

The viscosity of the air in the corresponding flow sections of the wall openings was calculated from the following relation correlated by Sutherland [14].

$$\mu = \mu_o \left(\frac{T}{T_o}\right) \frac{T_o + S}{T + S} \qquad (3.26)$$

where

S= Sutherland Constant (110).

To= 273°K.

μ_o= 1.72×10^{-5} N.S/m.

Chapter IV

EXPERIMENTAL STUDIES

In the previous chapter, the theoretical analysis of the characteristics of the stack effect for the case having the openings at the top and bottom levels only was presented and the effects of the wall openings and temperature difference across the wall on the neutral pressure level were evaluated analytically.

The main objective of the present study is to obtain an accurate means to calculate the pressure differentials induced by the stack effect, especially in highrise buildings.

As a first stage of a continuing study, the case of a building with no internal partition and with openings at four levels was investigated experimentally for various ranges of temperature differences and for different vertical distributions of exterior wall openings.

The test apparatus and instruments which were used in the present investigation are described in the following sections.

4.1 EXPERIMENTAL APPARATUS

The assembly of the experimental apparatus used in the present investigation is shown schematically in Fig.4.1. and the essential dimensions of the major components are illustrated in Figs.4.2 to 4.5.

The main apparatus is basically made up of a test section, pressure and temperature measuring devices, and a data acquisition system.

The basic concept of the test section was to simulate a high rise building with no internal partitions as shown in Fig.4.2.

To maintain a constant temperature difference between the inside and the outside of the building as in the real situations in the building[2], a specially designed multi-heater system was utilized. This was achived by having a 18.3 metre long copper pipe with 50.8 mm I.D., divided into 20 heating sections.

Each heating section is 0.91 m. in length and the power input is controlled independently. This system made it possible to achieve the requirement of the nearly constant wall temperature desired for the present experiment.

One K-type thermocouple was spotwelded on the outer wall of the pipe at the center of each heating section.

To simulate the distributions of the openings in the exterior wall of the building, six openings were provided on the outer wall of the test section at 4 different elevations as represented in Fig.4.2. The detailed construction of the openings of the test section is also shown in Fig.4.2.

To measure the inside air temperature of the test section with height, five tubes of 20.0 mm long, 17 gage hypodermic stainless steel tubings were mounted through the outer wall of the test section at 5 different elevations for the insertion of thermocouples as shown in Figs.4.1 and 4.5.

Seven pressure taps, connected to 76.2 mm. long, 17 gage hypodermic stainless steel tubing, were provided along the wall of the test section at seven different elevations for the measurement of the pressure differences across the wall as shown in Figs.4.3 and 4.5.

For the fabrication of the heating sections described before, the outer wall of the copper tube of the test section was initially painted with three coats of a thermally resistant, electric insulation paint ("RID-ARC" silicone spray). Having the insulation paint dried completely, the outer wall of the copper tube of the test section was carefully wrapped with three layers of 50 mm. wide fibreglass tape.

The test section was then divided into twenty 0.91 m. long heating segments and a 17 gage nichrome wire (20% Cr,80% Ni, resistivity 1.3352 Ω/m) was wound around the outside of each heating sections in 40 mm. pitches.

Two additional layers of fibreglass tape were wrapped around the outside of each section for further electrical insulation. After fabricating all the heating sections properly, the outside wall of the test section was covered with a 40 mm thick thermal insulation made of glassfibre with a thermal conductivity of 0.048 W/m.C.

Each heating section was then connected to its own variable transformer with an individual arrangement for power measurement. An example of a heating section is shown in Fig.4.4.

The whole test section was then installed in one of the staircases of Colonel By Hall of the University of Ottawa, mainly due to the unusual height of the test section as shown in Fig.4.9.

4.2 INSTRUMENTATION

4.2.1 PRESSURE MEASUREMENT

In order to measure the pressure difference across the test section wall induced by the temperature difference between the inside and outside at different elevations, seven sets of pressure tranducers were used. The pressure tranducers used were MKS Baratron type 220B with a maximum pressure head of one torr with 0.15% error at full scale.

The pressure transducers were installed at seven different elevations of the test section as shown in Fig.4.2. The locations of the pressure measurements at different heights of the test section, where the the pressure transducers were installed, are denoted as positions #1, 4, 7, 10, 14, 17 and 20 in Fig.4.1.

One of the two pressure ports for each pressure transducer was connected to the pressure tap of the test section at its corresponding elevations by flexible tygon tubing. The other pressure port of each pressure transducer was connected to a 17 gage hypodermic stainless tube bent 90 , which was mounted on the outside wall of the test section at the same elevation as the pressure tap, to measure the pressure difference between the inside and the outside of the test section at the corresponding level by the flexible tygon tubing. Fig.4.6. illustrates an example of the connection of the pressure transducers to the test section.

The D.C. signals from each pressure transducer were linked to 6 channels of HP Scanner of the Data Acqusition System with a shielded electric wire.

4.2.2 TEMPERATURE MEASUREMENTS

There were thirty-eight K-type thermocouples in total used for the measurement of the temperatures of the test section wall, of the inside air, and of the outside air at different elevations of the test section.

Twenty-eight thermocouples, spot-welded on the outer surface of the copper tube of the test section at the designated elevations, were used to measure the wall temperature of the test secton at positions #1 to #20 as shown in Fig.4.1.

Five thermocouples, sheathed in 15.2 cm. long stainless steel tube with a diameter of 0.82 mm., were used to measure the inside temperatures of the test section at positions #20 to #25 as shown in Fig.4.1.

Five additional thermocouples were installed on the outside wall of the test section insulation at the same elevations as the thermocouples measuring the inside air to measure the outside temperature of air of the test section at positions #26 to #30 as shown in Fig.4.1.

All thermocouples were connected to the terminal panel of the control stand which was linked to rotary switches. The positive side of each thermocouple was connected so as to pass through the ice-point junction via the rotary switches. The detailed circuit of the thermocouple connection is shown in Fig.4.7. By turning the rotary switches in sequence according to the experimental procedure predetermined, the D.C. signal from each thermocouple was processed by the Data Acquisition System through the HP Scanner.

4.3 CALIBRATION OF INSTRUMENTS

4.3.1 THERMOCOUPLES

The K-type thermocouples used in the present study were calibrated indirectly using a thermocouple which is made from the same spool of wire. This thermocouple is calibrated against a Fisher Nr15-155 precision thermometer in a temperature controlled oil bath. The result of the calibration is shown in Fig.4.10.

4.3.2 DIFFERENTIAL PRESSURE TRANSDUCERS

Before the initial pressure measurement, every pressure transducer was zero-adjusted in accordance with the

manufacturer's manual until it was set within the specified range. Having done the zero-adjustment of each pressure transducer, the calibration to obtain a correlation between the pressure measurement in units of D.C. output voltage(V) and units of pressure(Pa) was carried out. The results were compared against the calibration record sheet provided by the manufacturer and it was found that they were usually in good agreement with the record sheet from the manufacturer.

The procedures taken were as follows:

1) One of the two pressure ports of each pressure tranducer was connected to the pressure measuring side and the other port was connected to the reference pressure side of the device.

2) The D.C output connector of each pressure transducer was then linked to the HP Digital Voltmeter.

3) The measuring port of the transducer was then pressurized by means of a hydrostatic head.

4) The D.C. output signal from the transducers, measured by the HP Digital Voltmeter, was compared against the D.C output in the calibration record supplied by the manufacturer at the corresponding range of pressure difference.

5) Steps 2) to 4) were repeated for various ranges of pressure differences.

A typical example of the calibration of the pressure transducer expressed in terms of pressure drops(Pa) and D.C. output (V) is shown in Fig.4.11.

4.4 DATA ACQUISITION

4.4.1 DATA ACQUSITION SYSTEM

The data acquisition system used consists of a Hewlett Packard(HP) desk top computer and four other HP peripheral instruments.

Fig.4.8. shows a complete set-up of the data acquisition system. The following are brief descriptions of the data acquisition instruments.

(1) HP 9835A Desk Top Computer.

The desk top computer has a 115 K bytes memory, complete I/O capacity, a built-in tape cartridge drive for data storage on tape(217 K byte/tape), and an interactive key board with a cathode ray tube(CRT) display. The computer was employed throughout the present study in the acquisition of experimental data, data processing, data storage, and data reduction.

(2) HP 3455A Digital Voltmeter

The voltmeter has a capacity of up to 24 readings per second with 1μV sensitivity, true RMS, and automatic calibration capability. The voltmeter was utilized for all pressure and temperature measurements. All the measurements were in the form of D.C. signals from either the pressure transducers or the thermocouples.

(3) HP 3495A Scanner.

The 20 channels of reference assembly were used for the objectives of scanning either the pressures or temperatures. The instruments linked all the external instruments to the data acquisition system.

(4) HP 7245A Printer/Plotter.

This has the capability of being a printer as well as a plotter. All the experimental data obtained and processed by the computer were printed out by this printer/plotter. In addition to this process, the printer/plotter was extensively utilized during the data reduction.

(5) HP 98035 Real Time Clock.

The real time clock connected to the computer was used as a real time reference as well as a trigger mechanism. Besides being used to trigger the digital voltmeter at certain time interval for the acquisition of

data, this was also employed to set the system on idle for stabilization of the pressure transducers.

4.4.2 DATA ACQUSITION PROCEDURES

The data acquisition procedure for the present experiment was designed as follows:

(Step 1) In this stage, all the variables and arrays are initialized and all the instruments are addressed.

(Step 2) This stage includes the branching routines for all errors encountered in the instrument malfunctions or storage medium overflow.

(Step 3) A file name for the data storage of the current experiment undergoing is fed into the computer.

(Step 4) Temperatures of the inside, the wall, and the outside of the test section at each level are scanned from positions #1 to #38 shown in Fig.4.1 through the HP Scanner by turning the 2 channel rotary switch knob in sequence. The preliminary measurements of temperatures are repeated until the inside air and the wall temperatures of the test section stabilized uniformly along all the elevations of the test section.

(Step 5) After the predetermined optimum temperature uniformity is achieved, the temperatures of positions #1 to #38 shown in Fig.4.1. are measured through the HP Scanner by turning the 2 channel rotary switches in sequence manually.

(Step 6) In this step, the computer starts to measure the pressure differences across the wall of the test section at 7 different elevations for a given constant temperature difference and a particular distribution of the wall openings. These measurements are taken in sequence from pressure tap #1 to pressure tap #7 as shown in Fig.4.1. Each measurement is the average of 50 readings for a time period of 20 seconds. All of these measurements are automatically performed by the system using channels #2 to #7 of the HP Scanner.

(Step 7) In this step, the voltage and current provided to each heating section of the test section are read with an amperemeter and a handheld type digital multimeter by manually turning the rotary switches on the power control panel in sequence from heating sections #1 to #20 shown as in Fig.4.1. The data acquired from this step are fed into the computer manually.

(Step 8) After all the data are acquired, it is processed and stored in the tape cartridge. In addition, a hard copy printout of the processed data is provided the from printer.

(Step 9) As a final step, the system either starts a new test or stops and ends at the request of the operator. The flow chart of the data acqusition program can be found in Fig.4.12.

4.5 EXPERIMENTAL PROCEDURES

The present experiments were conducted in the following two stages: First, the system was idled for a given period of time to obtain the constant wall temperatures of the test section with height, meeting the predetermined ranges. Second, the temperatures, the pressure differentials across the test section wall and power input to each heating section were measured at the designated positions for various opening conditions under a given temperature difference. Prior to obtaining the data of the experiment undergoing, the following tasks were carried out:

1) the performance of the electrical insulation of all wiring of each heating section of the test section were examined carefully.

2) the zero adjustment was made on all pressure transducers.

3) the performance of all the connections of thermocouples, pressure transducers, and of the power supply to the heating sections were checked with a hand-held type multimeter.

4) The power switches of the system were then turned on and the voltages of the variable transformer of each heating section were adjusted to the predetermined scale.

4.5.1 Simulation of the Stack Effect

For the simulation of the stack effect in a high rise building, the constant wall temperature along all elevations the test section was produced.

This was obtained with the careful adjustment and control of the power supply for each heating section of the test section through continuous measurements of the currents and the voltages provided.

For the achievement of temperature stabilization and uniformity along all elevations of the test section within the range of ±3.0 °C, the previous procedures were conducted and idled for more than 10 hours.

After attaining the desired constant wall temperature of the test section, the measurements of the temperature were executed from positions #1 to #38 as shown in Fig.4.1.

Then a series of the tests, changing the vertical distribution of the wall opening of the test section, were conducted under a given temperature difference across the wall.

The test parameters used in the present experiment are as follows:

1) Five different temperature differences across the exterior wall of the test section were set for the cases with the same size of opening at the top and bottom elevations only: these temperature differences were 25°C, 30 °C, 40°C, 50°C, and 60°C.

2) Three different temperature differences across the exterior wall of the test section were set for the cases with the other wall opening conditions of 1).

4.5.2 MEASUREMENTS OF PRESSURE DIFFERENTIALS

At the moment of obtaining the designated condition of the temperature difference across the exterior wall of the test section along all the elevations, the pressure differentials were simultaneously measured from pressure tap #1 to pressure tap #7 for the predetermined wall opening conditions.

Maintaining the same temperature difference across the test section wall, 12 different kinds of the wall opening conditions, illustrated in Figs.5.2 to 5.4, were used for the measurements of the pressure differentials along the various elevations of the test section. Three sets

of data were obtained for each of the above test conditions. All the data are stored on the magnetic tape and plotted with the Printer/Plotter. Total time required for one complete measurement was in the order of 50 to 60 seconds.

Chapter V

RESULTS AND DISCUSSIONS

5.1 VALIDITY OF THE STACK EFFECT EQUATION

As noted in the theoretical analysis in Chapter III, the stack effect equation, Eq.(1.1), would accurately predict the vertical distribution of the pressure differentials across the exterior wall of the buildings induced by the temperature difference, provided that the coefficient, K_1, and the value of the neutral pressure level(NPL), N, are accurately known.

The stack effect equation, Eq.(1.1), is derived from the equation of state of a perfect gas and has been shown to be very correct in the actual situation, as long as the neutral pressure level is known[2].

In order to obtain the experimental value of the coefficient, K_1, in Eq.(1.1), the experimental results obtained under various ranges of temperature differences for a given distribution of wall openings are plotted as in Fig.5.1.

The values of the coefficient, K_1, in Eq.(1.1) which resulted from the experiments and the theoretical analysis are plotted against the temperature differences across the exterior wall in Fig.5.1.

As shown in the figure, the experiments have been carried out for six different ranges of temperature differences and six different modes of vertical distribution of wall openings. The values of the coefficient, K_1, obtained from the present experiment are found to be fairly constant and approximately equal to 3.53×10^3 Pa.K/m.

The theoretical value of the coefficient, K_1, assuming that the atmospheric pressure is 1 atm. at ground level, may be obtained as

$$K_1 = \frac{M g P_o}{R} = 3.44 \times 10^3 \text{ Pa K/m.}$$

where

g=9.81 m/s (the accelation due to gravity)

P =101.3×10^3 Pa.(1 atm)

M=28.8 g(the equivalent moleqular of air)

R=8.314 J/K(the universal gas constant)

The resultant, as shown in Fig.5.1., shows that the agreement between the value of K_1 obtained from the experiment, and the theoretical estimation is excellent and the coefficient, K_1, is not affected by the distribution of the wall opening conditions as well as by the temperature differences.

This result represents an indication that the air behaves like a perfect gas and therefore the assumption employed in the derivation of Eq.(1.1) is well justified.

This also confirms the findings reported by Lee et al.[2] with regard to Eq.(1.1), which showed that the coefficient, K_1, is constant and is neither affected by the temperature differences across the exterior wall of the building, nor by the wall opening distribution.

Therefore, this may lead to the conclusion that the equation of the stack effect, Eq.(1.1), can provide a means for the correct prediction of the pressure differentials caused by the stack effect, provided that the value of the neutral pressure level is correctly known.

5.2 EFFECT OF THE VERTICAL DISTRIBUTION OF THE EXTERIOR WALL OPENINGS

For the accurate prediction of the pressure differentials induced by the stack effect, the location of the neutral pressure level should be known correctly, as shown in the preceeding sections.

A series of experiments was carried out to investigate the effect of the vertical distribution of wall openings along the elevations of building on the location of the neutral pressure level and also on the vertical distribution of the pressure differentials. The experiments were conducted with variations of vertical distribution of the wall openings under a given temperature difference as shown in Figs.5.2. through 5.4.

The figures show the vertical distribution of the pressure differentials along the elevations of the building for various opening conditions under a constant temperature difference, where the pressure differentials of twelve different opening conditions are plotted versus the elevations. The ranges of the temperature differences across the exterior wall used in the experiments were 25°C, 40°C, and 60°C.

As represented in Figs.5.2. to 5.4., the results of the present experiment positively manifest that the location of the neutral pressure level is affected significantly by the distribution of the wall openings. The experimental results also show that each different mode of opening condition has a different value for the neutral pressure level.

The results obtained also illustrate that the slope of the pressure gradient along the elevations is constant for a given temperature difference across the wall regardless of the vertical distribution of the wall openings.

The case having two openings at the top and bottom elevations only, shown as Test #4 in the figures, the neutral pressure level is located at about 38% of the total height over all ranges of temperature differences.

But in Test #5 represented in Figs.5.2 to 5.4., which is the case with a single opening at the top and bottom levels only, the neutral pressure level occured at about 42% of the total height, thus having moved up to 4%.

The case having one opening at the top level and two openings at the bottom level, shown as Test #3 in the

figures, the neutral pressure level occured at about 22% of the total height.

In test #10, in which there are two openings at the top and one opening at the bottom level, and therefore opposite to the case in Test #3, the neutral pressure level is located at about 22% of the height in all temperature difference ranges.

Test #1 and #12 shown in Figs.5.2. to 5.4. represent the extreme cases which have the wall opening at the top or at the bottom level only, respectively. In Test #1, which is the case with the wall opening at the bottom only, the neutral pressure level is located at the level of the opening as shown in the figures.

Test #12, in which the wall opening is at the top elevation only, showed the opposite result of Test #1. The neutral pressure level in this case occured at the level of the top opening exists. The same results were obtained in the cases having a single opening at the top or at the bottom elevation only.

In Test #8, which has a uniform distribution of the wall openings with the elevations, the neutral pressure level occured at approximately 50% of the total height. The

result of Test #8 showed a similarity with the outcome of Tamura and Wilson[9], which used a mathematical model of a ten storey building with a uniform vertical distribution of openings.

In Test #9, which is another case of multi-opening along the elevations, having one opening at the bottom, one opening at the elevation of H1, and two openings at the top elevation, the neutral pressure level is located at a higher elevation than that of Test #8.

The results obtained from Test #1 and #12 coincide exactly with the predictions discussed in the theoretical analysis of the chapter III. These results also indicate that the test procedures followed in the experiments were adequate and reliable.

The experimental results obtained, as represented in the figures, revealed distinctly that the vertical profile of the pressure differentials and the location of the neutral pressure level were affected strongly by the arrangement of the vertical opening distribution.

As noted from the functional relationship of the neutral pressure level, Eq.(3.25), the dependence of the neutral pressure level on the distribution of opening conditions can clearly be expected. In the preceeding

chapter, the analysis for the case with the opening at the top and bottom only showed that the value of the neutral pressure level has close relationships with the area, A, with the size of the openings, and with the length of flow paths, L. The results of the theoretical analysis, which considered the effect of the flow resistance and the distribution of the wall opening conditions, were in excellent agreement with the experimental results shown in Figs.5.5. to 5.11., as it was predicted.

5.3 EFFECT OF THE TEMPERATURE DIFFERENCES ACROSS THE EXTERIOR WALLS

The equation of the stack effect, Eq.(1.1), shows that the pressure differentials induced by the stack effect are proportional to difference of the reciprocal of the outside and inside absolute temperatures for a given value of the neutral pressure level.

To investigate the effect of the temperaure differences across the exterior wall on the stack effect, a series of the experiments shown in Figs.5.12. to 5.19 were carried out. The figures represent the results of the experiment showing the effect of the temperature differences across the wall on the neutral pressure level for a given condition of the wall openings, where the pressure differentials are plotted against the elevation(Z).

The experimental results shown in the figures reveal that the stack effect is proportional to the difference of the reciprocal of the inside and outside absolute temperature, but the neutral pressure level is hardly affected by by the temperature differences for a given distribution of the wall opening condition.

Fig.5.12 shows the results of the experiment for the case in which a single opening is placed at the top and bottom elevations only under the temperature differences from 25°C to 60 °C. The result shows that the neutral pressure level has a constant value and is fixed at about 42% of the total height.

The result of the case having two openings at the top and bottom levels only, shown in Fig.5.13, presents the same trend shown in Fig.5.12. In this case, the neutral pressure level occured at approximately 38% of the total height over various ranges of the temperature differences.

All the other results of the experiments for the cases shown in Fig.5.14 to 5.17 illustrate the same trend observed in the cases shown in Figs.5.12 to 5.13 evidently.

The equation for the calculation of the neutral pressure level, Eq.(1.2), recommended by ASHRAE, shows the

effect of the temperature of inside and outside of the building on the value of the neutral pressure level. But, both in the results of the present experiment and in the analytical studies, it has been shown evidently that the location of the neutral pressure level is little affected by the temperature differences for a given distribution of the wall opening condition. This result may give evidence that the temperature difference across the wall would not be a decisive factor for the accurate prediction of the neutral pressure level under a given wall opening condition. The outcome of the present experiments also showed a reasonably good agreement with the results observed in the field studies by Tamura and Wilson[7,8], which is shown in Fig.2.1.

The comparisons of the experimental results with the present theoretical analysis and that of Eq.(1.2), recommended by ASHRAE, are shown in Figs.5.5 to 5.11.

5.4 COMPARISON OF THE PRESENT ANALYSIS AND ASHRAE RECOMMENDATION WITH THE EXPERIMENTAL RESULTS

As was discussed in the preceeding chapters, it is very important to know the accurate value of the neutral pressure level for the correct prediction of the pressure differences induced by the stack effect. The correct information of the pressure differentials caused by the

stack effect is also significantly valuable for the accurate estimation of the air infiltration rate by the stack effect.

The neutral pressure level, as shown in the previous sections, is significantly affected by the vertical distribution of the wall openings, and the flow resistance of the wall openings, but is hardly affected by the temperature difference for a given condition of the wall opening arrangement.

The values of the neutral pressure level resulting from Eq.(1.2), which is recommended by ASHRAE[4], and our theoretical analysis are compared with the experimental results in Figs.5.5 to 5.11.

The values of the neutral pressure level obtained from Eq.(1.2) recommended by ASHRAE, as can be seen in the figures, showed a considerable discrepancy with the results of the experiment. However, the results obtained from our theoretical analysis presented excellent agreement with the experimental results.

The discrepancy between the results from ASHRAE's recommendation and the results from the experiments are illustrated clearly in Figs.5.8 to 5.11, where $\left[\frac{NPL}{NPL_{(exp)}} - 1\right]$ % is plotted versus the temperature differences across the exterior wall(ΔT°C). While the results from Eq.(1.2),

recommended by ASHRAE, showed up to a maximum 25% of deviation from the experimental results, the present analysis presented less than +6.0% in all the cases studied.

In the analysis, the following assumption was made: $C1 \approx Ca1 \approx Cb1 \approx 150$ and $C2 \approx Ca2 \approx Cb2 \approx 280$. This is because the flow in short length of channels as in the case of the present study(Fig.4.2) does not have smooth transition at the entrance. The values of 150 and 280 were obtained from the sensitive analysis.

The significant disagreement of the results from ASHRAE recommendation with the experimental results may be explained from the fact that the recommendation of ASHRAE, Eq.(1.2), is derived from the Bernoulli's principle, thus neglecting the effect of the real flow resistances along the flow paths in the wall openings. ASHRAE's recommendation, Eq.(1.2), considers the effect of the temperature difference across the wall on the neutral pressure level. However, the temperature difference, as shown on our experiments and theretical analysis, is a factor that is not decisive for the prediction of the neutral pressure level.

Therefore, it may lead to the conclusion from the present study that the method for the prediction of the neutral pressure level recommended by ASHRAE, Eq.(1.2), has overly simplified the actual flow conditions and is therefore not appropriate for the accurare prediction of the

neutral pressure level in actual situations. This result may also give a conclusion that the flow resistance along the flow paths should be taken into the consideration for the accurate prediction of the neutral pressure level and is not a negligible factor affecting the neutral pressure level, but the temperature difference across the wall is not a major factor affecting the neutral pressure level.

5.5 EFFECT OF PHYSICAL DIMENSION OF BUILDING

As discussed in the previous sections 5.2 to 5.4, it has been shown that the equation for the calculation of the neutral pressure level, Eq.(3.23), which is derived from the present analysis, presents an excellent agreement with the experimental results.

This, in turn, would lead to a conclusion that the equation, Eq.(3.23), considering the actual flow resistance along the flow paths, could be applied in the accurate prediction of the neutral pressure level for the cases in which the openings are at the top and bottom elevations only.

An analysis was made, using the result of the present theoretical method, to study the effect of the physical dimensions of the building on the location of the neutral pressure level for the cases in which the wall openings are at the top and bottom elevations only.

In the analysis of the effect of physical dimensions on the neutral pressure level, the length of the test section(18.3 m) and inside diameter of the test section were used as the value of Lo and Do, repectively. Fig.5.20 illustrates the effect of the vertical height ratio of the building (L/Lo) on the location of the neutral pressure level, where the ratio of the vertical height (L/Lo) is plotted against the ratio of the neutral pressure level to the height of the building (N/Z) for a given opening condition and temperature difference across the wall.

The result of the analysis shown in Fig.5.20 shows that the effect of the vertical dimension of the building on the location of the neutral pressure level in the cases having openings only at the top and bottom levels may not be significant where the ratio of L/Lo is greater than 0.5.

Fig.5.21 also illustrates the effect of the lateral dimension of the building on the location of the neutral pressure level, where the ratio of the lateral dimension (D/Do) is plotted against the ratio of the neutral pressure level to the height of the building (N/Z) for a given opening condition and temperature difference across the wall.

The analytical result shown in Fig.5.21 indicates that the effect of the lateral dimension of the building on

the location of the neutral pressure level in the cases having openings only at the top and bottom levels may not be significant where D/Do is greater than 0.4.

Chapter VI

CONCLUSIONS

In the present study, the characteristics of the pressure differentials induced by the temperature difference across the building envelope (which is generally termed as "stack effect") was investigated both analytically and experimentally.

In the present study, the stress was placed on the prediction of the correct value of the neutral pressure level (NPL) as it has been previously shown that the stack effect equation, derived from the equation of the state of perfect gas, can correctly calculate the pressure difference due to the stack effect, provided that the correct value of the neutral pressure level is given.

The results of the present analysis based on the energy equation applied to a hypothetical high-rise building with no internal partitions have shown to agree well with those obtained from the present experimental program.

The model of the building which was utilized in the experiment was made of copper tube having 50.8 mm I.D, 18.3

m in length and consisted of 20 individually heated test-sections to simulate the constant temperature difference across the exterior wall of building in all the elevations.

The following conclusions were drawn from the present study:

1) It has been confirmed that the stack effect equation derived from the equation of the state of perfect gas can correctly predict the pressure difference across the exterior wall of a high-rise building induced by the temperature difference as long as the value of the neutral pressure level (NPL) is correct.

2) The pressure differentials induced by the stack effect is shown to be linearly proportional to the difference of the reciprocal of the absolute temperature of the inside and outside of building.

3) The recommendation of ASHRAE for the calculation of the value of the neutral pressure level is shown to be extremly inadequate and the value of the neutral pressure level is strongly affected by the charateristics of the exterior wall openings (numbers and vertical distribution).

4) The effect of the flow resistance in the flow passages on the value of the neutral pressure level is considerable and its effect should be taken into consideration for the accurate prediction of the stack effect.

5) The effect of the temperature differences across the exterior wall of building on the value of the neutral pressure level is shown to be negligibly small.

6) The effect of the physical sizes of buildings on the value of the neutral pressure level has been shown to be insignificant when the dimensionless parameter D/Do and L/Lo are greater than 0.4 and 0.5, respectively.

REFERENCES

1. Tamura,G.T and C.Y. Shaw.,"Studies of Exterior Wall Tightness and Air-Infiltration of Tall Building",ASHRAE Transsactions, Vol.82,P.122-134,1976.

2. Lee,Y.,H.Tanaka and C.Y.Shaw,"Distribution of Wind and Temperature Induced Pressure Differences across the Walls of a Twenty Storey Compartmentalized Building ",Journal of Wind Engineering and Industrial Aerodynamics,Vol.10,P.287-301,1982.

3. Shaw,C.Y."Air Tightness and Air Infiltration of School Buildings" ASHRAE Transactions,Vol.85,P.85-95,1979.

4. American Society of Heating, Refrigerating and Air-Conditioning Engineers Inc,."ASHRAE HANDBOOK 1977 FUNDMENTALS",ASHRAE,Chap.21 1978.

5. Shaw,C.Y and G.T.Tamura,"The Calculation of Air Infiltration Rate by Wind and Stack Action for Tall Building",ASHRAE Transactions, Vol.83,P.145-158,1977.

6. Shaw,C.Y."Method for Conducting Small Scale Pressurization Test and Air Leakage Data of Multistory Apartment Buildings",Prepared submission to ASHRAE Semiannual Meeting,LA,California,Feb.1980.

7. Tamura,G.T and A.G.Wilson, "Pressure Differences for a Nine Story Building as a Result of Chimney Effect and Ventilation System Operation",ASHRAE Transactions,Vol.72,Part.I,P.180,1966.

8. Tamura,G.T and A.G.Wilson,"Pressure Differences Caused by Chimney Effect in Three High Buildings",ASHRAE Transactions,Vol.73,Part.II 1967.

9. Tamura,G.T and A.G.Wilson,"Building Pressures Caused by Chimney Action and Mechanical Ventilation",ASHRAE Transactions,Vol.73, Part.II,P.II.2.1,1967.

10. Barret,R.E and D.W.Locklin,"Computer Analysis of Stack Effect in High -rise Buildings",ASHRAE Transactions,Vol.74,Part.II, P.155-169,1968.

11. Shaw,C.Y., D.M.Sander and G.T.Tamura ,"Air Leakage Measurement Exterior Walls of Tall Buildings",ASHRAE Transactions,Vol.79, P.40-48,1973.

12. Goel,Kailash.C,"Fffect of Free Stream Turbulence on Fluid Flow and Heat Transfer",MaSc.Thesis,Dept of Mech Eng., Univ of Ottawa,April,1972.

13. Streeter,V.L.and E.B.Wylie,"Fluid Mechanics",McGraw Hill Book Company,New York,1979.

14. Fox,W and Alan.T.McDonald,"Introduction to Fluid Mechanics", 2nd.Ed,John Wiley & Sons,N.Y.1978.

15. Building Research Estabishment Digest,"Principle of Natural Ventilation ",BRED Digest,No.210,London,HMSO.,1978.

16. Chatswood,G.,"Natural Ventilation of Building",NSB, No.43, Dept of Works,Commonwealth Building Station,Australia,1957.

17. Cockroft,J.P and P.Robertson,"Ventilation of an Enclososure through a Single Opening",Building and Environment,Vol.II, P.29-35,1976.

18. Etheridge,D.W.,"Crack Flow Equation and Scale Effect", Building and Environment,Vol.12,P.181-189,1977.

19. Kays,W.M.,"Loss Coefficients for Abrupt Changes in Flow Cross Section with Low Reynolds Number Flow in Single and Multiple Tube System",ASME Transactions,Vol.72,P.1067-1074 ,1950.

20. Nylund,Per.O.,"Infiltration and Ventilation",Swedish Council for Buildibg Research,D22,Stockholm,Sweden,1980.

21. Schrichting,H.,"Boundary Layer Theory",McGraw Hill Book Company N.Y.,1968.

22. Smith,G.L.,"Air Leakage Due To Stack Effect in Multi-Story Buildings", Air Conditioning, Heating and Ventilating, July P.73-75,1958.

23. Tamura,G.T.,"Computer Analysis of Smoke Movement in Tall Buildings",ASHRAE Transactions,Vol.75,P.81-92,1969.

24. Tamura,G.T and C.Y.Shaw,"Air Leakage Data for the Design of Elevator and Stair Shaft Pressurization System",ASHRAE Transactions,Vol.82,P.179-190,1976.

25. Tamura,G.T.,"The Calculation of House Infiltration Rates", ASHRAE Transactions,Vol.85,P.58-71,1979.

26. Wilson,A.G.,"Influence of The House on Chimney Draft", ASHRAE Journal ,Vol.2,No.12,Dec.P.63,1960.

26. Wilson,A.G. and G.T.Tamura,"Stack Effect in Buildings", Canadian Building Digest,CBD 104,Aug,P.4,National Research Council of Canada,Ottawa,1968.

27. Wilson,A.G. and G.T.Tamura,"Stack Effect and Building Design", Canadian Building Digest,CBD 107,National Research Council of Canada,Ottawa,1968.

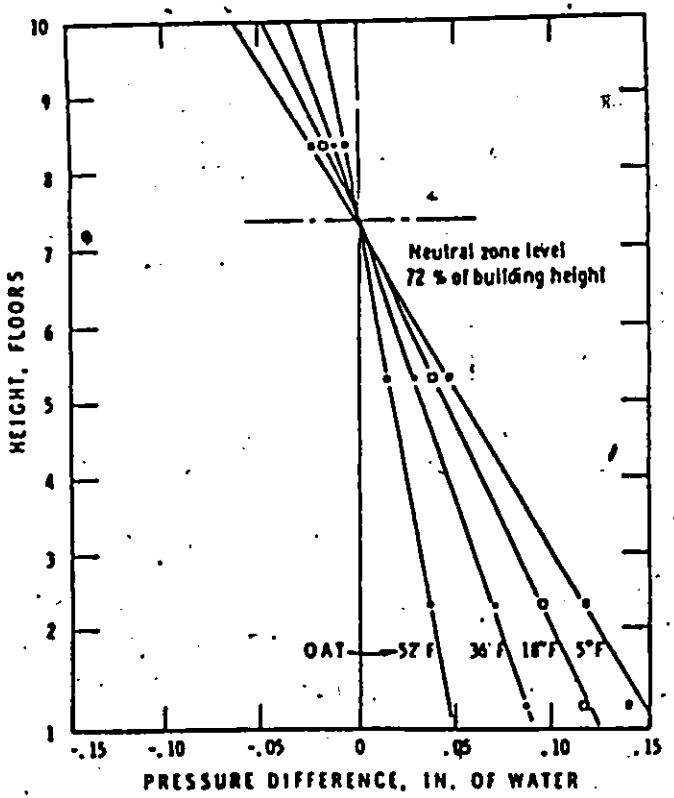

(a) Exterior Wall Pressure difference caused by stack effect

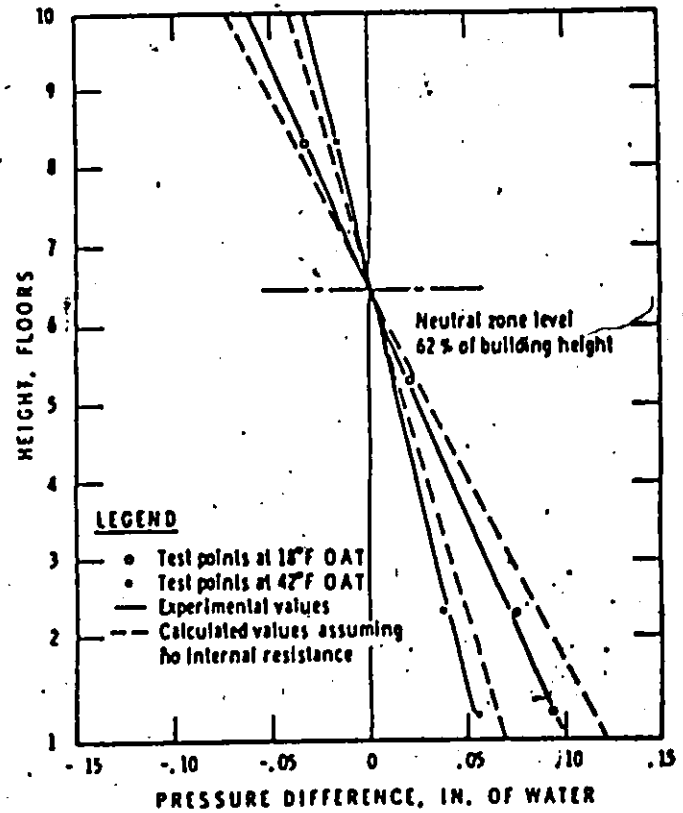

(b) Exterior Wall Pressure difference caused by stack effect with vertical air shaft sealed.

Fig.2.1 The Result of A Field Measurement of A Nine Story Building for Stack Effect by Tamura and Wilson [7]

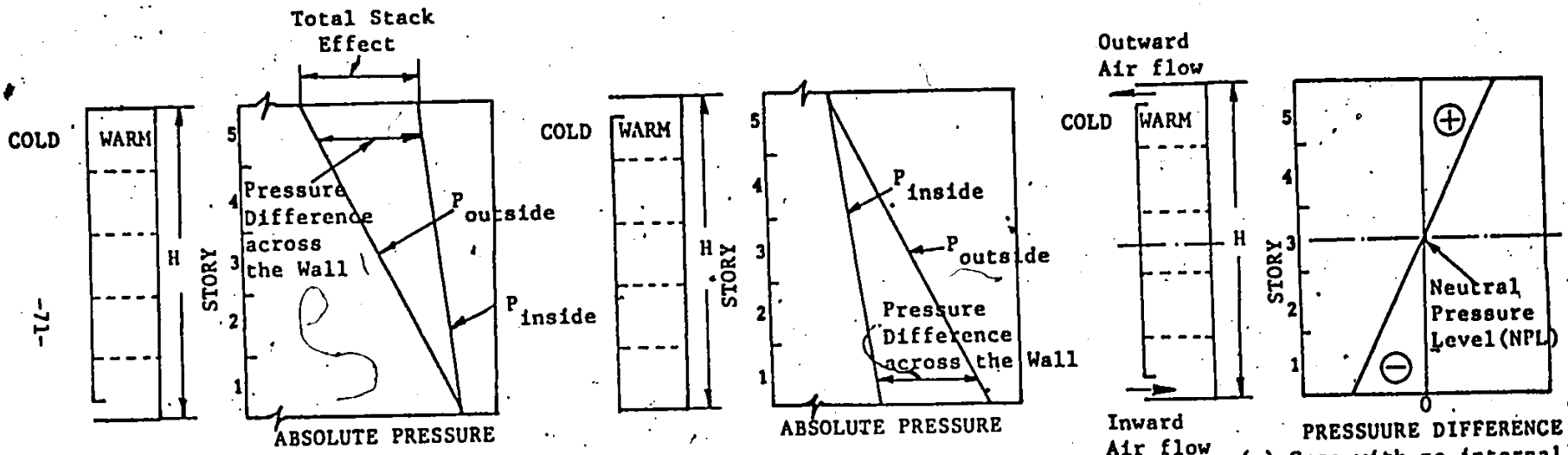

(a) Case with no internal partition, single opening at bottom level.

(b) Case with no internal partition, single opening at top level.

(c) Case with no internal partition, and equal at top and bottom level.

Fig.3.1 The Stack Effect in a Idealized Building.

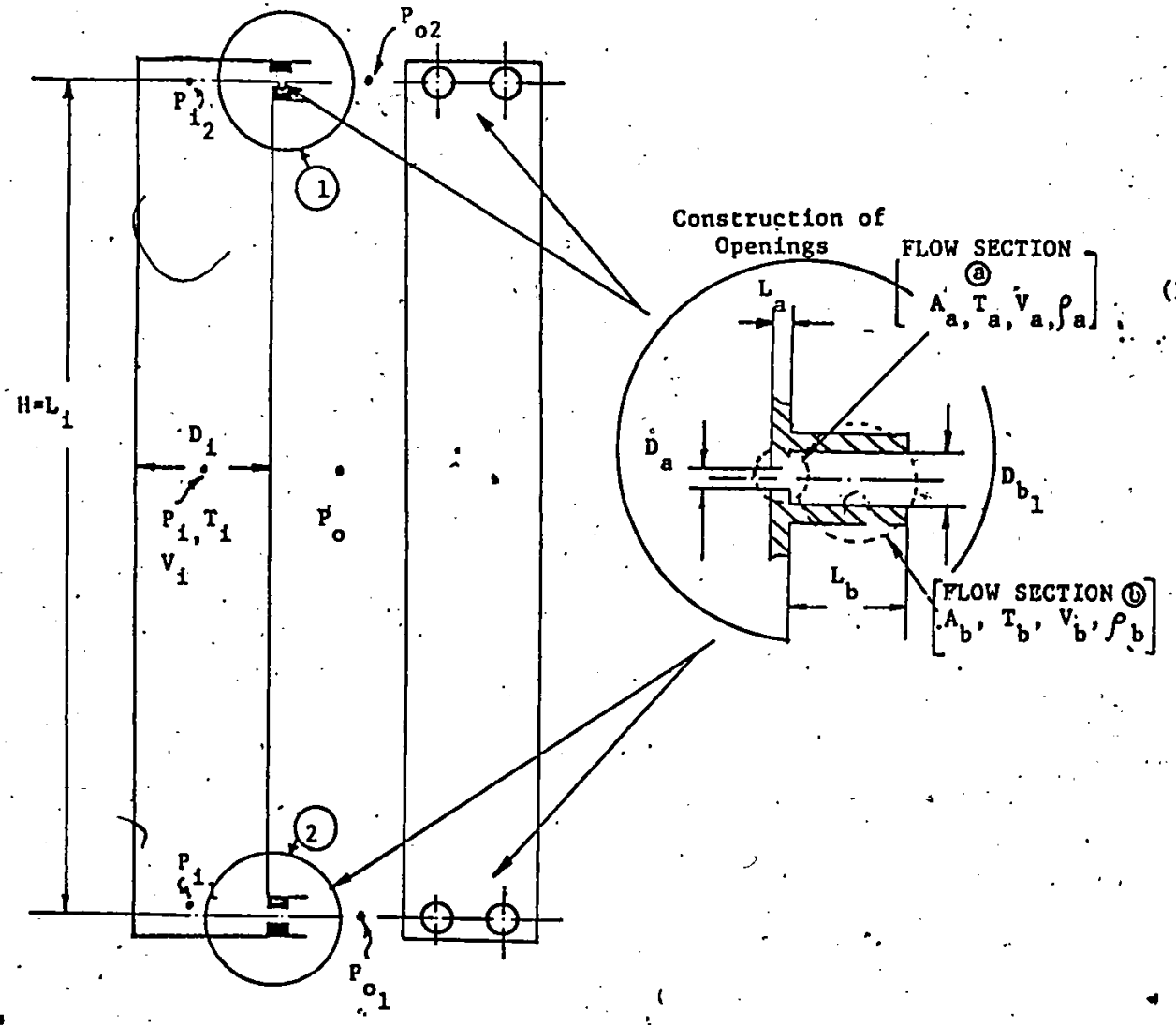

VARIABLES

(1) TEMPERATURES

T_i, T_o

T_{a_1}, T_{b_1}

T_{a_2}, T_{b_2}

(2) AREA OF OPENINGS

A_{a_1}, A_{b_1} (D_{a_1}, D_{b_1})--OPENING AREA AT BOTTOM LEVEL

A_{a_2}, A_{b_2} (D_{a_2}, D_{b_2})--OPENING AREA AT TOP LEV

(3) FLOW LENGTH

L_{a_1}, L_{b_1}

L_{a_2}, L_{b_2}

L_i

Fig.3.2 A Simplified Model of Building with No Internal Partitions and Openings at Top and Bottom Level only for Stack Effect Analysis.

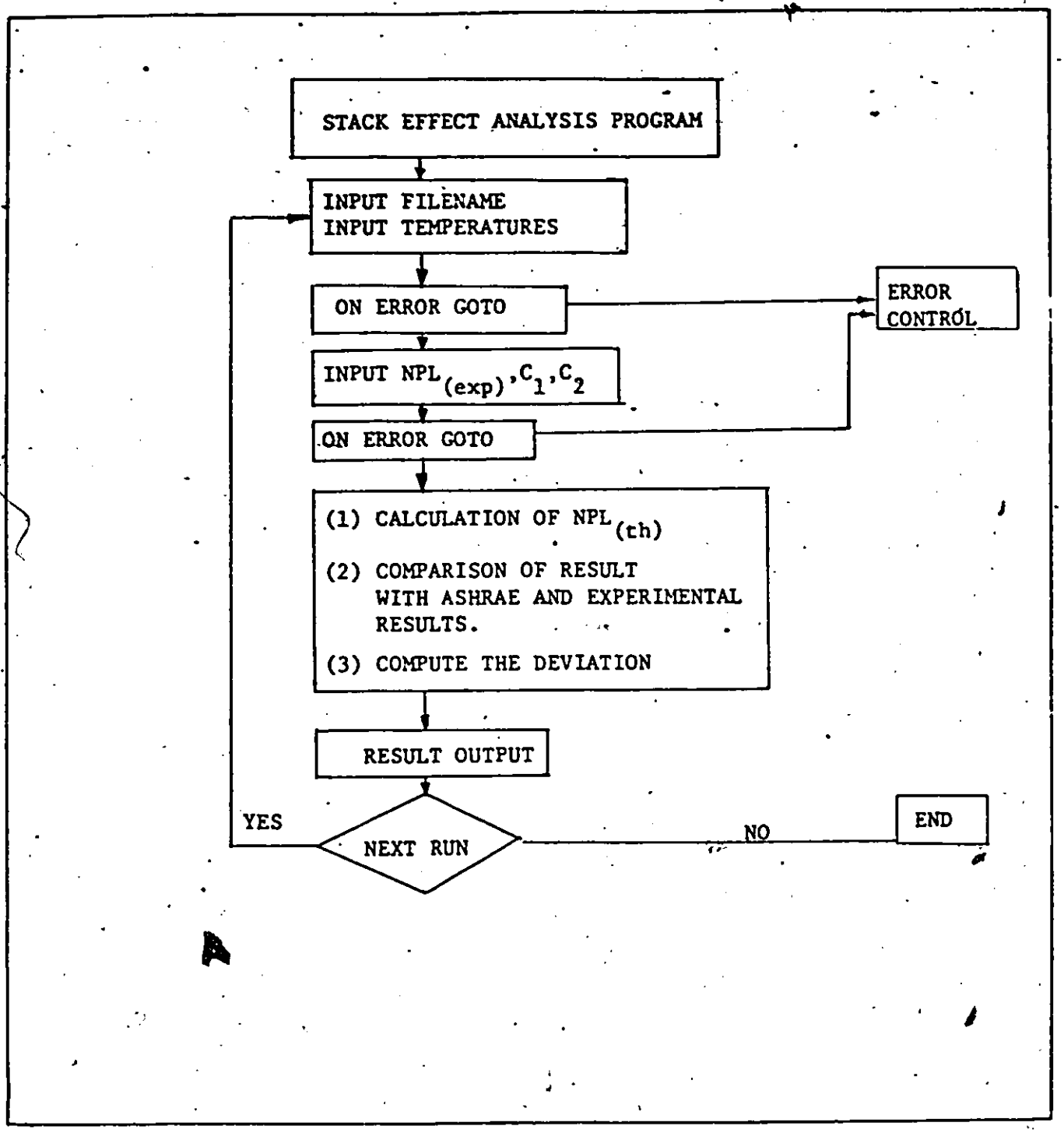

Fig.3.3 Flow Chart of Stack Effect Analysis Program

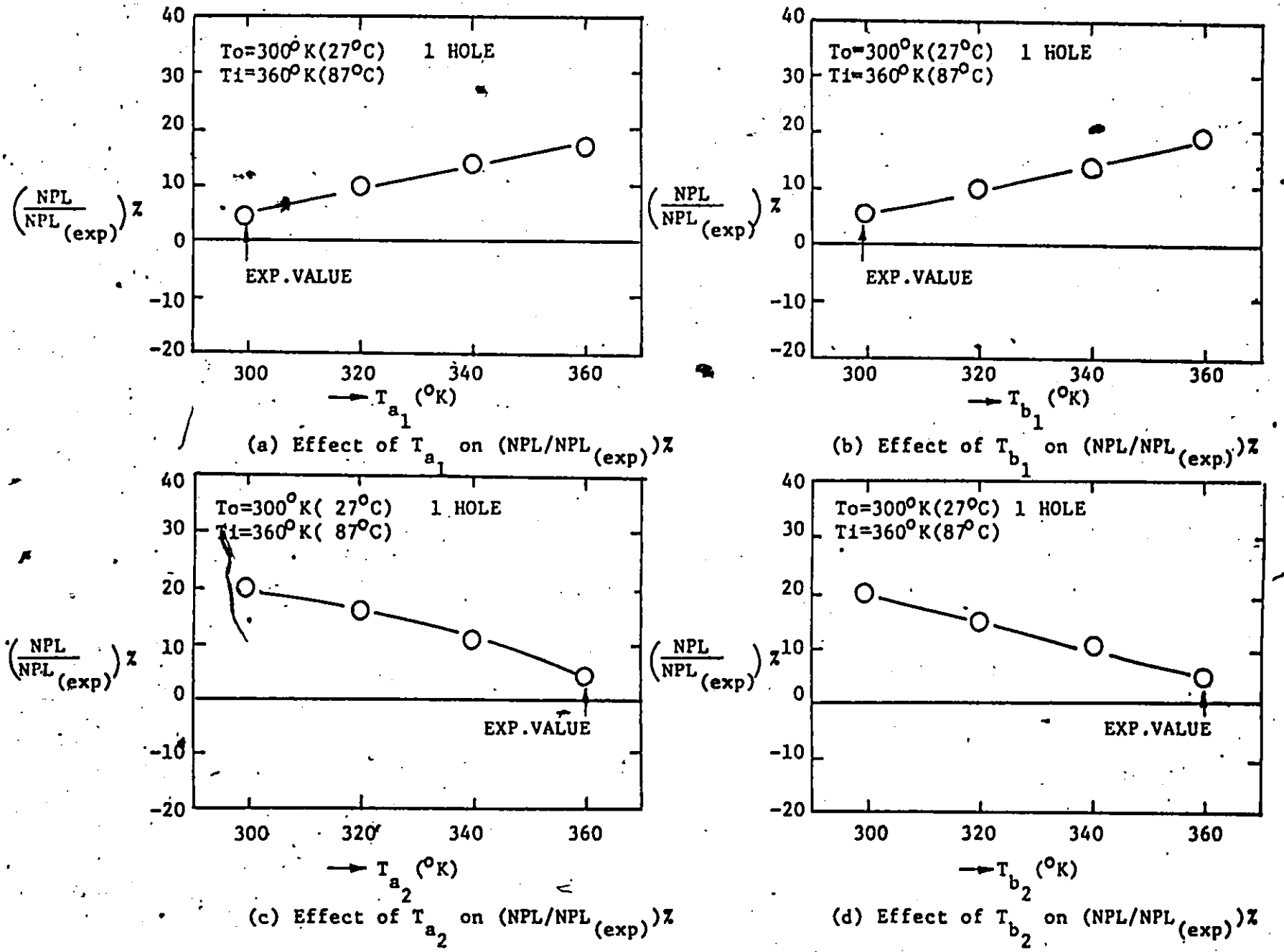

Fig.3.4 Effect of Temperatures at Flow Section of Openings on the Calculation of the Neutral Pressure Level(NPL).

$$C_1 = \frac{\int_0^L C_x dx}{\int_0^L dx} \qquad C_2 = \frac{\int_0^L C_x dx}{\int_0^L dx}$$

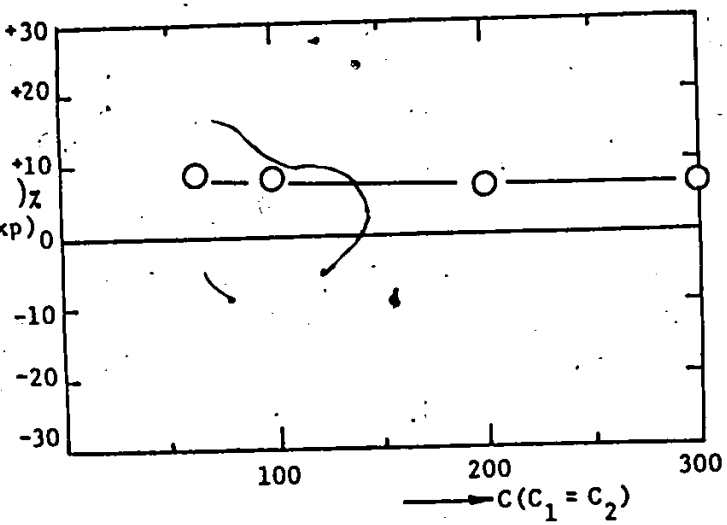

Effect of C on $(NPL/NPL_{(exp)})\%$ for the case $(C=C_1=C_2)$.

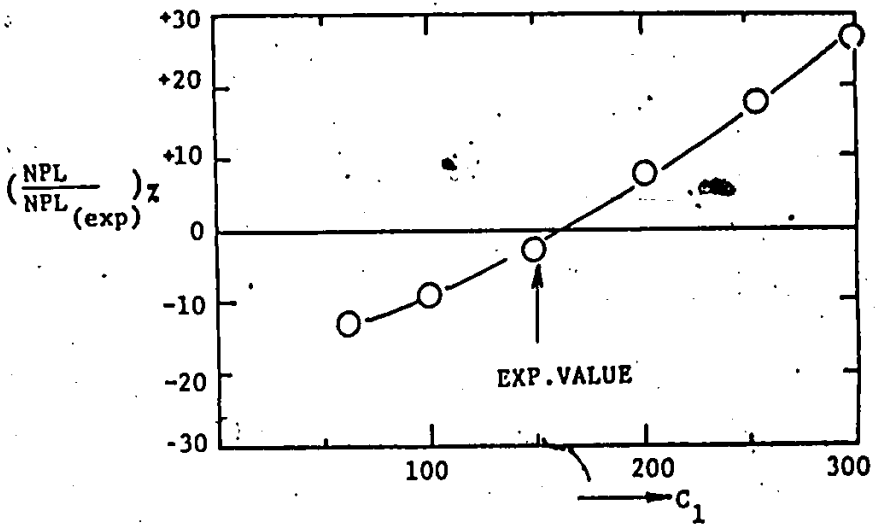

Effect of C_1 on $(NPL/NPL_{(exp)})\%$

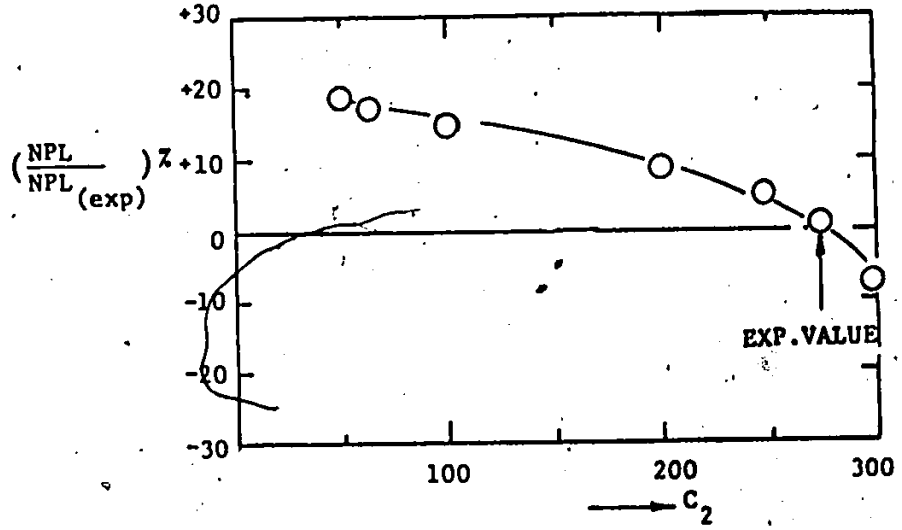

Effect of C_2 on $(NPL/NPL_{(exp)})\%$

Fig.3.5 Effect of C_1, C_2 on the Calculation of NPL under a given Condition(1 Opening at Top and Bottom Level and $\Delta T=60^{\circ}C$).

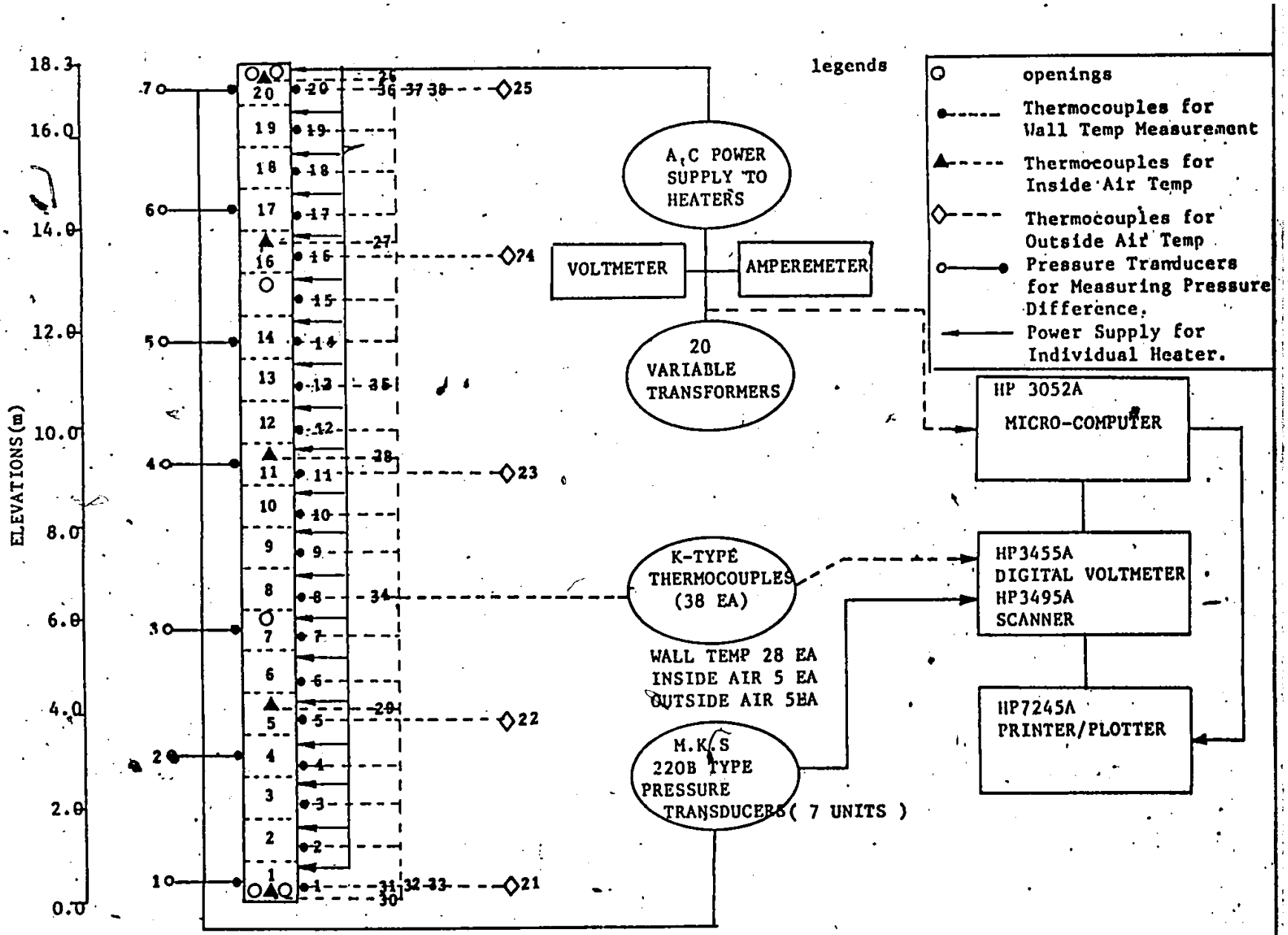

Fig.4.1 Schematic Diagram of Set-up of Experimental Apparatus

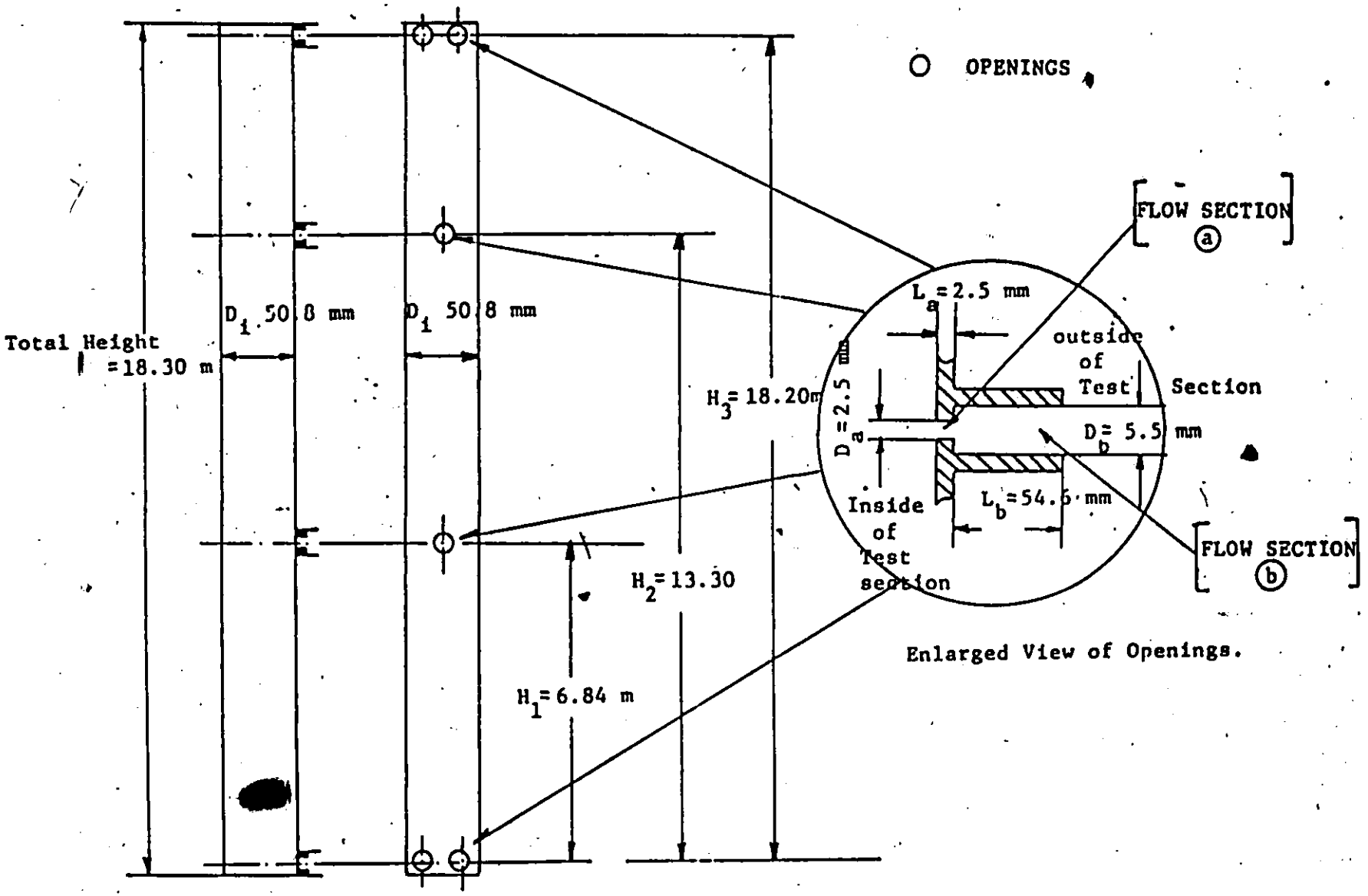

Fig.4.2 Locations and Construction of the Vertical Openings in the Test Section.

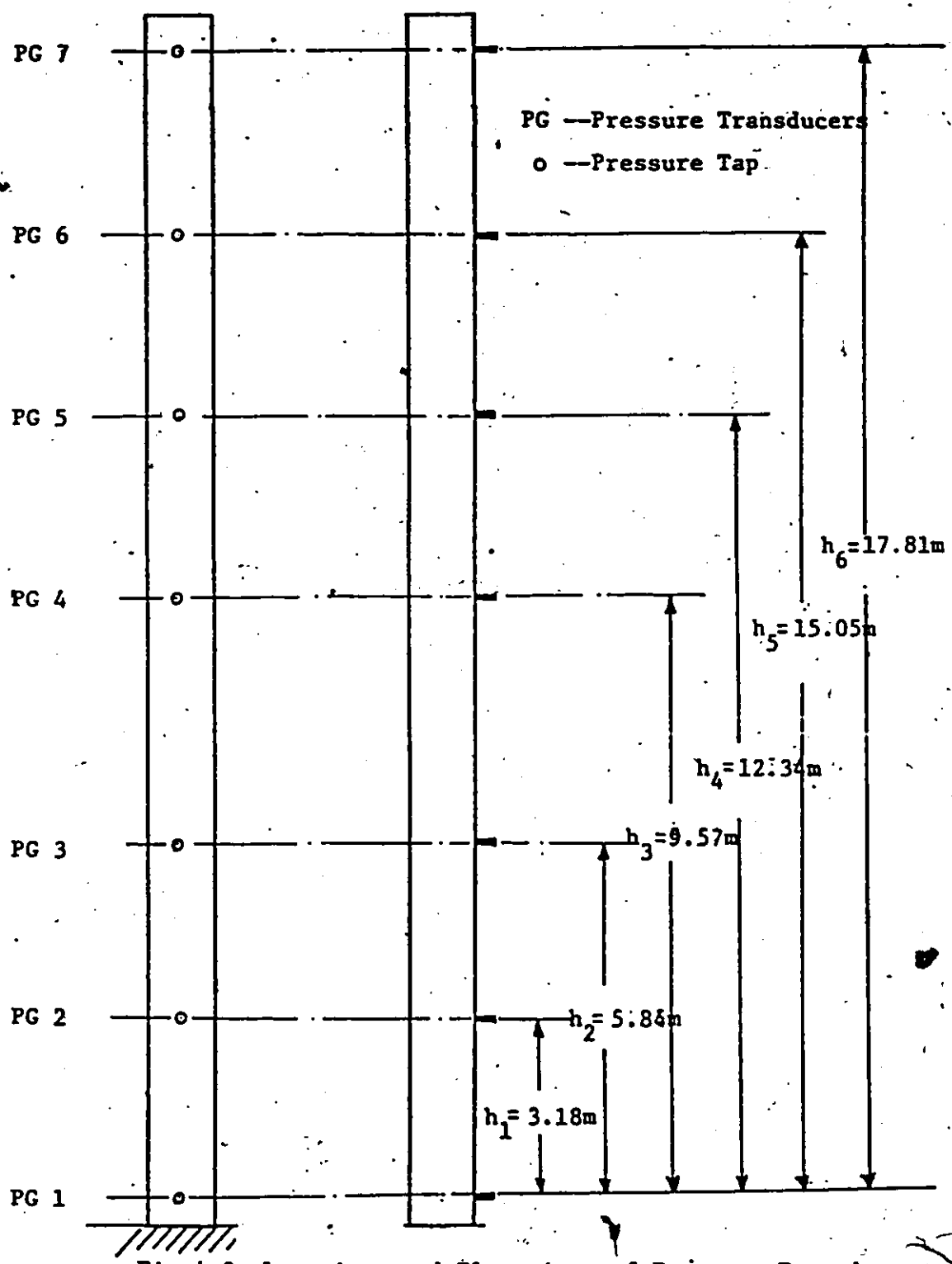

Fig.4.3 Locations and Elevations of Pressure Transducers Measuring Pressure Differentials along elevations of the Test Section.

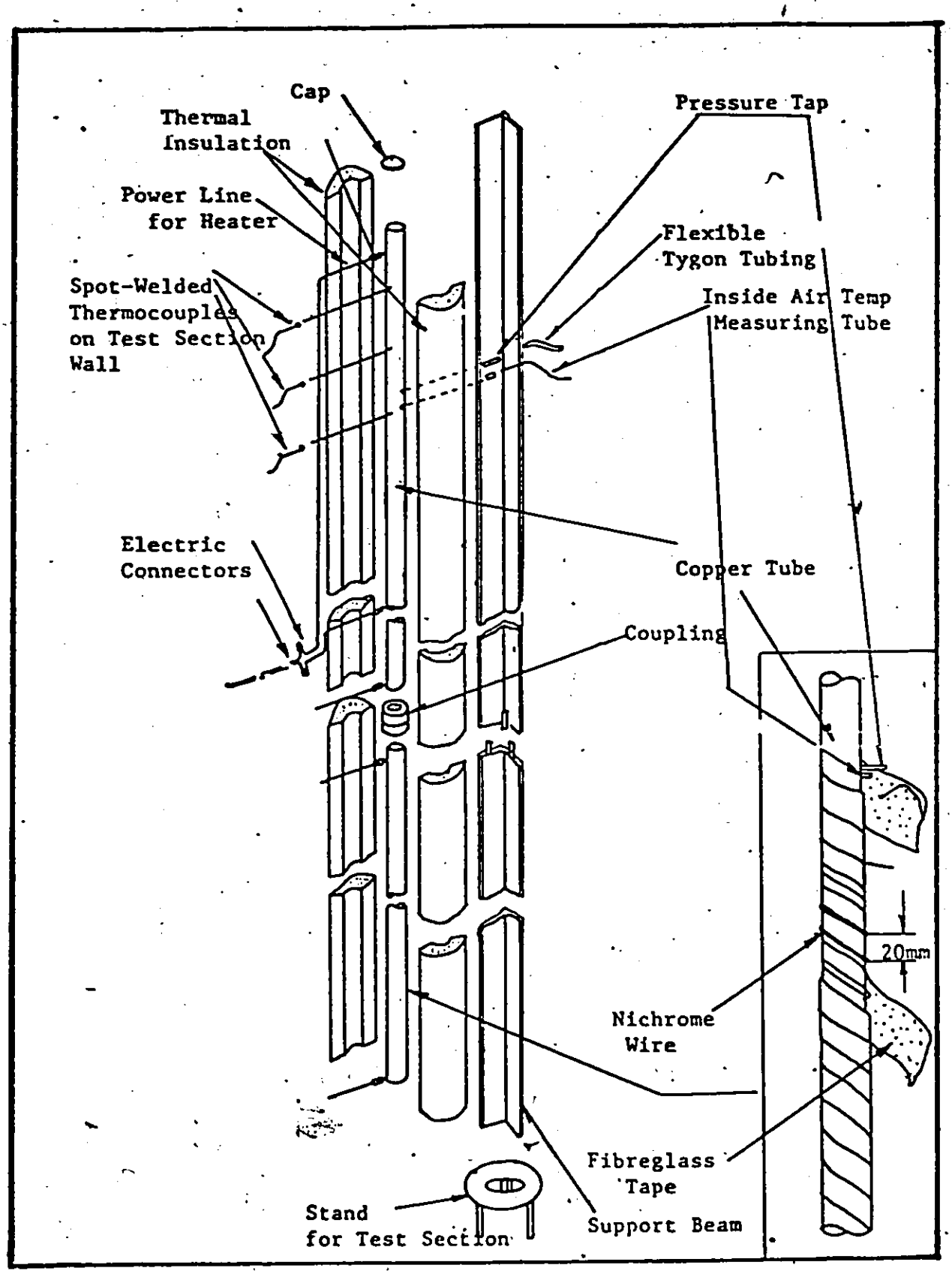

Fig.4.4 Assembly Drawing of Test Section

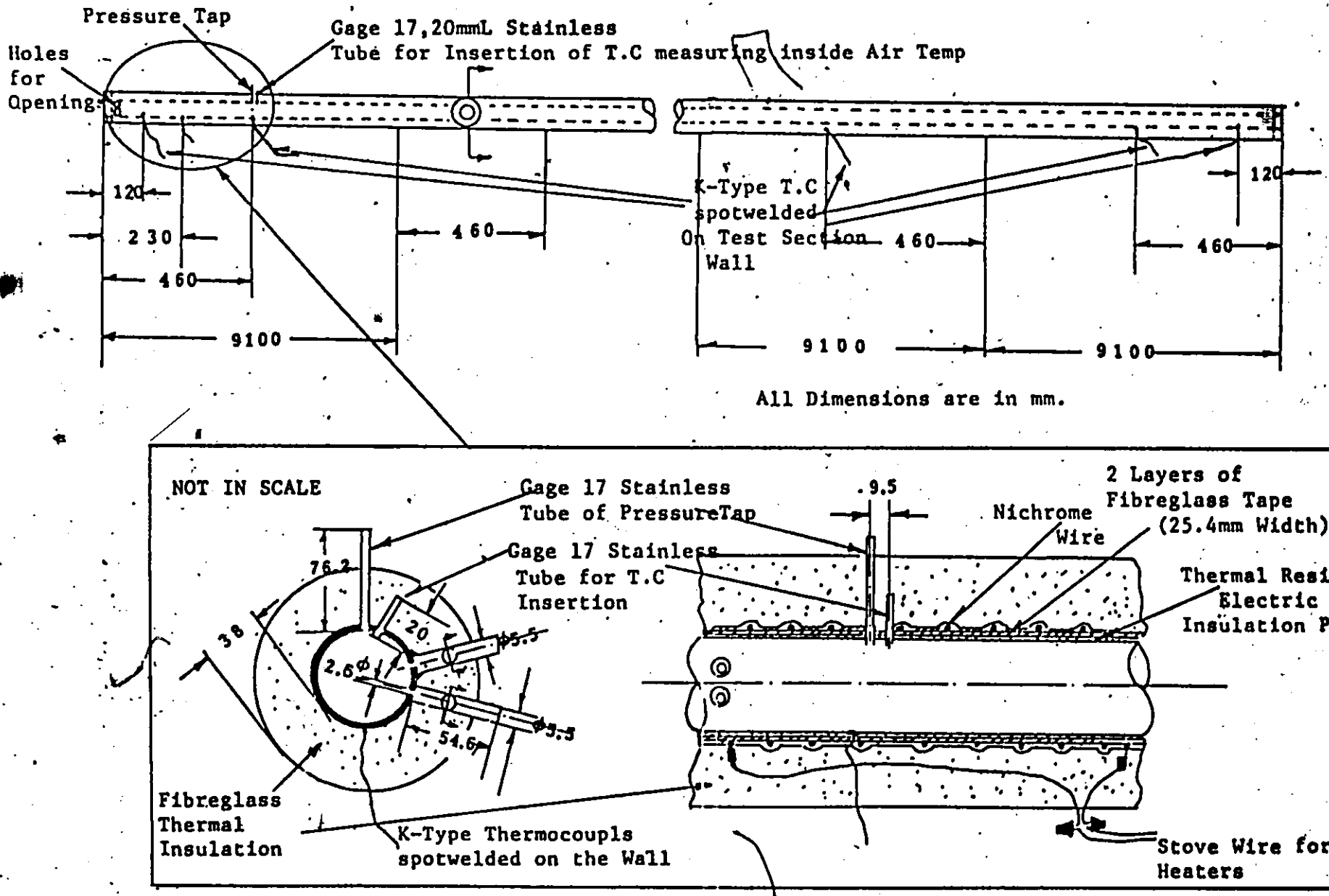

Fig.4.5 Sectional View of Consruction of Test Section and Heating Sections.

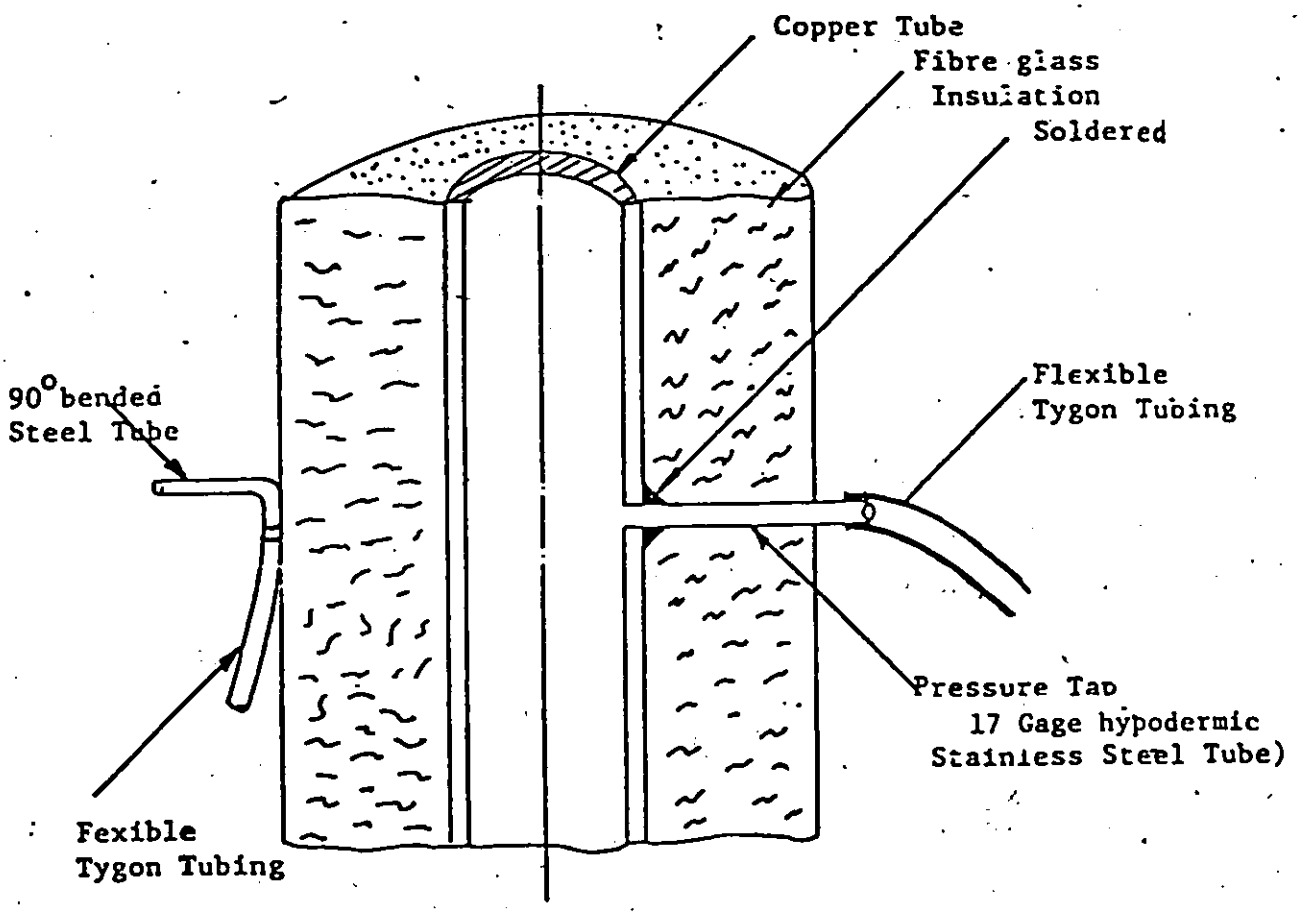

Fig.4.6. Illustration of Connection of Pressure Tap for Pressure Measurement.

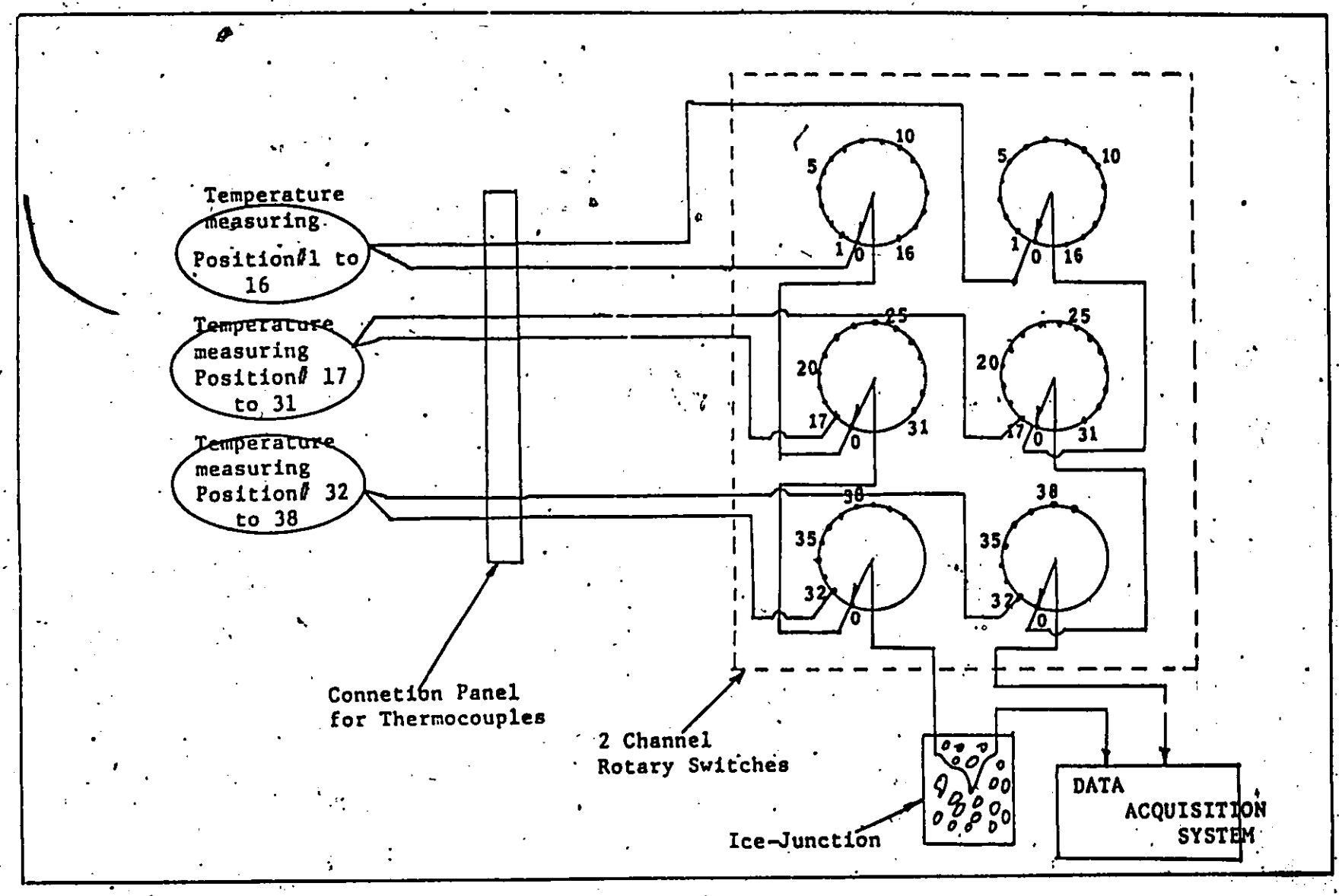

Fig.4.7 Circuit Diagram of Thermocouples

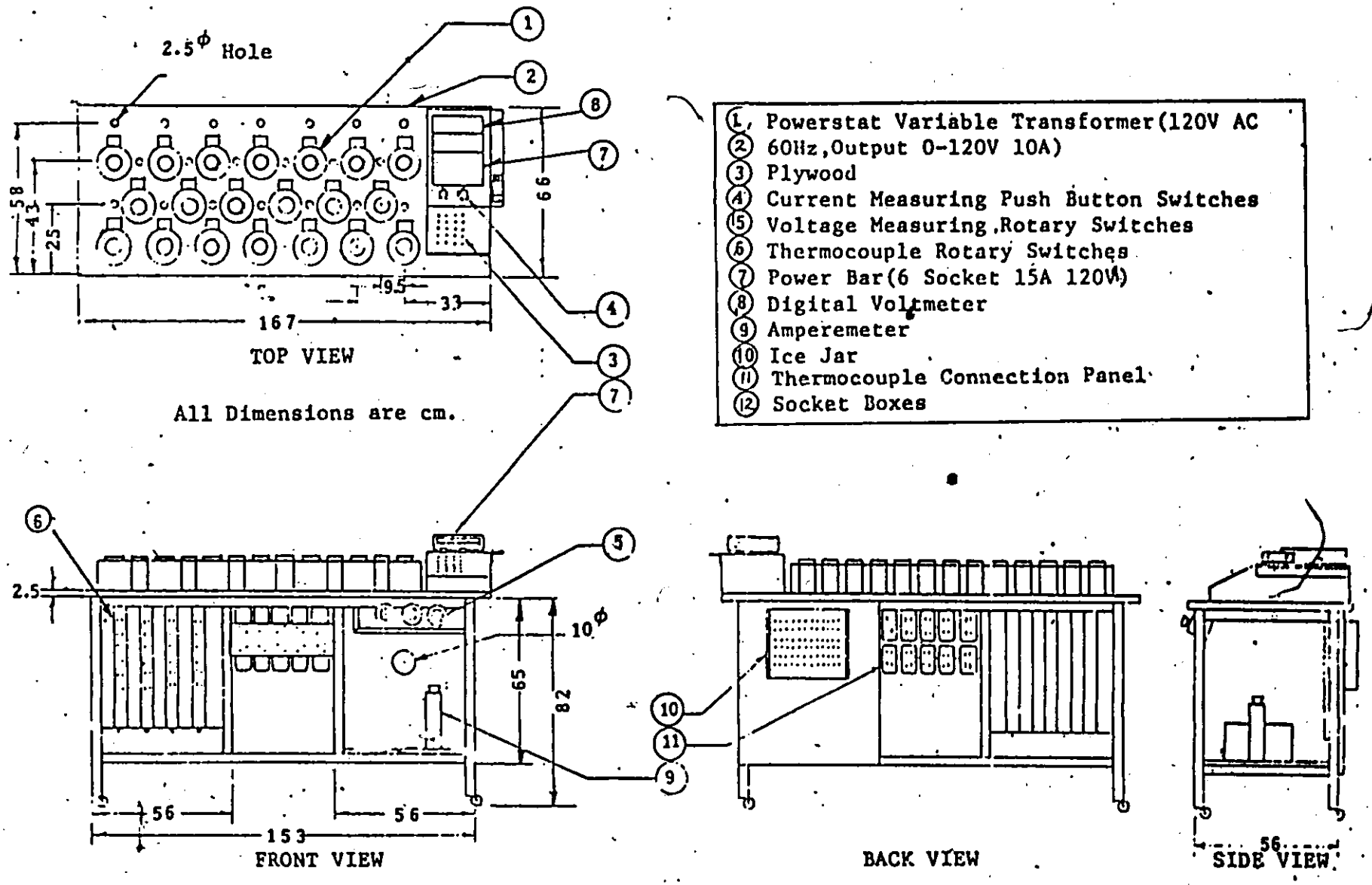

Fig.4.8 Plane View of Power Control and Measurement System in Experimental Apparatus.

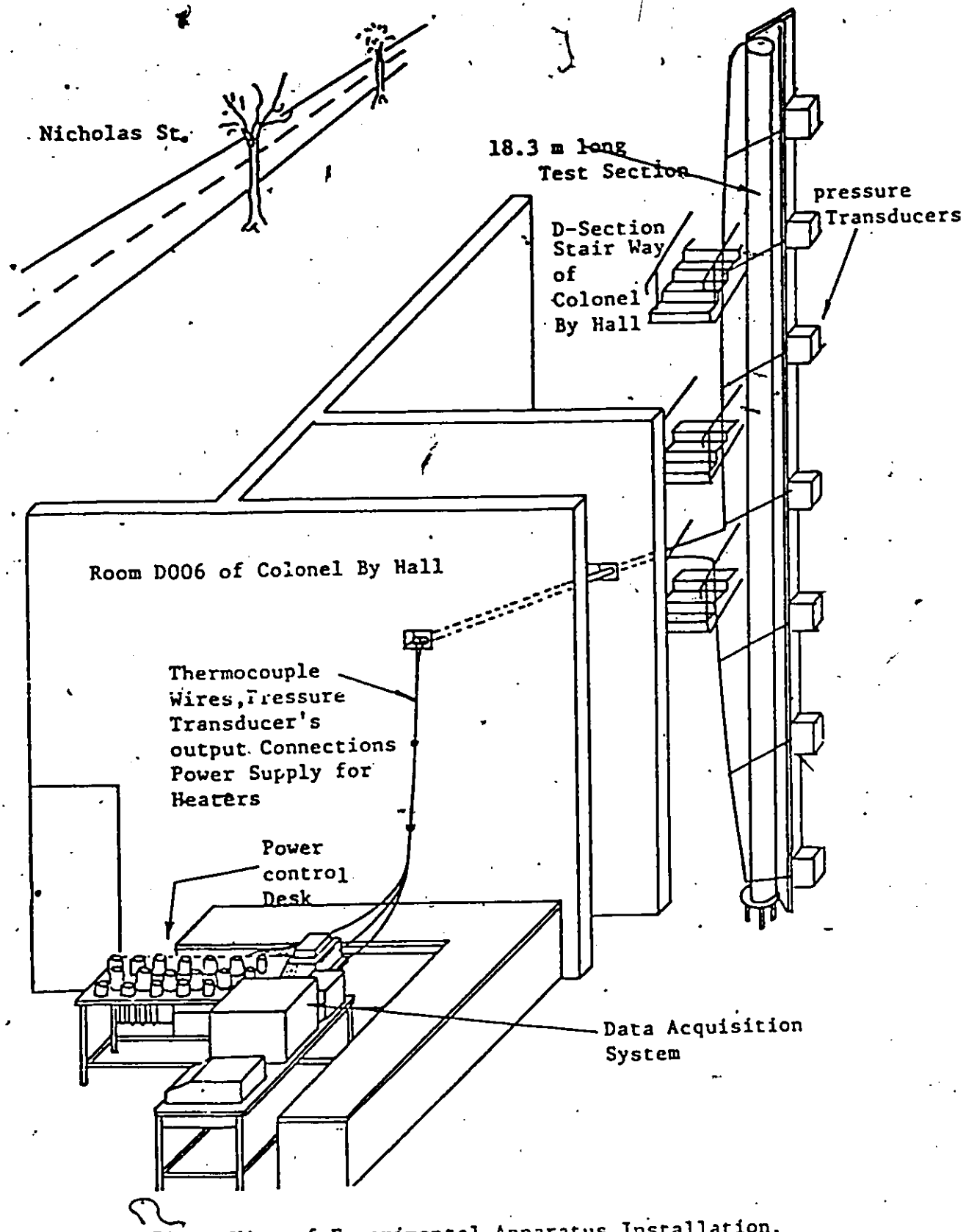

Fig.4.9 Plane View of Experimental Apparatus Installation.

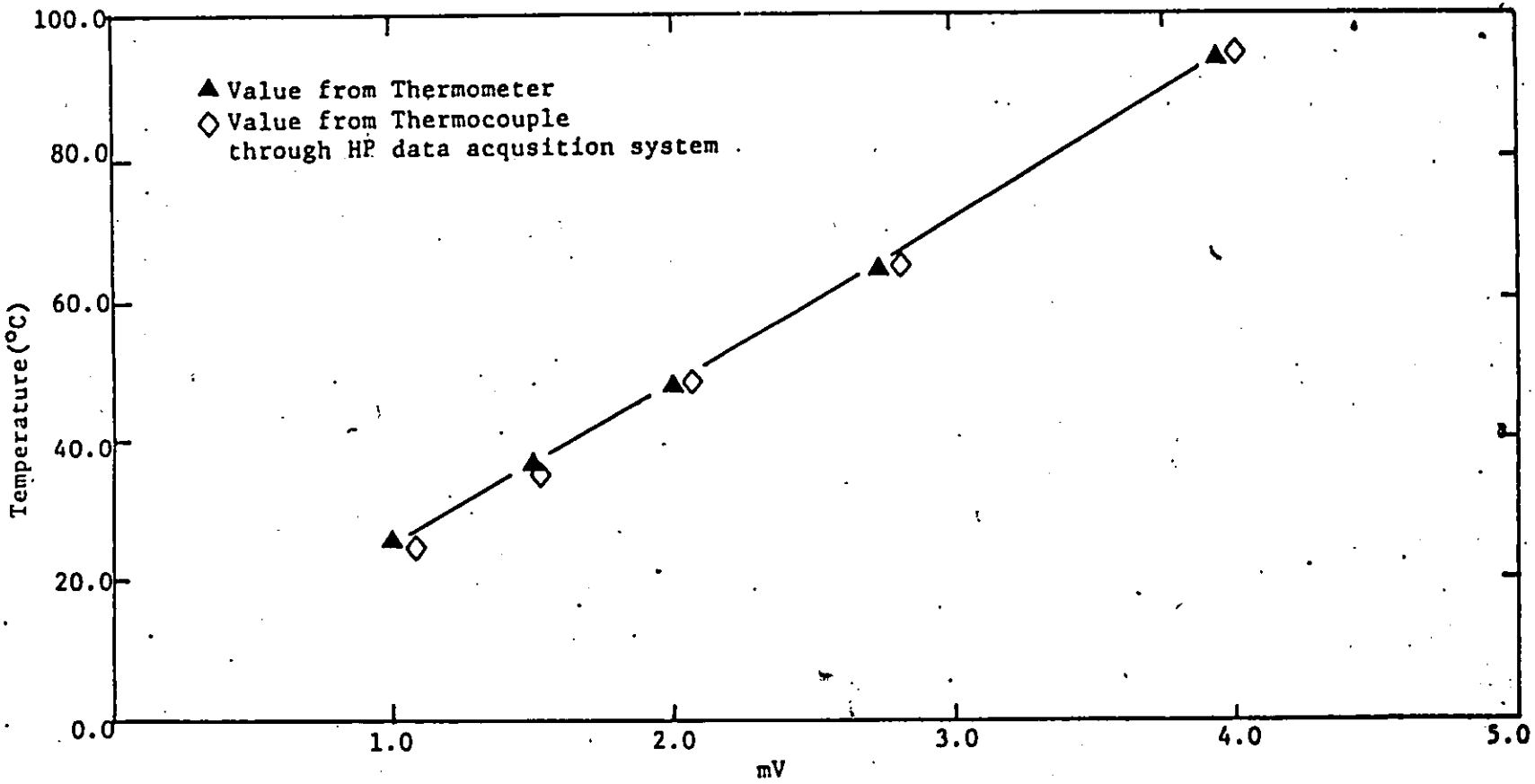

Fig.4.10 Calibration Curve of Thermocouple

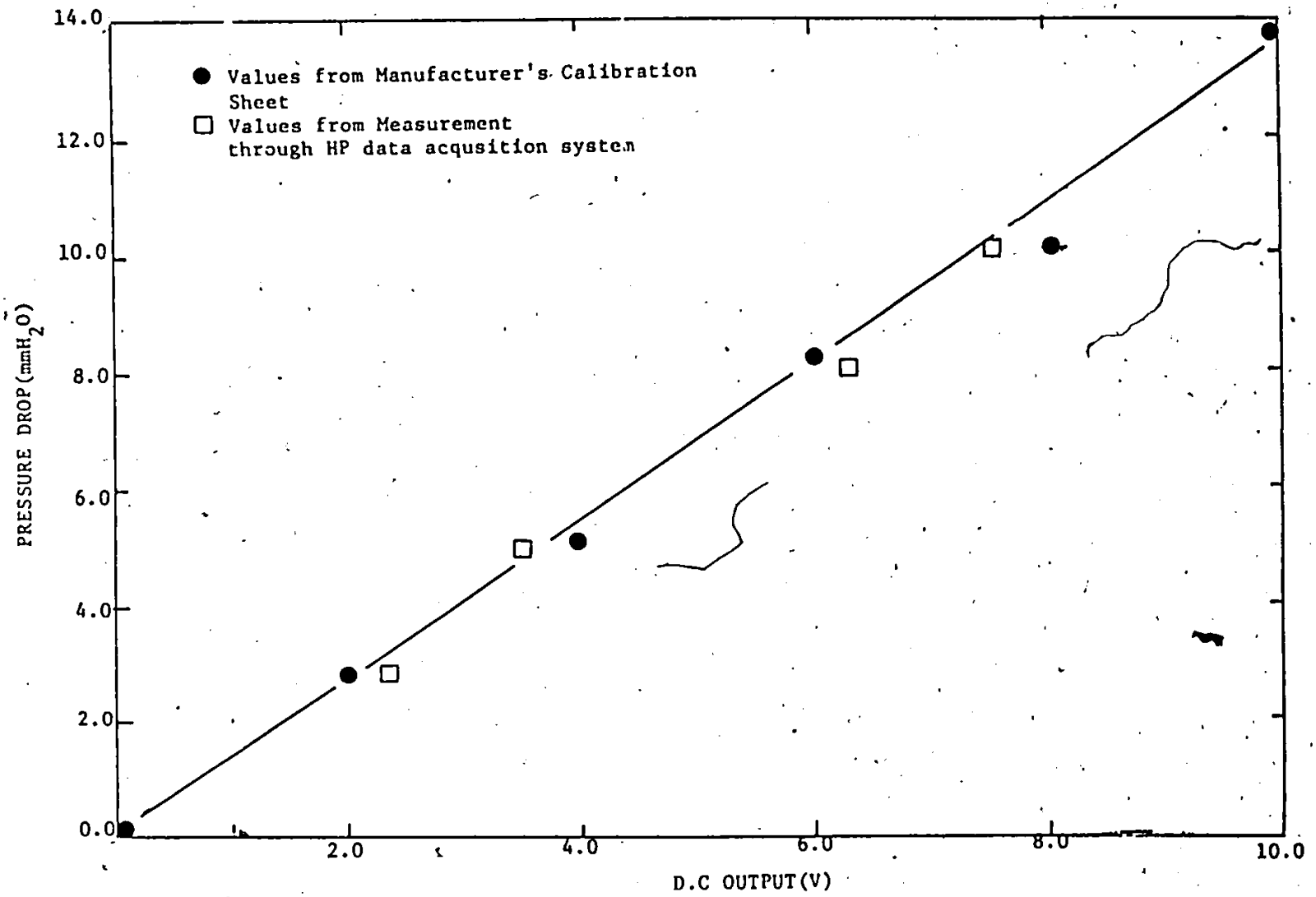

Fig.4.11 Calibration Curve of Pressure Transducer

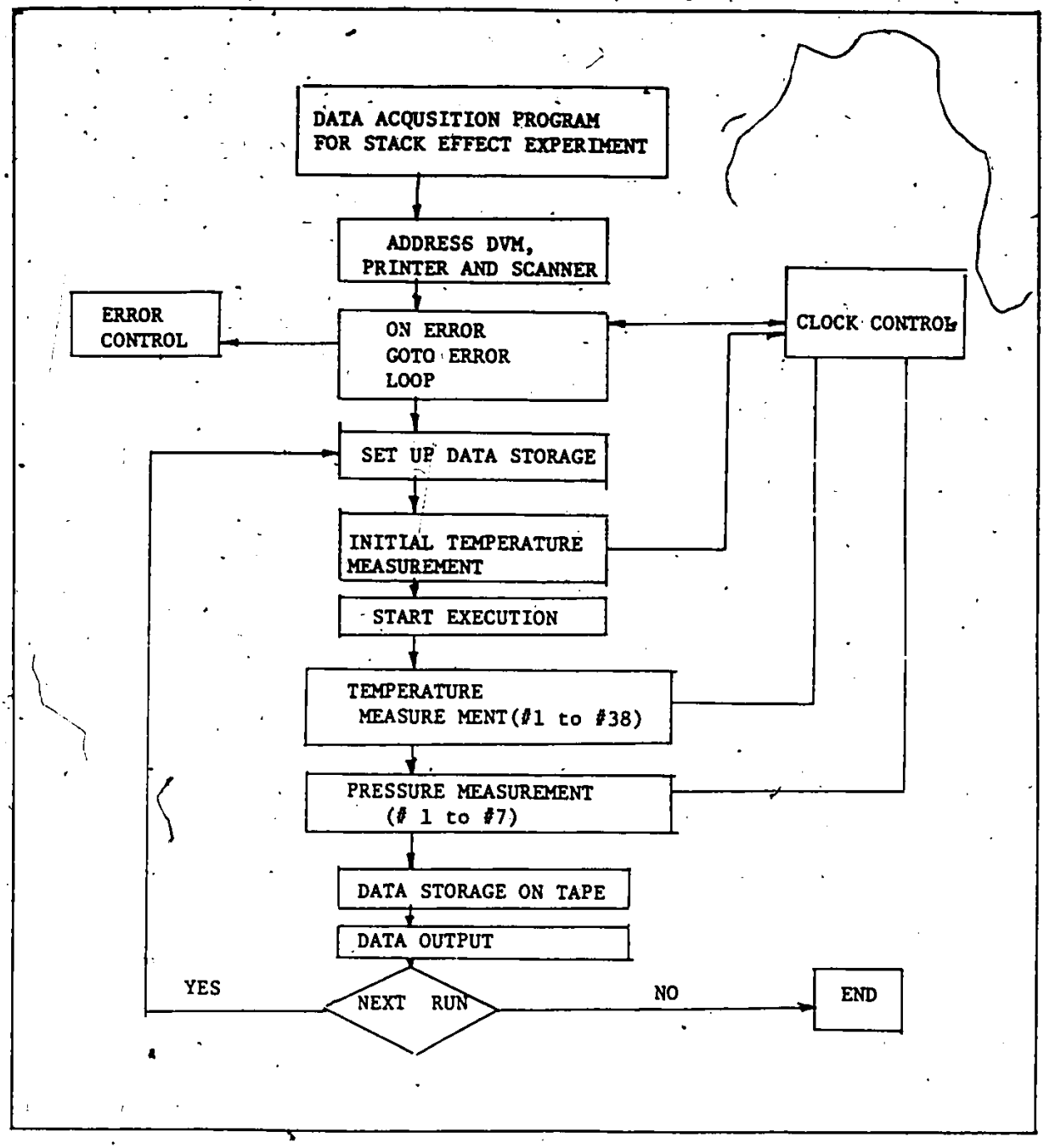

Fig.4.12 Flow Chart of Data Acqusition Program for the Stack Effect Experiment.

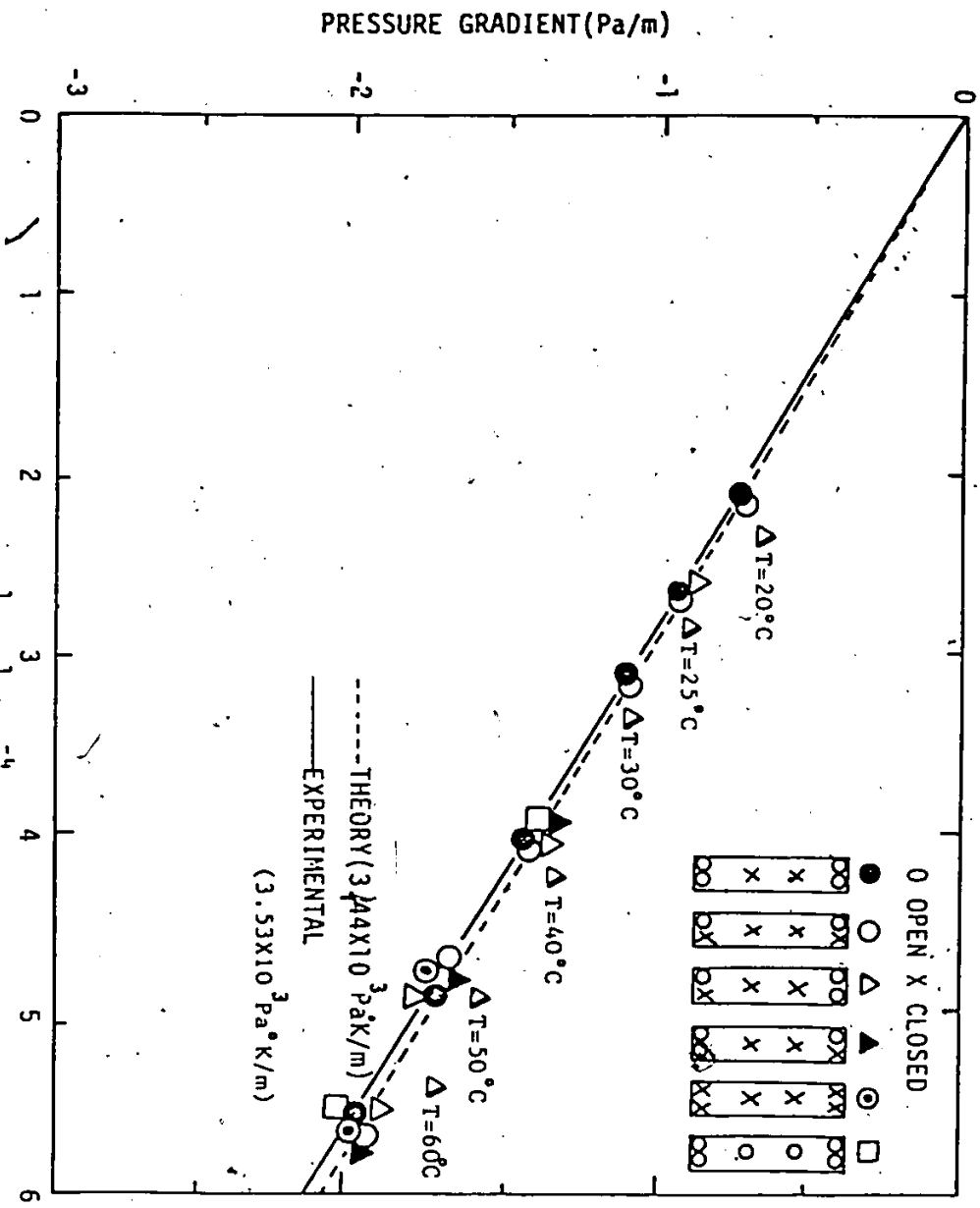

Fig.5.1 Vertical Pressure Gradient due to Stack Effect

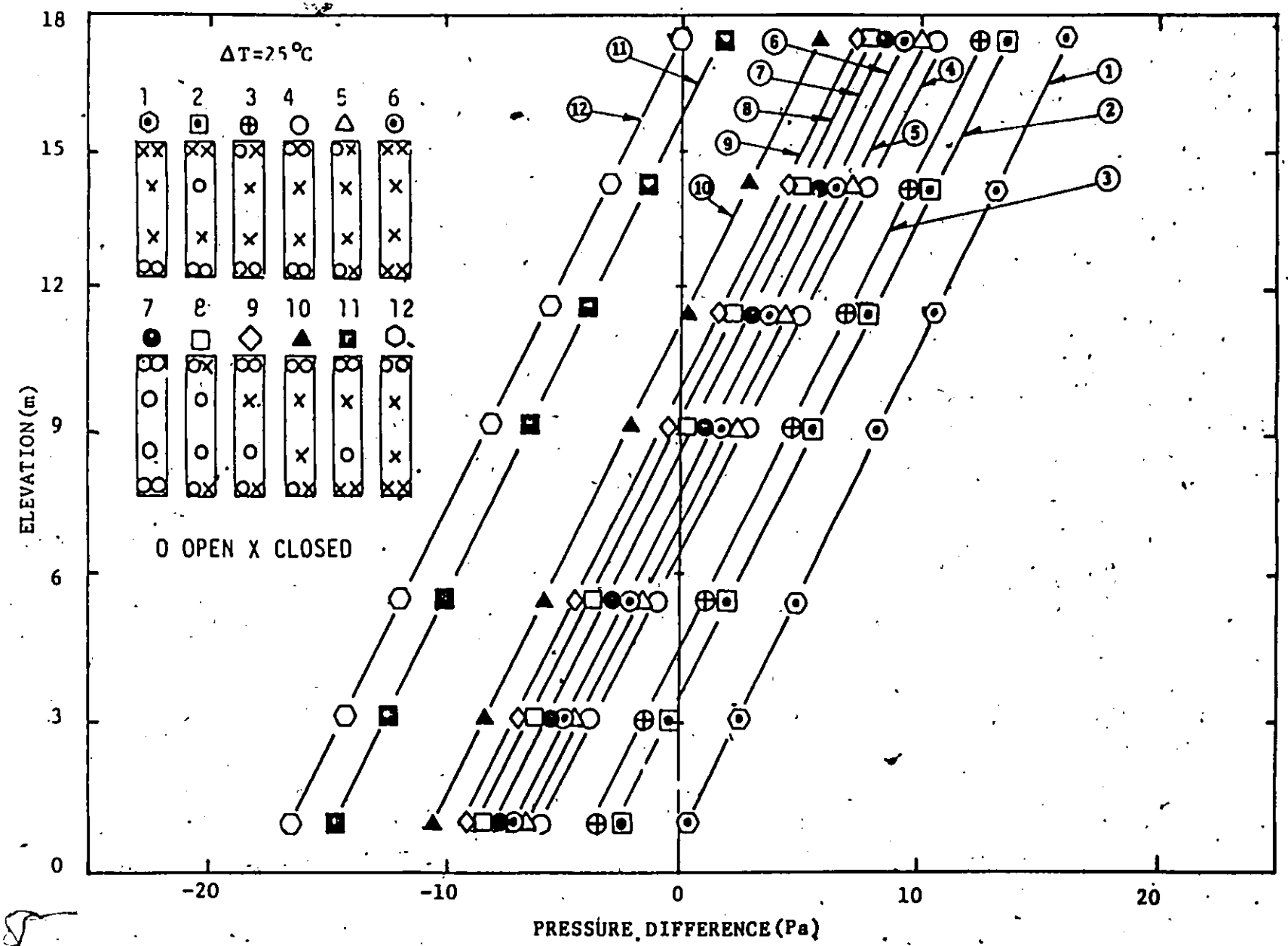

Fig.5.2 Profile of Pressure Differentials obtained in the Experiment with variation of Openings under a given Constant Temperature Difference across the Wall ($\Delta T = 25^{o}C$).

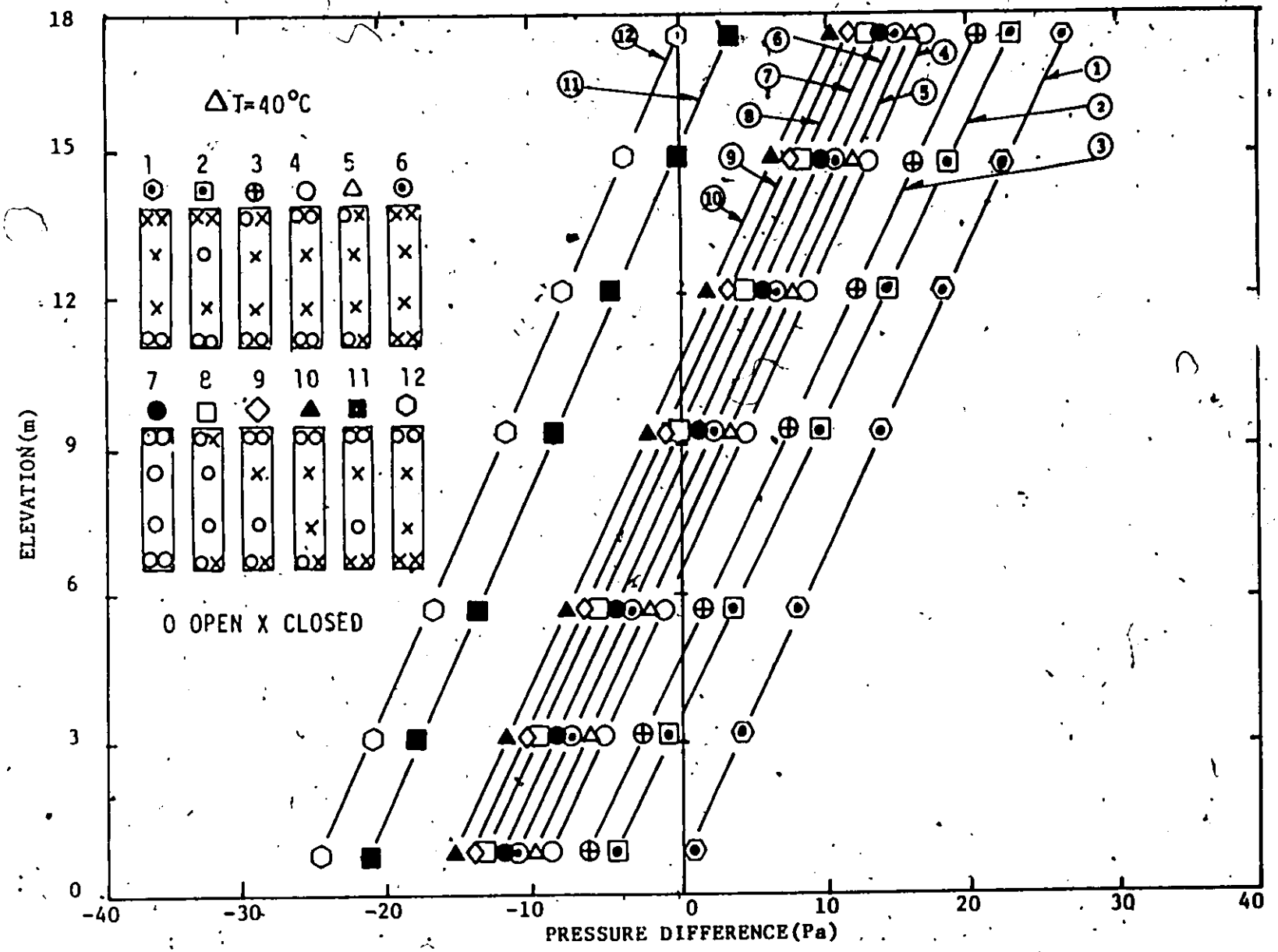

Fig.5.3 Profile of Pressure Differentials obtained in the Experiment with Variation Openings under a given Constant Temperature Difference ($\Delta T = 40^{\circ}C$).

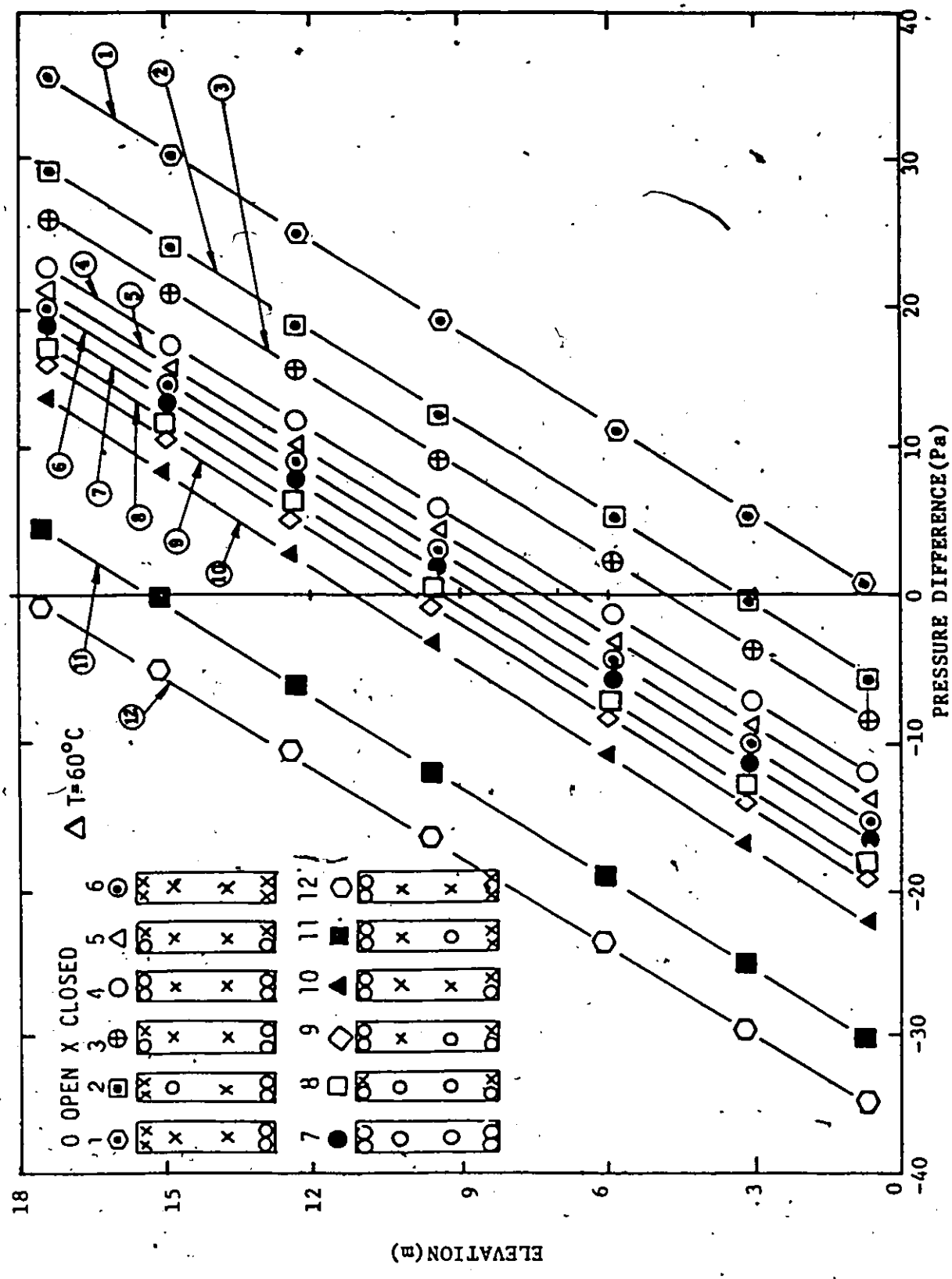

Fig.5.4 Profile of Pressure Differentials obtained in the Experiment with Variation of Openings under a given Constant Temperature Difference($\Delta T = 60^{o}C$).

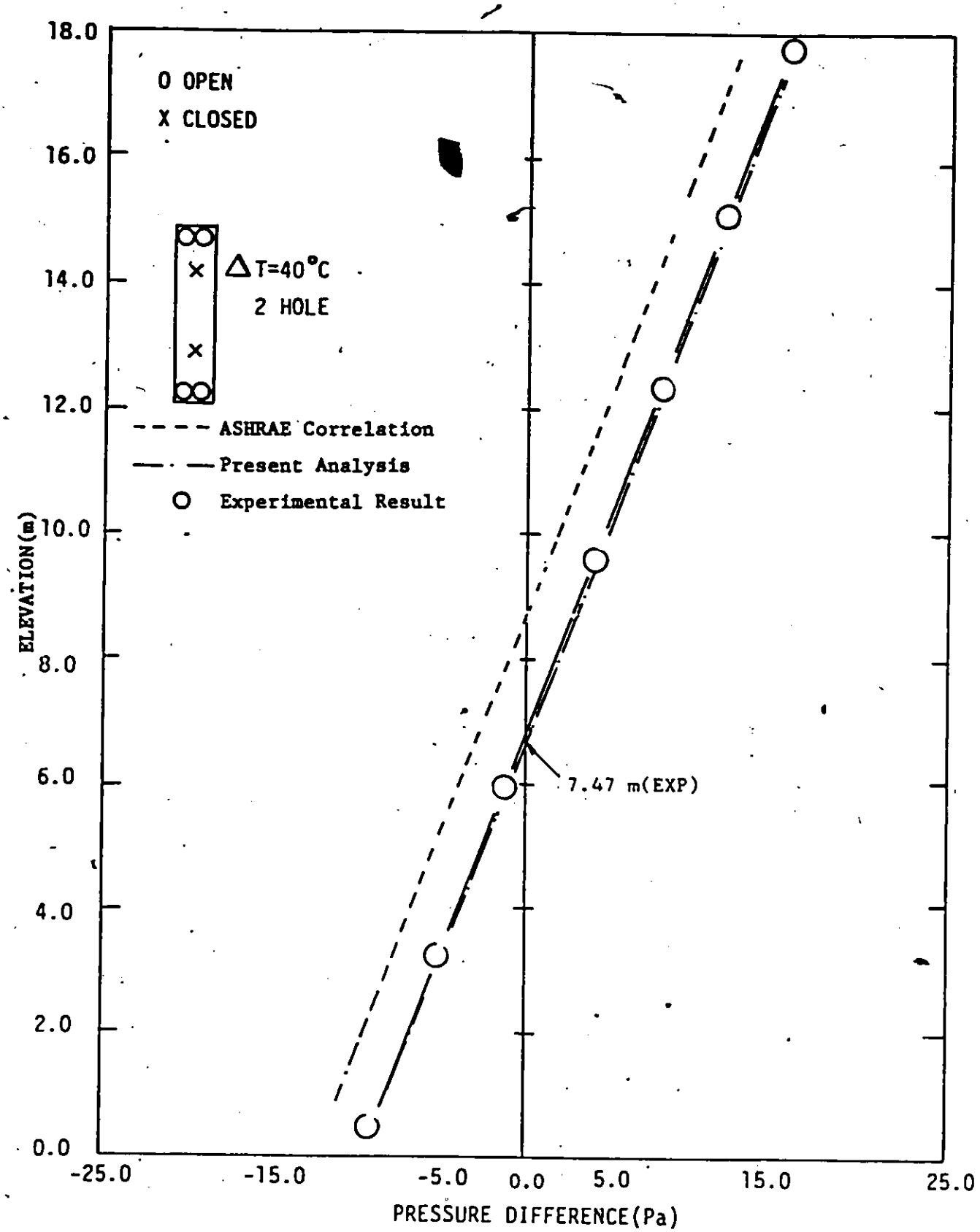

Fig.5.5 Comparison of Experimental Result with ASHRAE Recommedation and Theoretical Analysis in the Case with two openings at the top and bottom levels only for a given Temperature Difference.

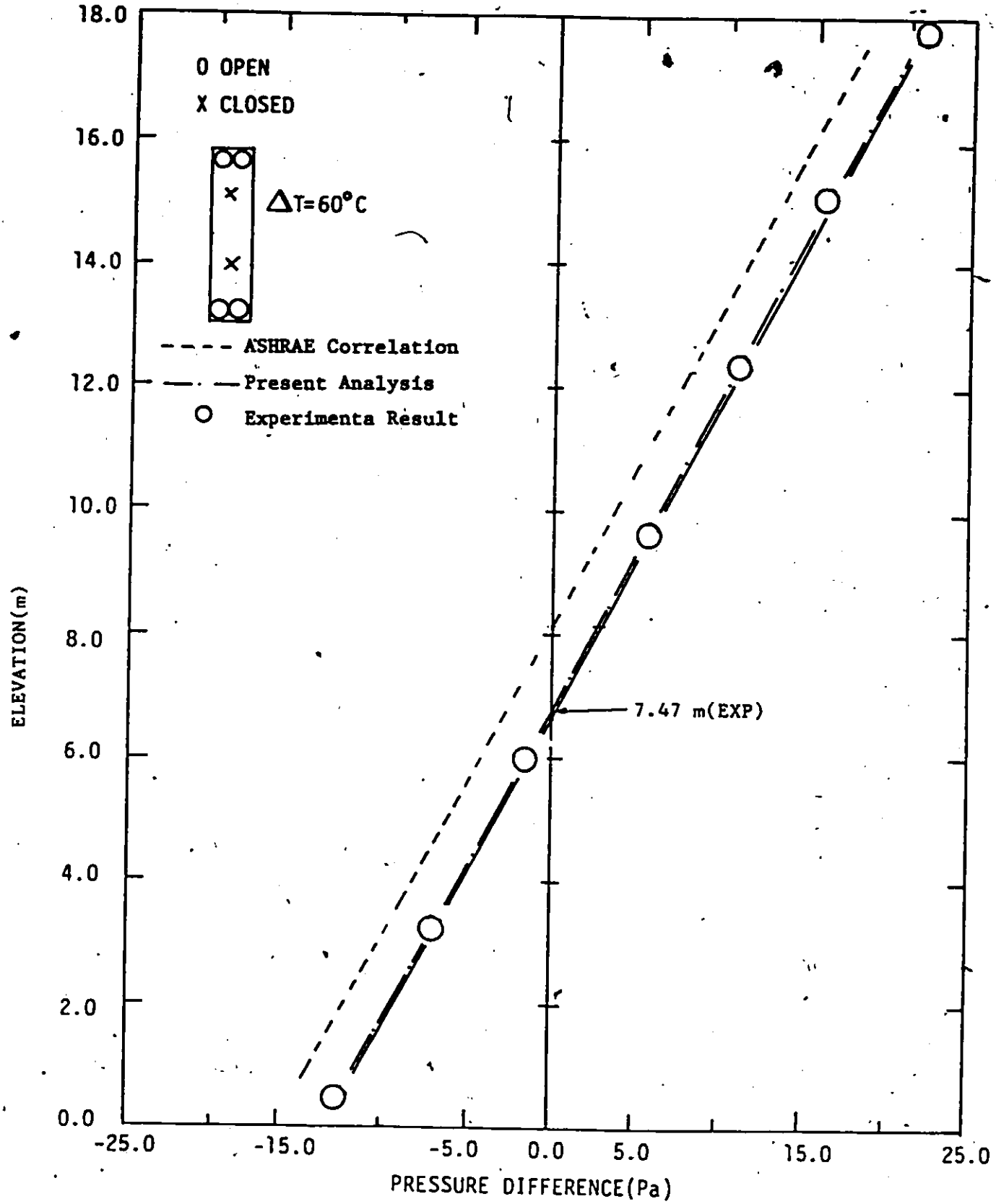

Fig.5.6 Comparison of Experimental Result with ASHRAE Recommendation and Theretical Analysis in the Case with two Openings at the top and bottom Elevations only for a given Temperature Difference (ΔT=60°C).

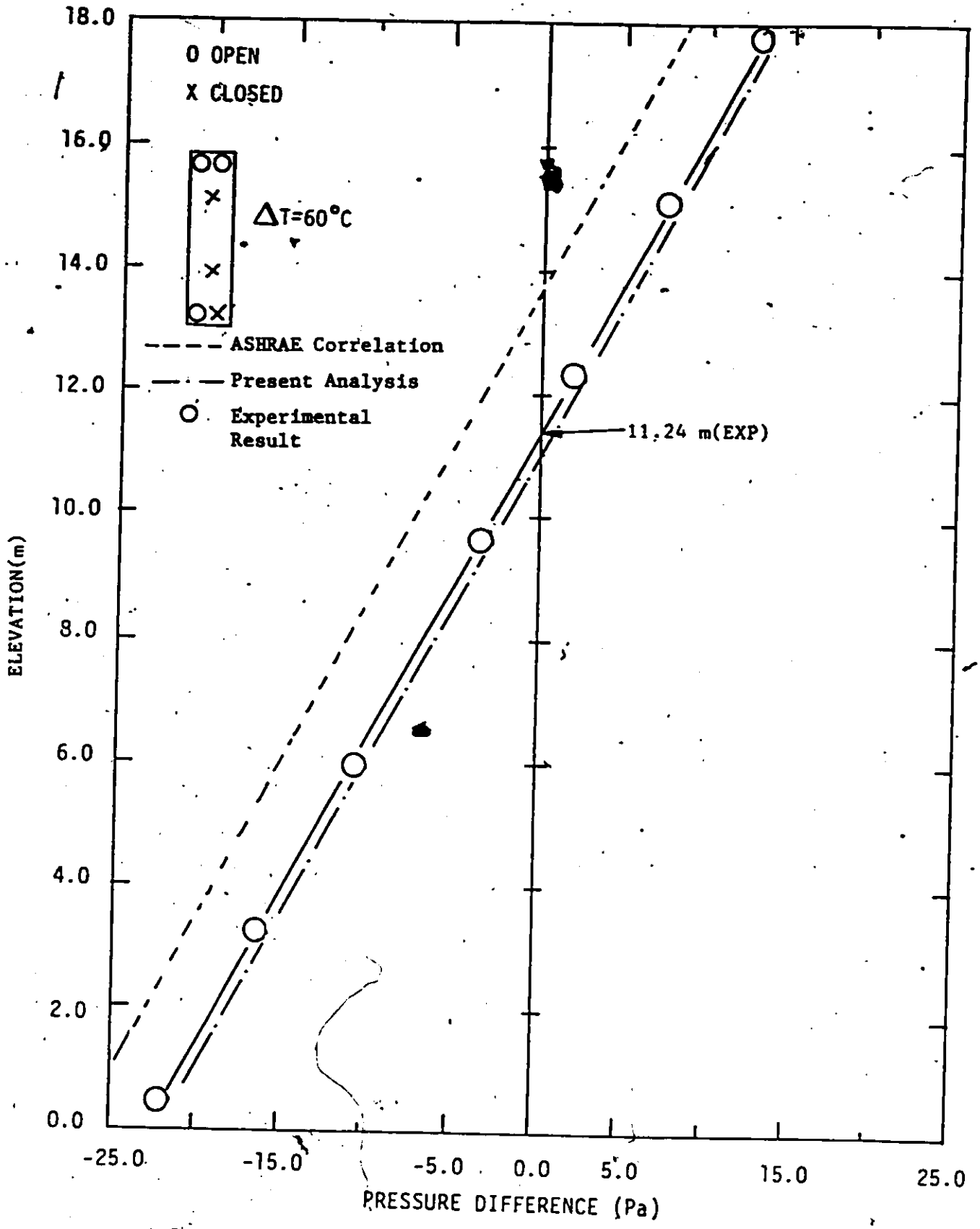

Fig.5.7 Comparison of Experimental Result with ASHRAE Recommendation and Theoretical Analysis in the Case with two Openings at top and one Opening at bottom level for a given Temperature Difference.

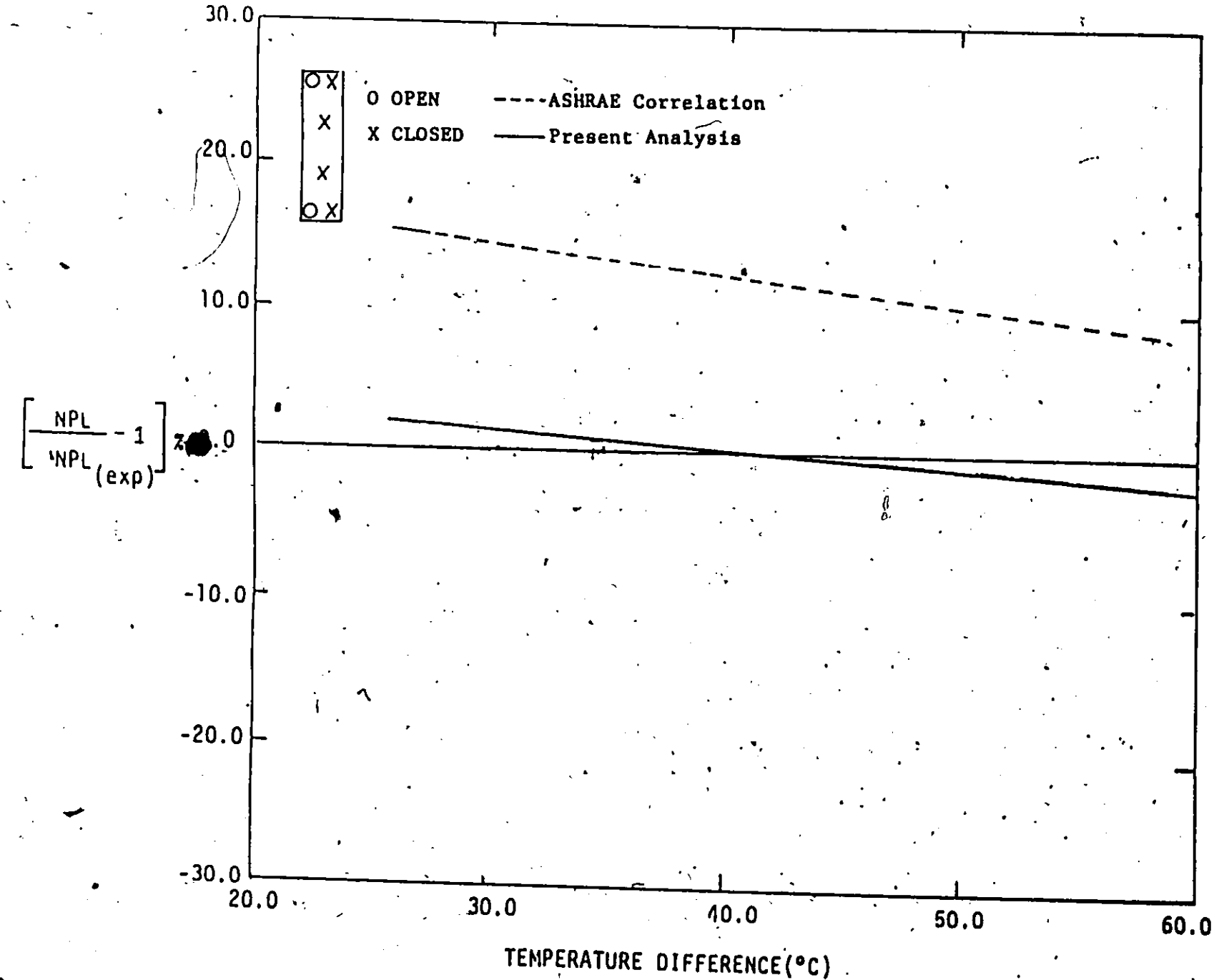

Fig.5.8 Comparison of Experimental Results with ASHRAE Recommendation and Theoretical Analysis for a given Opening Condition(One Opening at top and bottom level only).

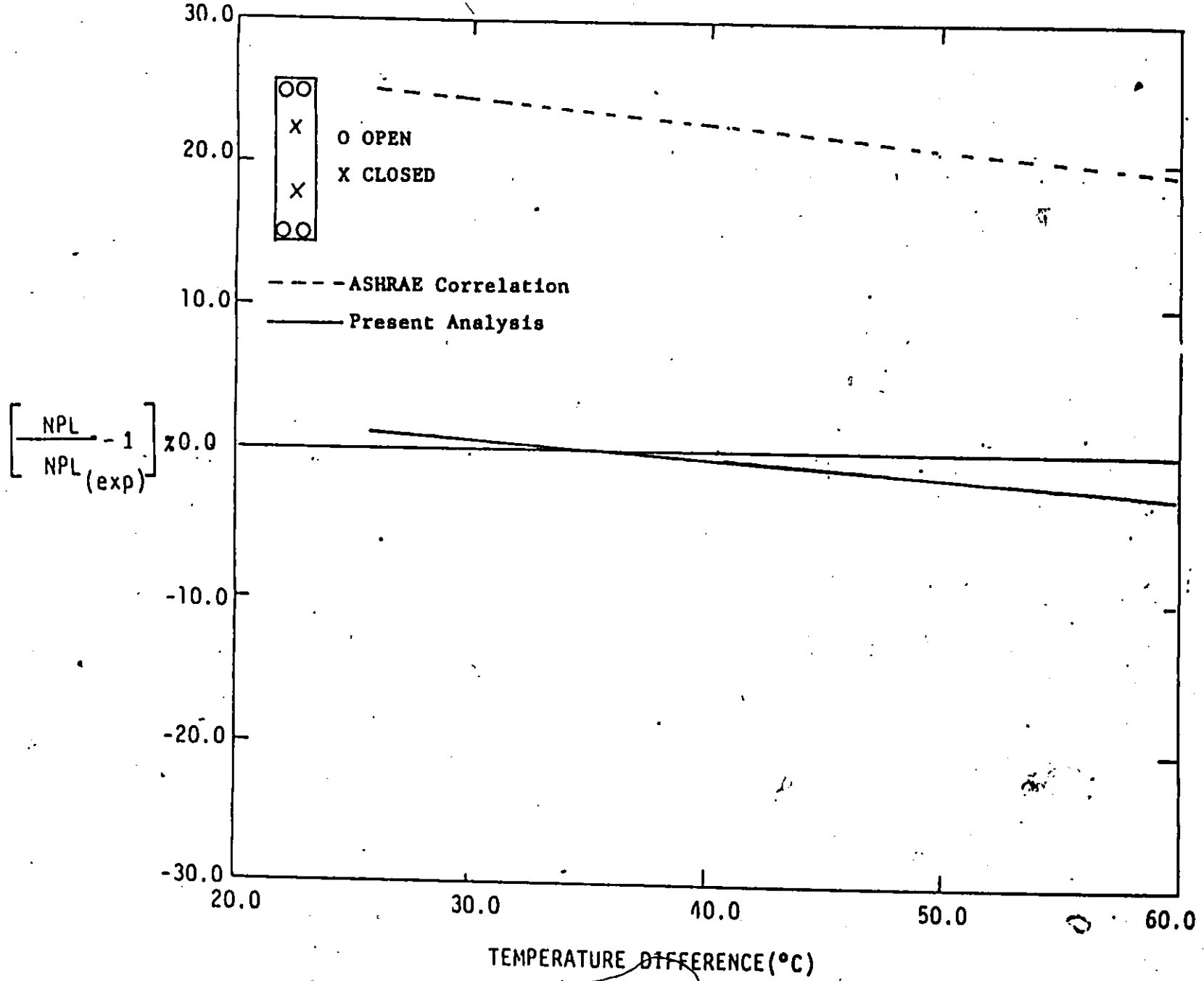

Fig.5.9 Comparison of Experimental Result with ASHRAE Recommendation and Theoretical Analysis for a given Opening Condition(Two Openings at top and bottom levels only).

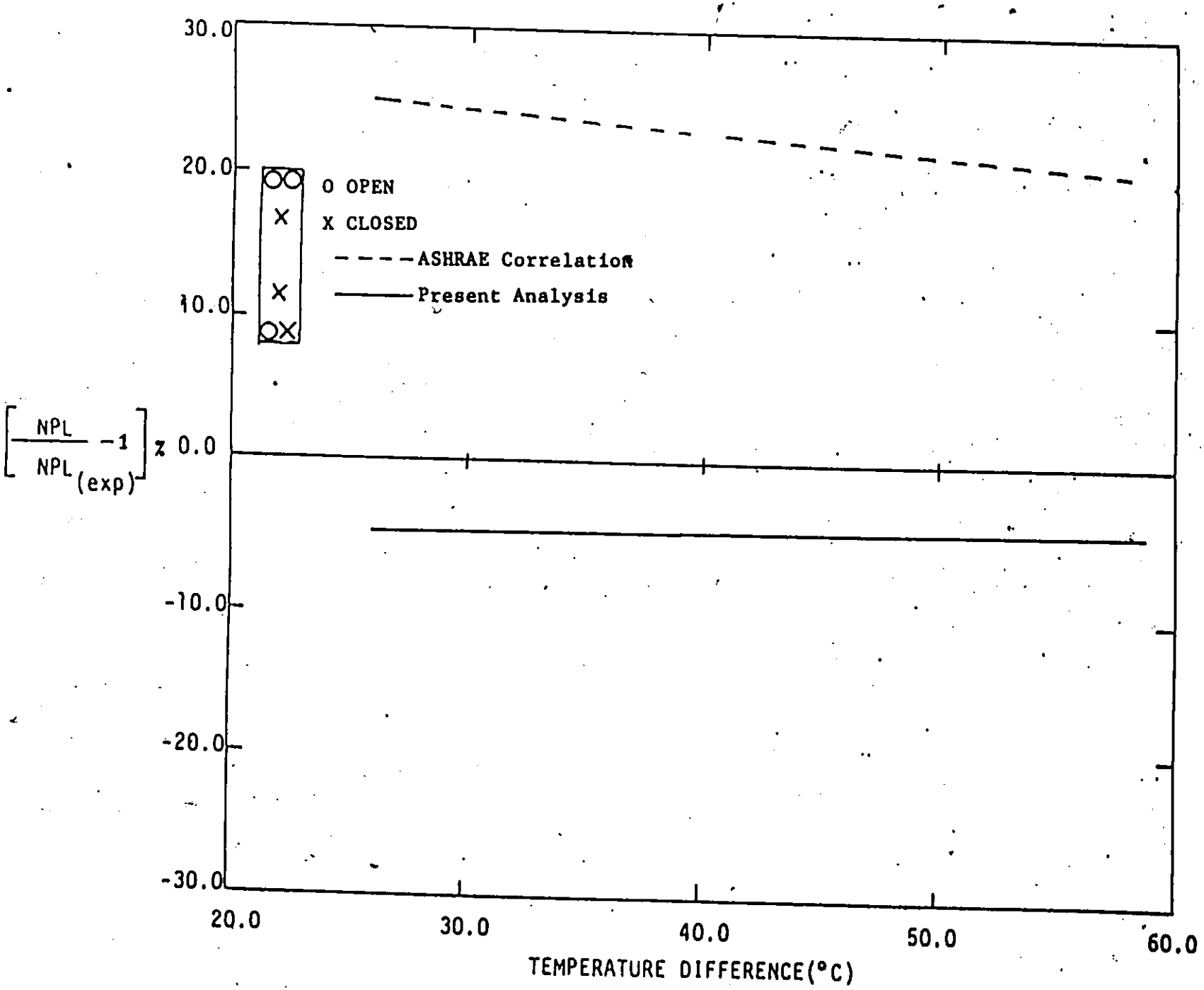

Fig.5.10 Comparison of Experimental Result with ASHRAE Recommendation and Theoretical Analysis for a given Opening Condition(Two Openings at top level and One Opening at bottom level).

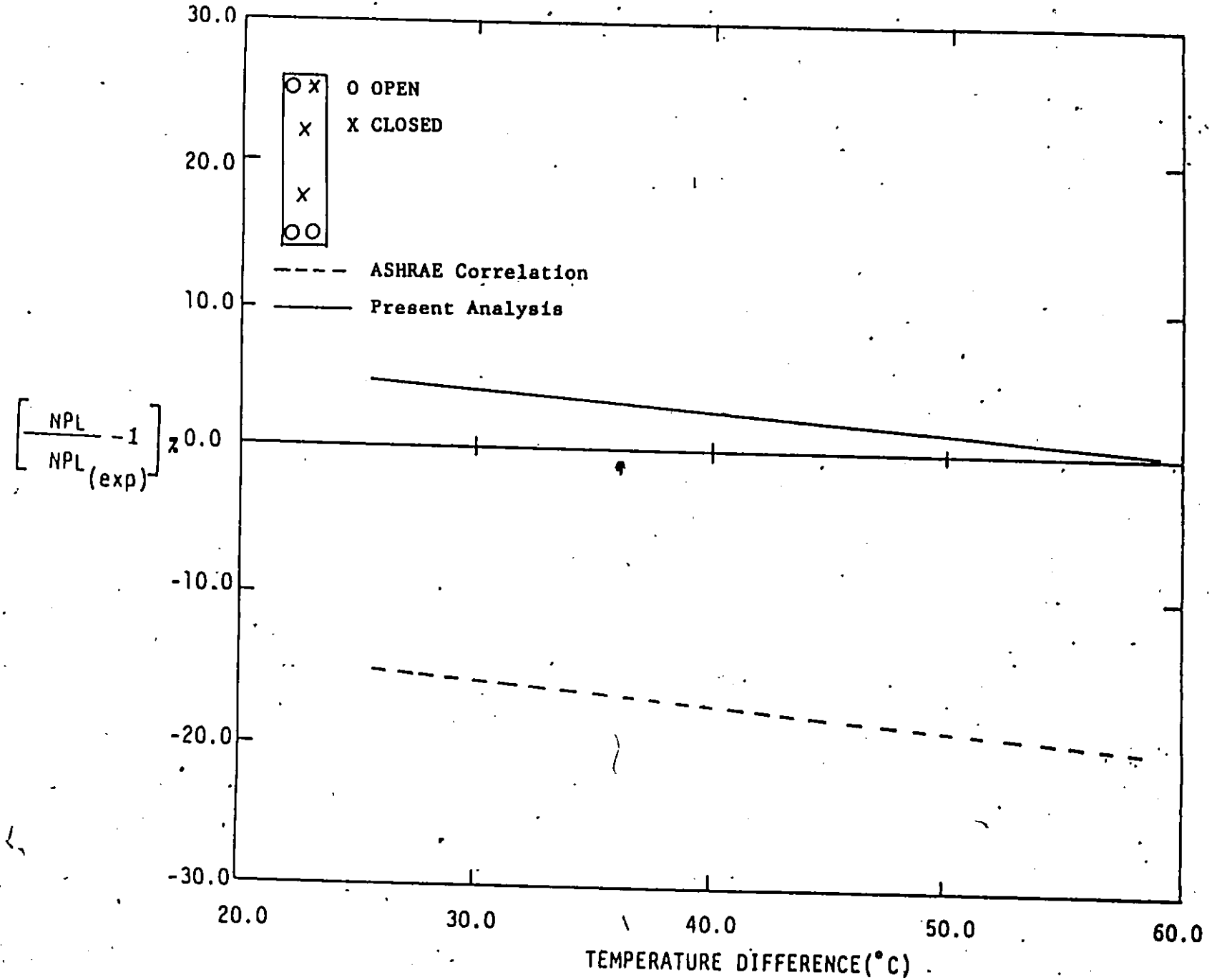

Fig.5.11 Comparison of Experimental Result with ASHRAE Recommendation and Theoretical Analysis for a given Opening Condition

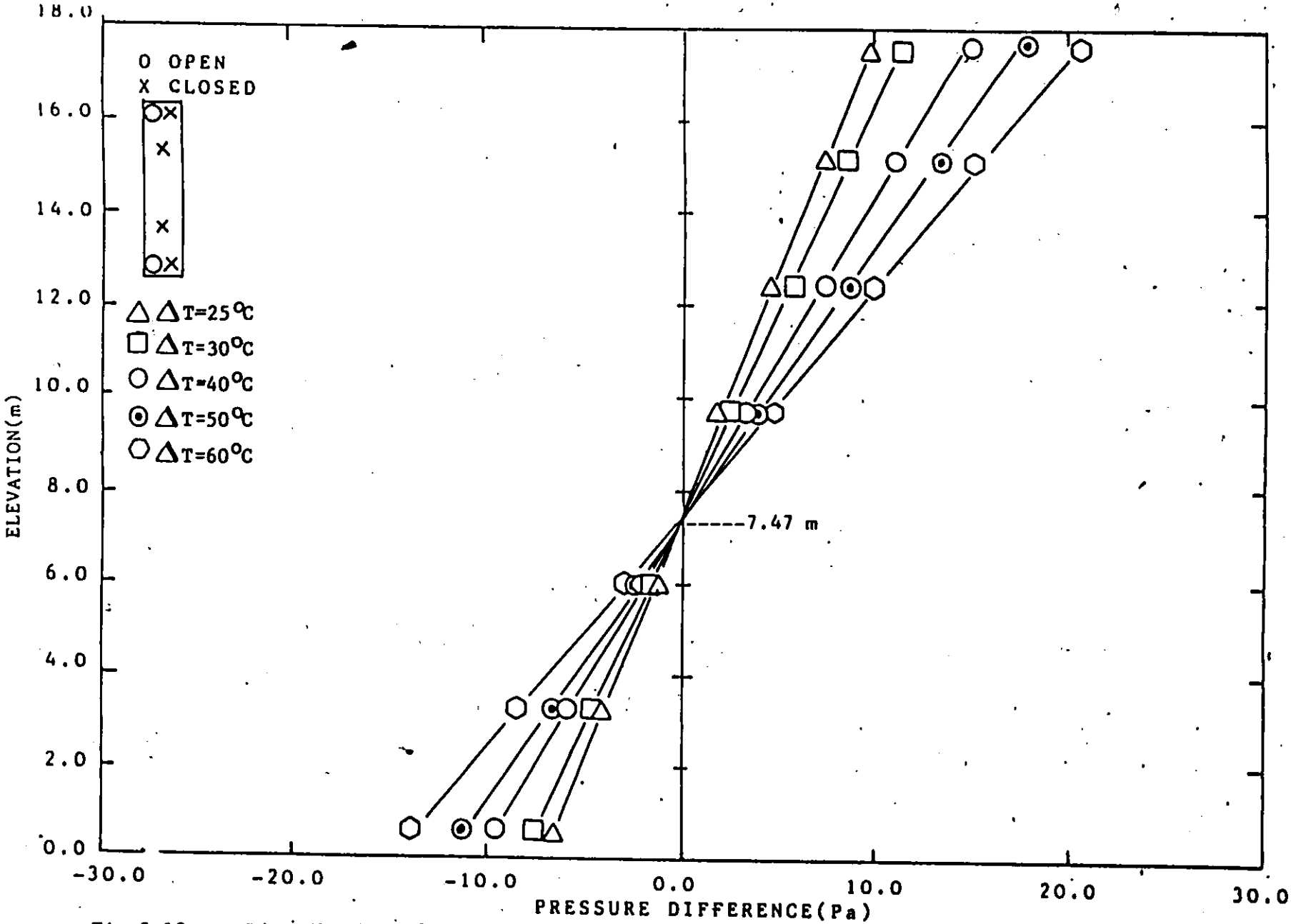

Fig.5.12 Distribution of Pressure Differentials in the Experiment with the variation of Temperature Differences across the Exterior Wall for a given Opening Condition(One Opening at top and bottom elevations only).

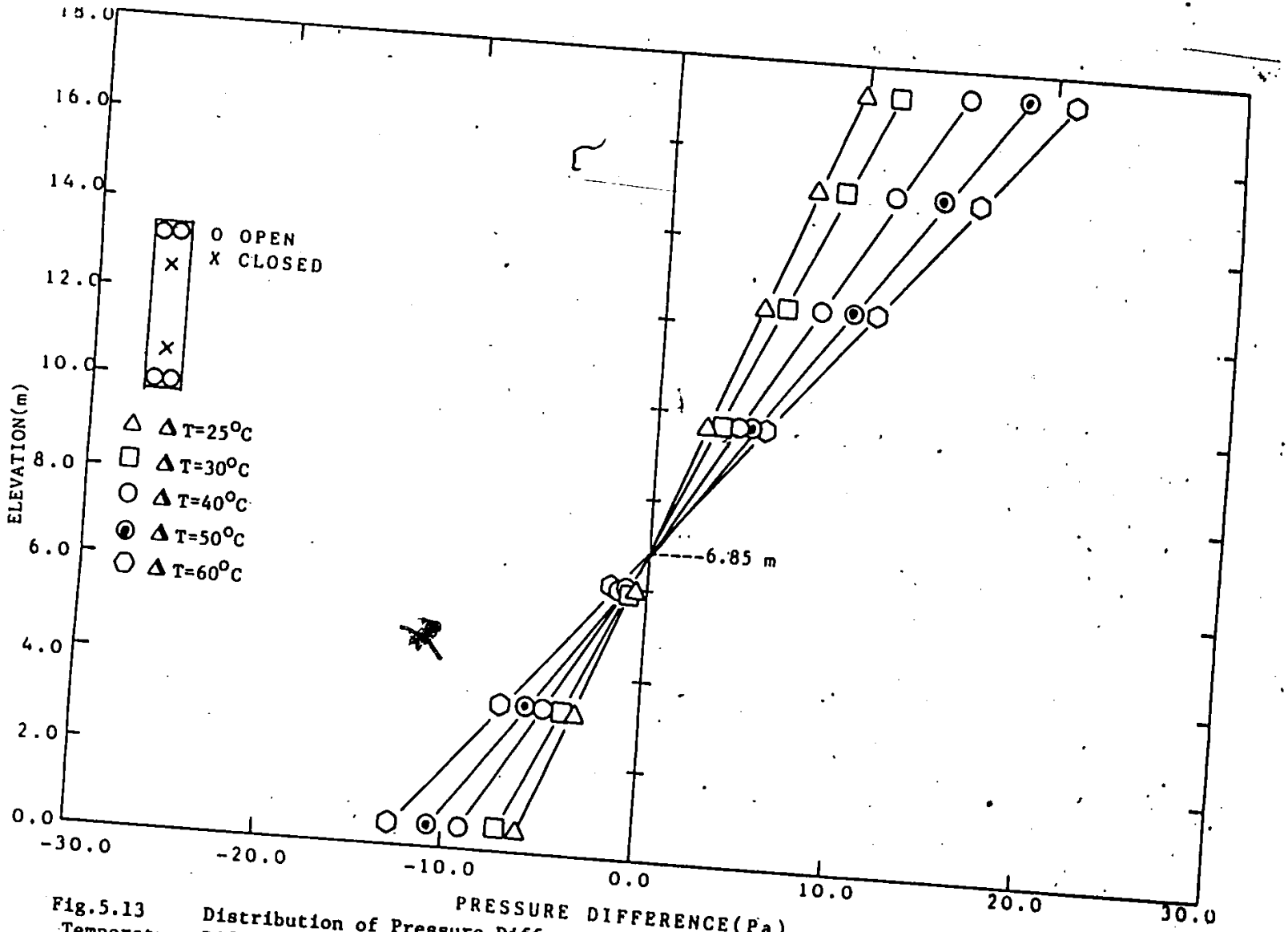

Fig.5.13 Distribution of Pressure Differentials obtained in the Experiment with the variation of Temperature Differences across the Exterior Wall for a given Opening Condition.

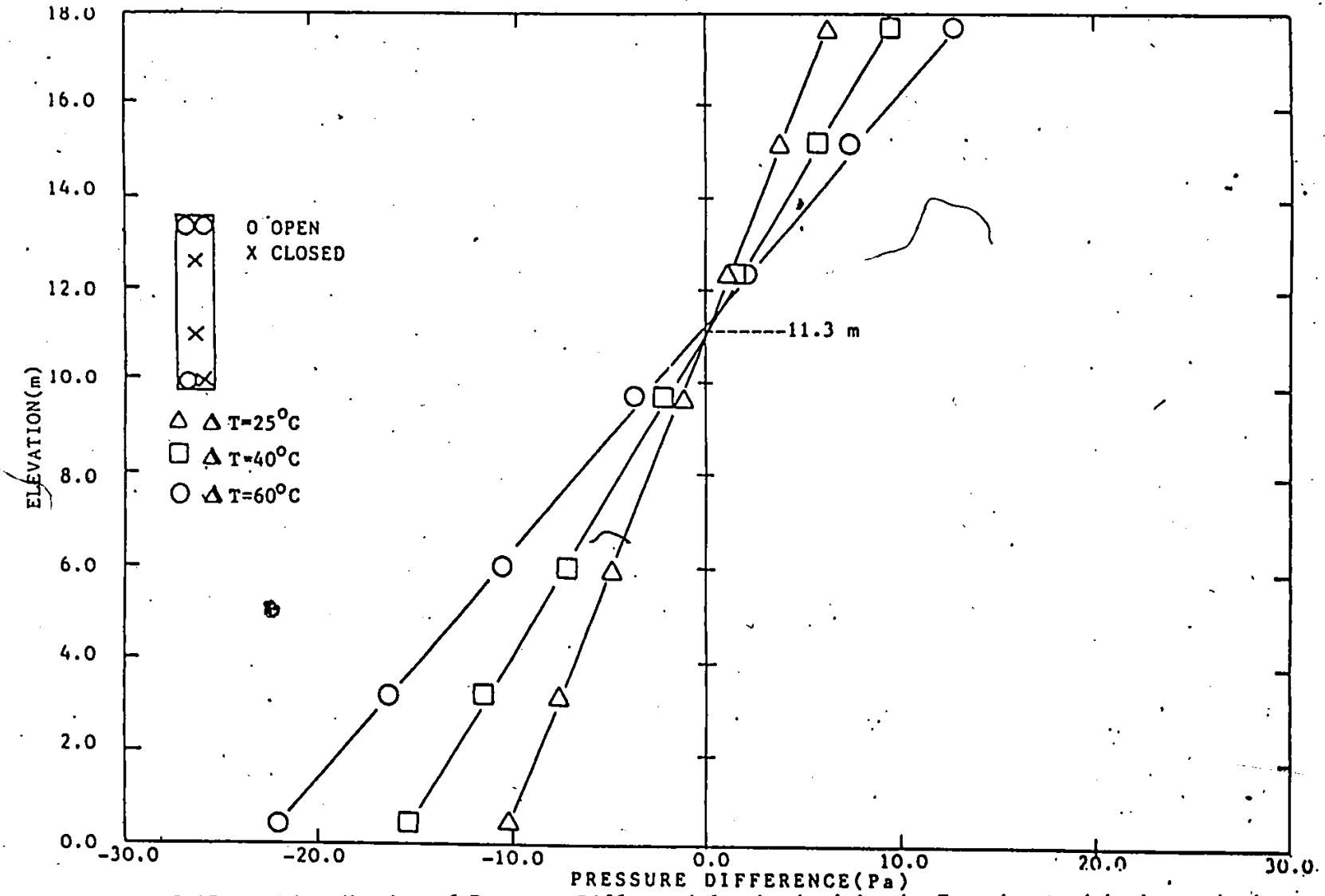

Fig.5.15 Distribution of Pressure Differentials obtained in the Experiment with the variation of Temperature Differences across the Exterior Wall for a given Opening Condition(Two Openings at top level and One Opening at bottom level).

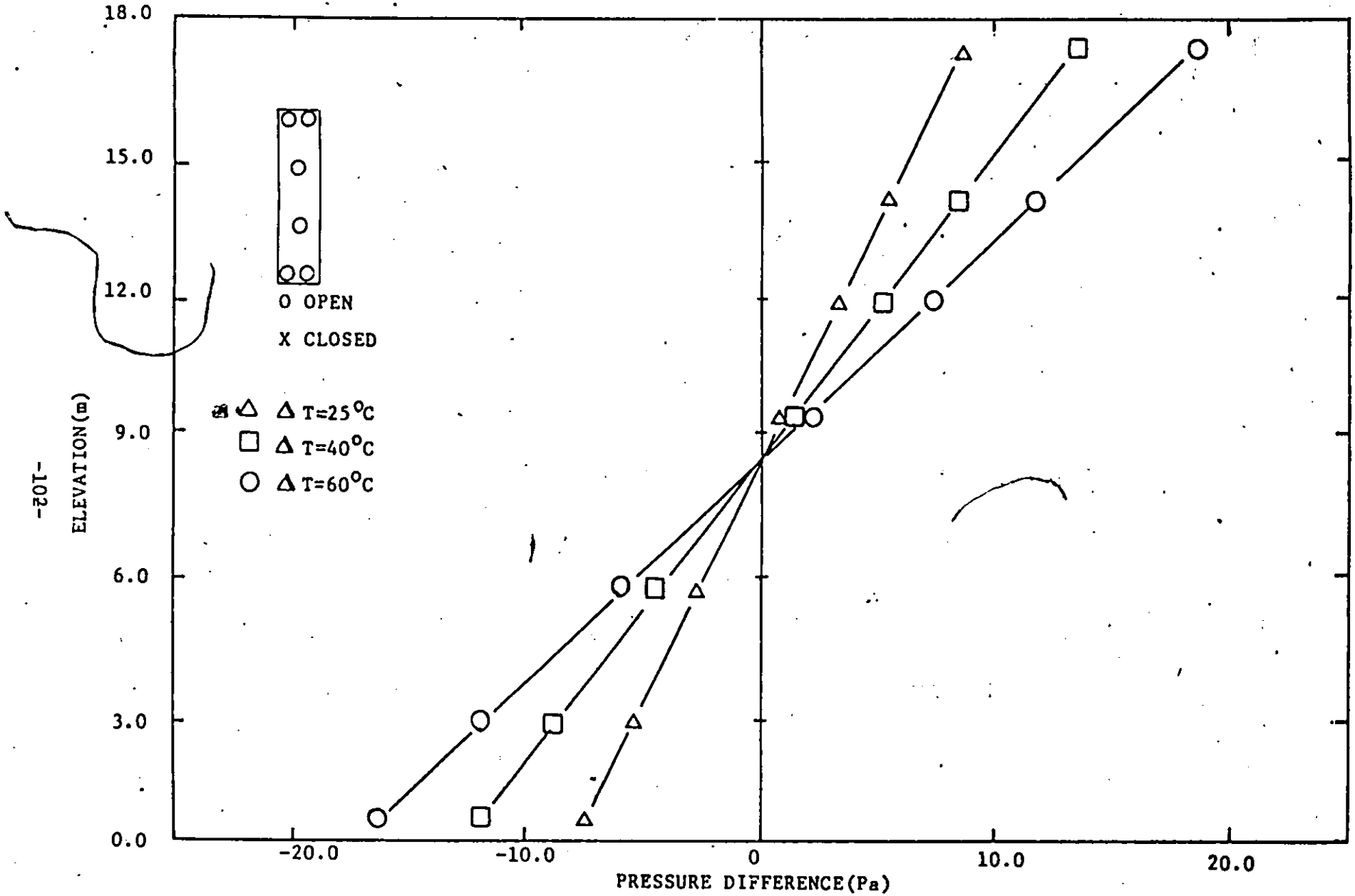

Fig.5.17 Distribution of Pressure Differentials obtained in the Experiment with Variation of Temperature Differences across Wall under a given Opening Condition(Openings at Four Elevations).

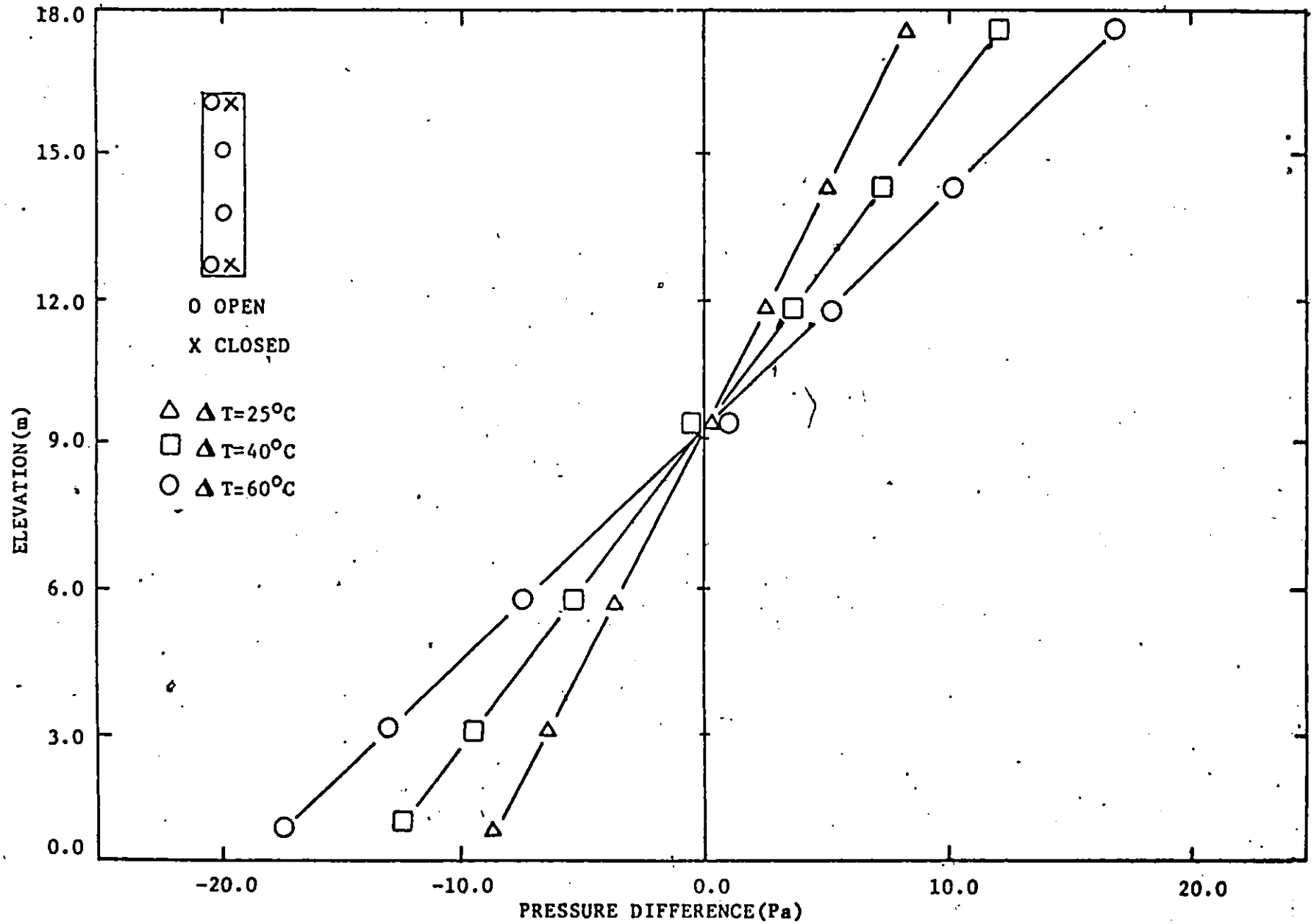

Fig.5.16 Distribution of Pressure Differentials obtained in the Experiment with Variation of Temperature Differences across Wall under a given Opening Condition(Uniform Opening at Four Level).

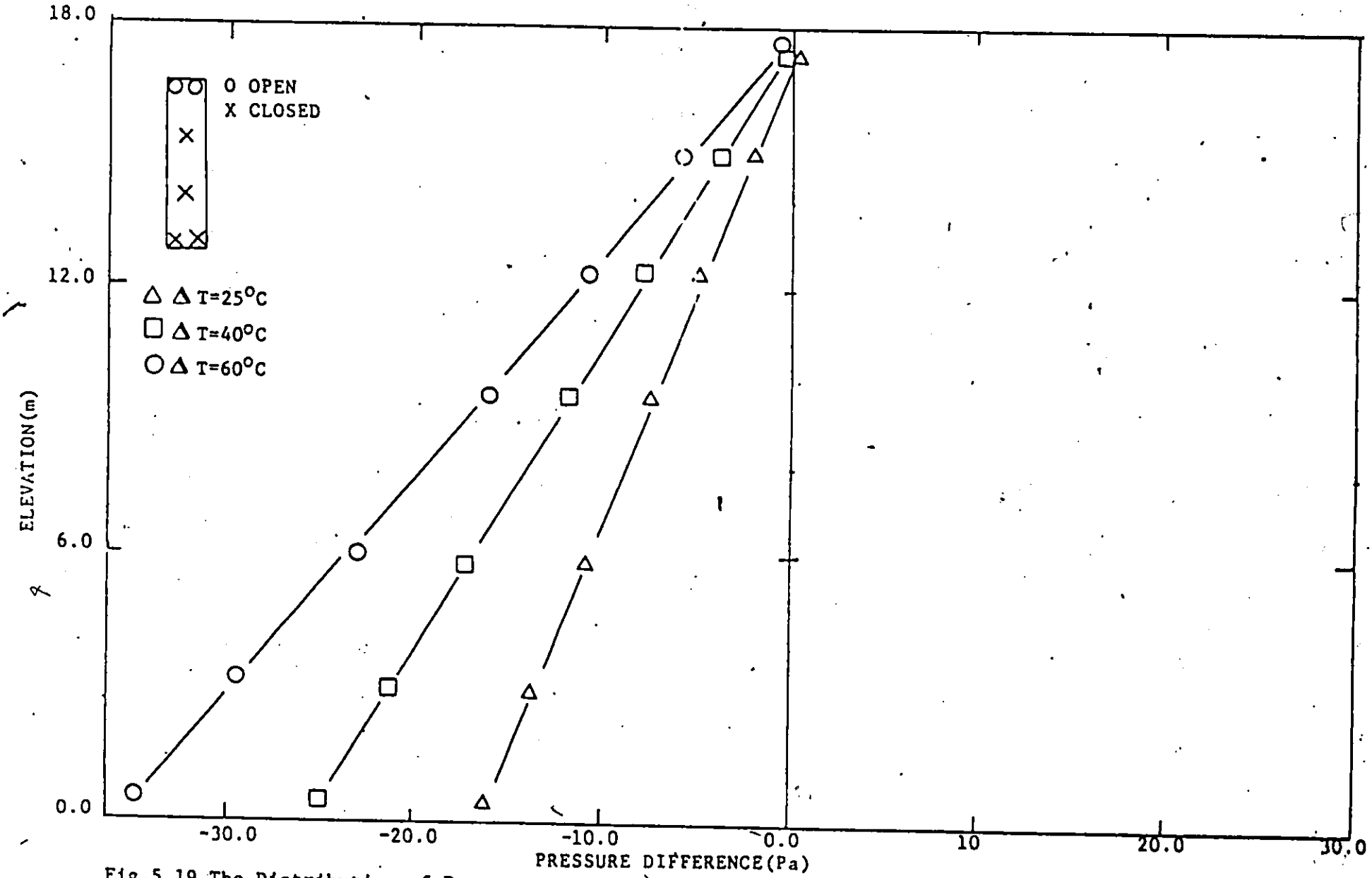

Fig.5.19 The Distribution of Pressure Difference obtained in the Experiment with the variation of Temperature Difference across the Exterior Wall for a given Opening Condition(Two Openings at top level only)

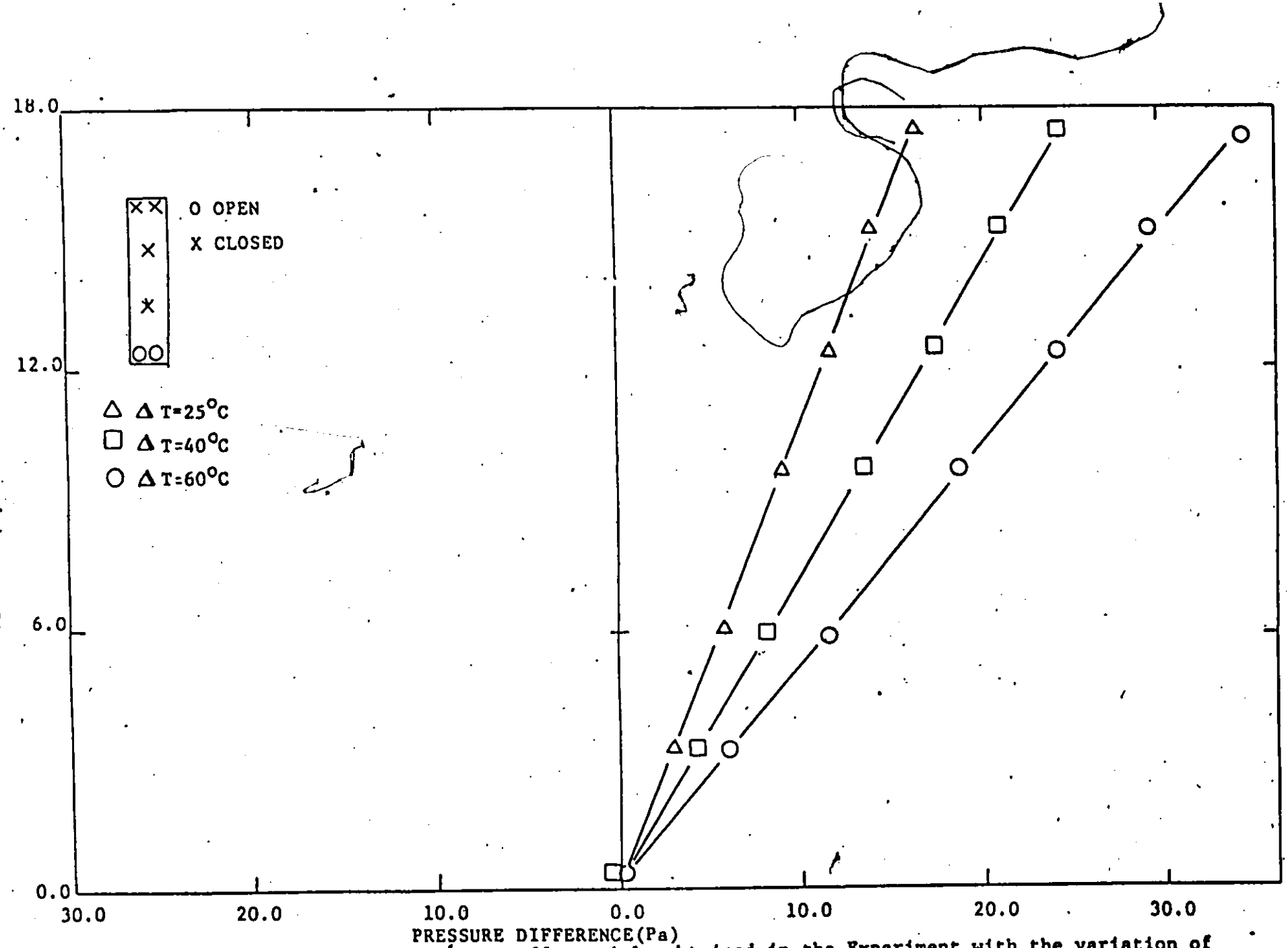

Fig.5.18 The Distribution of Pressure Differentials obtained in the Experiment with the variation of Temperature Differences across the Exterior Wall for a given opening Condition(Two Openings at bottom level only).

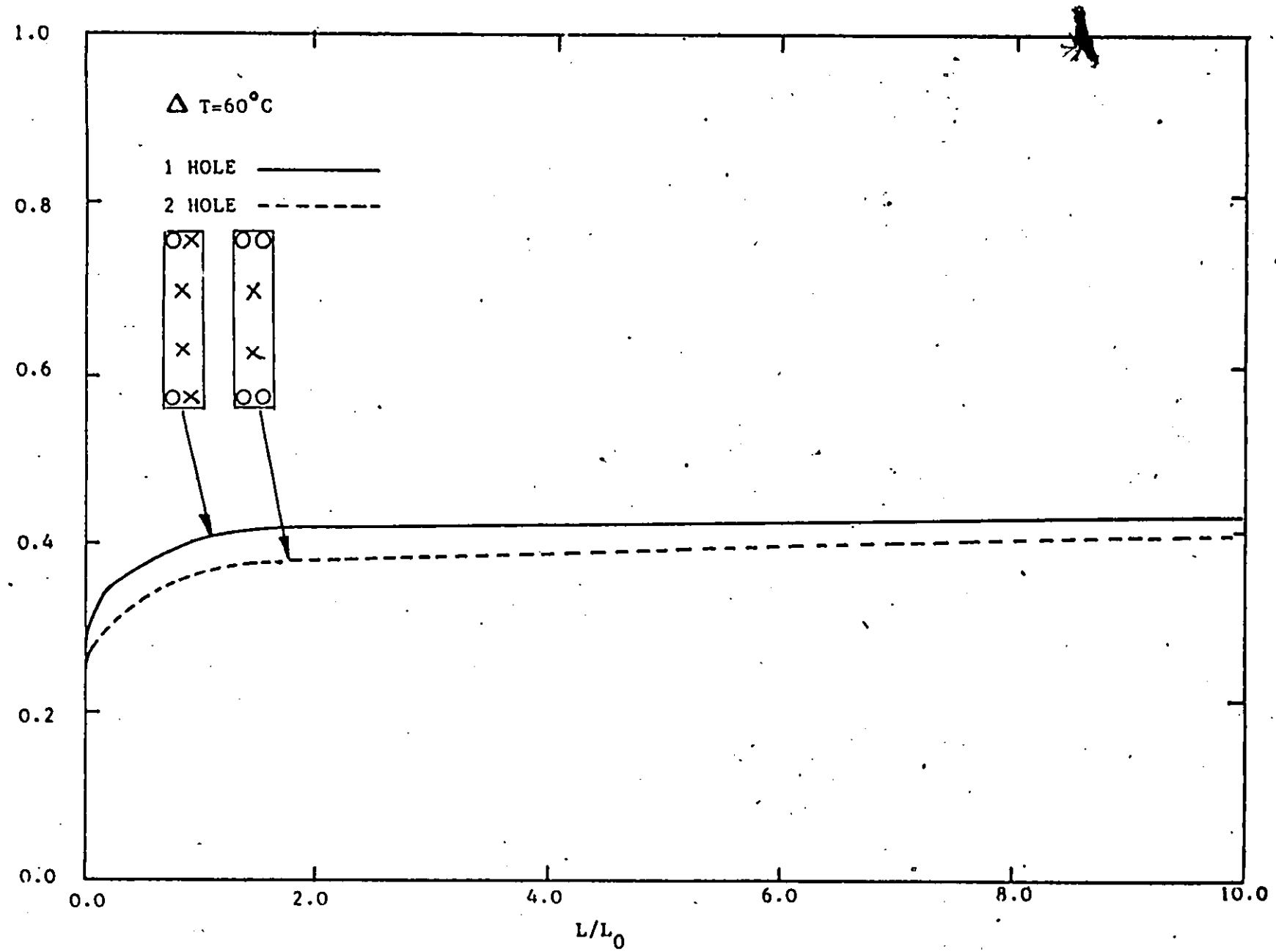

Fig.5.20 Theoretical Analysis of Effect of Vertical Dimension of Building on the Neutral Pressure Level for a given Opening Condition and Temperature Difference.

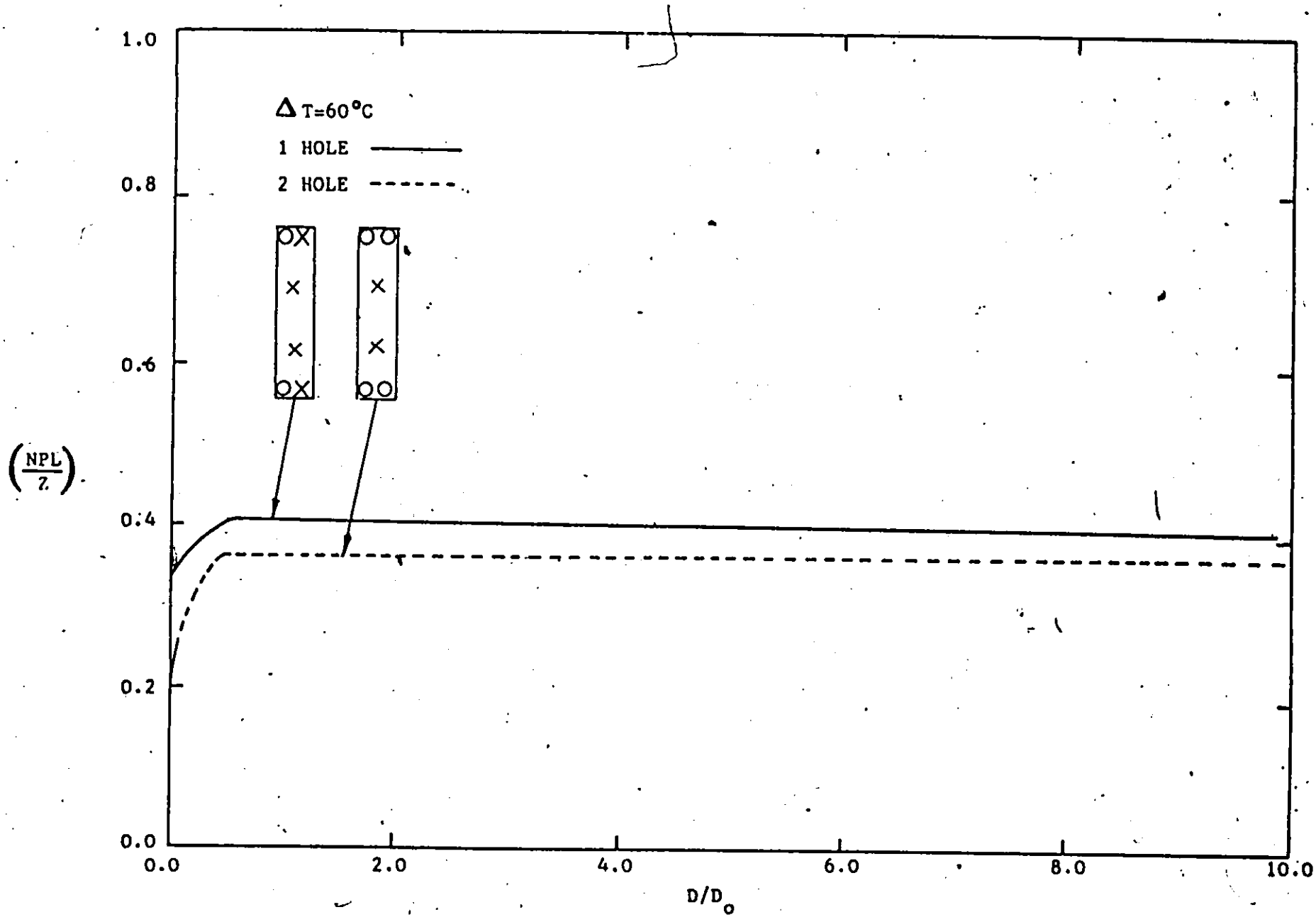

Fig.5.21 Theoretical Analysis of Effect of Lateral Dimension of Building on the Neutral Pressure Level for a given Opening Condition and Temperature Difference.

Tab 3.1 Calculated Value of C_x from Eq.(3.12)

L/D	Value of C_x
1	1143.3
2	759.7
3	574.8
4	275.2
5	221.5
6	198.9
8	168.8
10	145.5
15	120.1
17	109.5
20	93.1
25	69.2
30	65.3
35	64.2
35 $-\infty$	64.2